

27 July, 1994

*Rapport BIPM -94/9*

*document CCPR / 94 - 2*

***REPORT ON THE INTERNATIONAL COMPARISON OF  
SPECTRAL RESPONSIVITY OF SILICON DETECTORS***

**R. Köhler, R. Goebel, R. Pello**

*Bureau International des Poids et Mesures, Pavillon de Breteuil, 92312 Sèvres,  
Cedex, France*





## TABLE OF CONTENTS

Abstract .....	5
Introduction .....	7
Participating laboratories .....	7
Time schedule .....	8
Pilot comparison .....	8
Detector sets .....	9
Protocol for the comparison .....	13
Experimental arrangement .....	14
Method of the comparison .....	17
Related measurements .....	19
Amplifier calibration .....	19
Shunt resistance .....	20
Linearity .....	21
Temperature coefficient .....	22
Uniformity .....	24
Photodiodes .....	24
Trap detectors .....	26
Spot .....	26
Uncertainties arising from non-uniformities .....	27
Monochromator .....	27
Summary of uncertainties .....	27
Uncertainties in the absolute scales .....	29
Measurement of relative spectral responsivity .....	31
Effects of UV radiation .....	34
Measurements after return of the detectors .....	36
National scales .....	39
CSIR .....	38
CSIRO .....	38
CSMU .....	38
ETL .....	39
INM .....	39
IRL .....	40
KRISS .....	40
NIM .....	40
NIST .....	41
NPL .....	41
NRC .....	42
OMH .....	42
PTB .....	43
VNIIOFI .....	43
Comparison of national scales .....	43
Photodiodes .....	45
Traps .....	48
Agreement of the national scales .....	52
Individual national scales .....	54
Trap measurements at 633 nm .....	64
Conclusions .....	66
Acknowledgement .....	66
Appendix A: The BIPM absolute responsivity scale .....	67
Appendix B: List of acronyms .....	69
List of figures .....	70
List of tables .....	71
References .....	71



***ABSTRACT***

The spectral responsivity scales of fourteen national standards laboratories have been compared within the wavelength range from 250 nm to 1000 nm using two different types of silicon photodetectors. In a second round of this comparison another four laboratories participated.

The repeated measurements of such a large batch of identical photodiodes over a large wavelength range, and over a long period of time has provided interesting information on the stability of these detectors, especially in the UV.

Overall, good agreement was found between the scales of the participating laboratories, although some large deviations were also observed.



## INTRODUCTION

At the 1990 meeting of the Comité Consultatif de Photométrie et Radiométrie (CCPR) it was decided that an international comparison of spectral responsivity<sup>1</sup> should be carried out by the BIPM.

It was agreed to use windowed silicon photodiodes with incoherent radiation in the wavelength range from 250 nm to 1000 nm.

The protocol of the comparison was drawn up by a working group consisting of NPL, PTB and the BIPM. The aim was to prepare a final report, (this report) by June 1994 so that it could be discussed at the following CCPR meeting planned for September 1994.

## PARTICIPATING LABORATORIES

All member laboratories of the CCPR were invited to participate in this comparison. Fifteen responded to a questionnaire and fourteen finally agreed to participate. These are (in alphabetical order of their acronyms<sup>2</sup>):

CSIR	South-Africa
CSIRO	Australia
CSMU	Czechoslovakia
ETL	Japan
INM	France
IRL	New Zealand
KRISS	Korea (Rep. of)
NIM	China
NIST	USA
NPL	Great Britain
NRC	Canada
OMH	Hungary
PTB	Germany
VNIIOFI	Russia

**Table 1:** List of participants in the first round of the comparison.

The VNIIOFI did not receive the original invitation and heard about the comparison rather later. It was able to participate however, using a spare set of detectors which

<sup>1</sup>The spectral responsivity (or spectral sensitivity)  $S(\lambda)$  is defined as the quotient of the detector output  $dY(\lambda)$  by the monochromatic detector input  $dX_e(\lambda) = X_{e,\lambda}(\lambda) d\lambda$  in the wavelength interval  $d\lambda$  as a function of the wavelength  $\lambda$  [1]. For silicon photodiodes, which is the case in this report, the spectral responsivity is expressed in A/W as a function of wavelength.

<sup>2</sup>A list of acronyms can be found in appendix B

had been retained by the BIPM. Consequently its time schedule was different from that of the other laboratories in the first round.

When the comparison was already well under way, four other laboratories expressed their interest in participating. In the absence of spare detector sets, it was decided that these laboratories would receive detector sets returned to the BIPM after measurement at other laboratories. They are:

IENGF	Italy
IOM	Spain
SP	Sweden
VSL	Netherlands

**Table 2:** List of second round participants.

The results of the comparison for the participants of the second round will be discussed in a supplement to this report, available in the middle of 1994.

### ***TIME SCHEDULE FOR THE COMPARISON***

The photodiodes for use during the comparison were purchased in November 1991 and measurements on them began in March 1992. The detector sets were dispatched to laboratories at the beginning of July 1992. The laboratories were given five months to calibrate the detectors and return them to the BIPM, the deadline being the 1 December 1992. The last of the detector sets was in fact returned to the BIPM in March 1993. The second round of measurements at the BIPM finished in the Spring of 1993 which allowed four of the sets to be sent to the second round laboratories in April 1993. Again, five months were given to measure the detectors, their return to the BIPM being scheduled for 1 October 1993.

### ***PILOT COMPARISON***

Before the main comparison began, to check the BIPM facilities and methods of measurement, a pilot comparison was performed between the NPL and the PTB. This pilot comparison, using four photodiodes of exactly the same type as for the main comparison, gave satisfactory results so that the main comparison could go ahead without procedural changes. The results of this pilot comparison are not discussed here, as they are very similar to those of the main comparison.

## DETECTOR SETS

Fifteen detector sets were prepared at the BIPM. Each set comprised three Hamamatsu S1337-1010BQ silicon photodiodes (10x10 mm, quartz window) and one trap detector of BIPM design. The detectors were shipped in a wooden box equipped with a shock absorbing compartment for each detector. Each set also included a cable fitted at one end with a connector matching the connectors on the detector housings. This allowed the laboratories to fit the other end with a connector of the type normally used in their measurements. Finally, an alignment device for the trap detector was added to each set.

The photodiodes were mounted on one side of a cylindrical housing with a BR2 connector attached on the opposite site (see Fig.1). A protective cap over the active surface of the detector could easily be removed for the measurements.

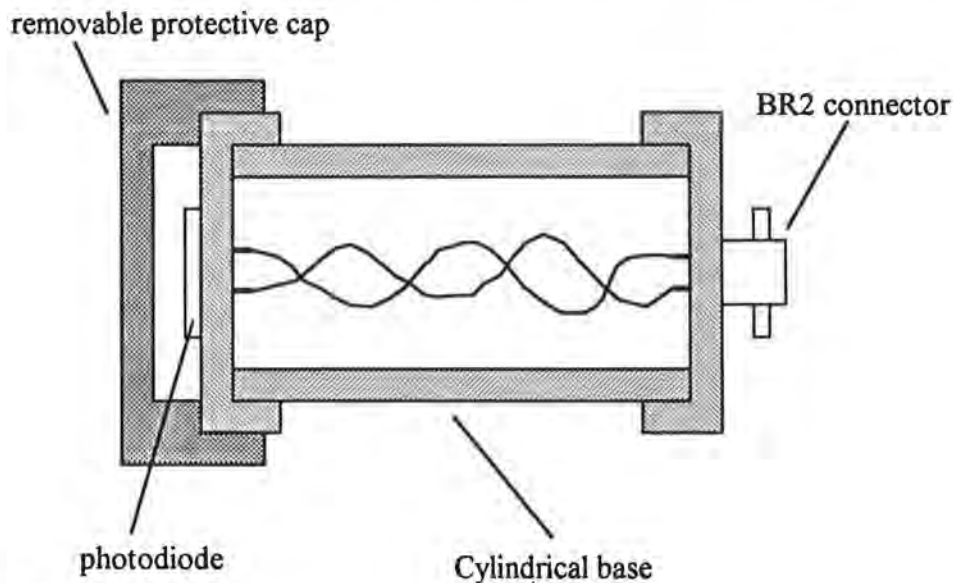


**Fig.1:** The photodiode assembly.

The trap detectors take the form of three photodiodes S1337-1010 N (no window) aligned in such a way that incoming radiation undergoes five specular reflections before leaving the detector. This is shown schematically in Fig.2.

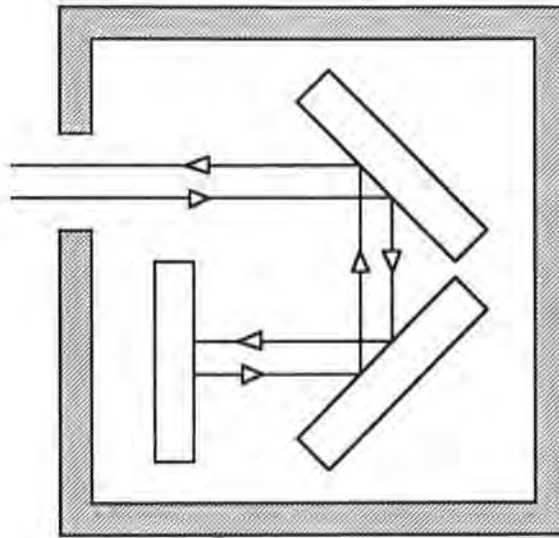


**Fig.2:** Schematic of the trap detector, return beams offset for clarity.

In the practical realization of the device the individual detectors are arranged to lie each in a different plane to reduce any sensitivity to polarization [1] (Fig.3).

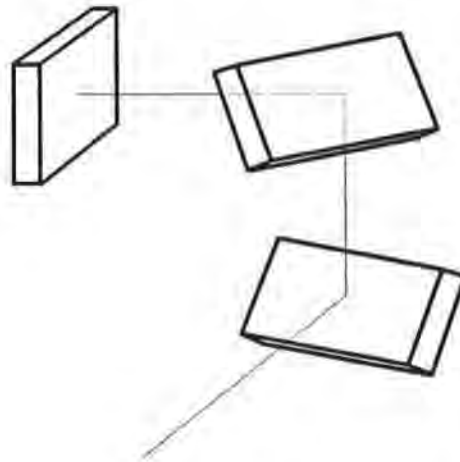


**Fig.3:** Three-dimensional arrangement of the photodiodes in the trap.

To compensate for small misalignments of the photodiodes in their housings, it was found that the last photodiode of each trap had to be adjustable in orientation. This adjustment is made by means of three screws under the diode. The last photodiode of each individual trap was aligned with a laser beam, so that the light returning from the trap was within  $0,5^\circ$  with respect to the incoming beam, when the trap itself had been aligned correctly (see below for the procedure).

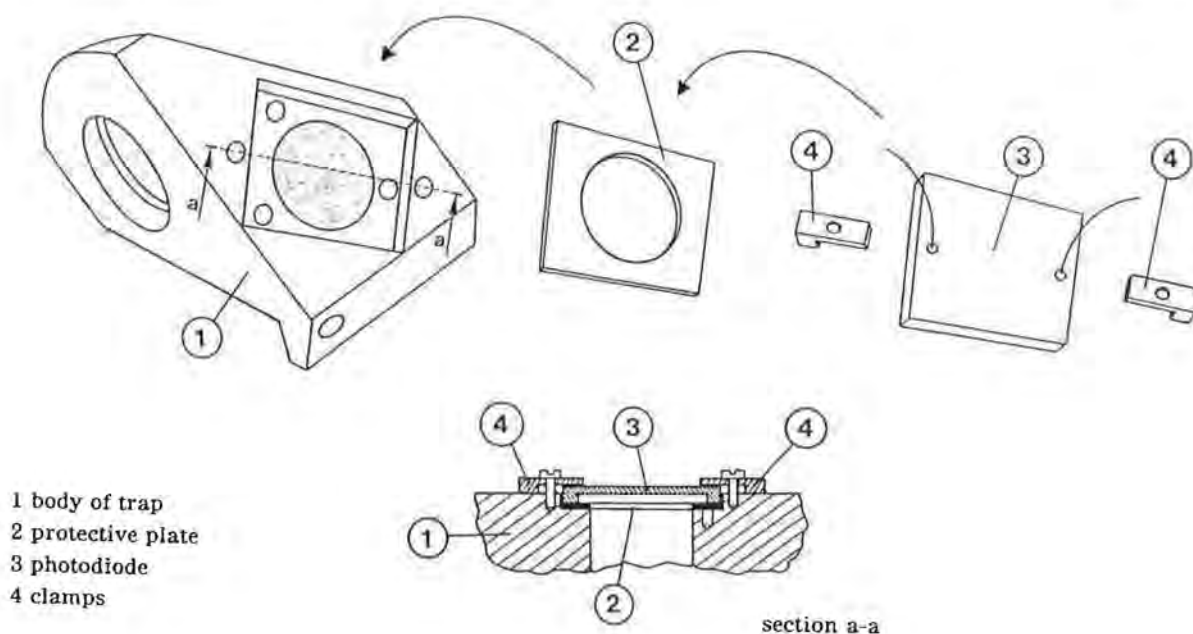


**Fig.4:** Trap assembly drawing 1) body of trap, 2) protective plate, 3) photodiode, 4) clamps.

The alignment of the trap detectors is critical when used with large, non-parallel beams. A comprehensive alignment procedure was explained in the letter accompanying the detectors and is as follows:

The reference surface is the front surface of the assembly with the dust-cap assembly removed. This surface should be aligned with the help of a mirror to be perpendicular to the beam axis. The trap should then be translated until the optical axis lies in the centre of the entrance opening of the device. For this purpose, a device is supplied with the detector. This can be inserted in the entrance hole of the trap, with the protective cap still removed. A small hole in the device indicates the centre of the optical axis. Once properly aligned, the alignment device is removed and the protective cap can be replaced and opened for measurements by rotating the disk fixed to the cap.

Photodiodes Nos 1 and 2 of the device are turned  $45^\circ$  around the optical axis and tilted another  $45^\circ$ . For this reason the first photodiode appears as shown in Fig.5 when observed from the entrance hole. The (theoretical) maximum beam diameter (parallel beam) for the trap is 8,1 mm.

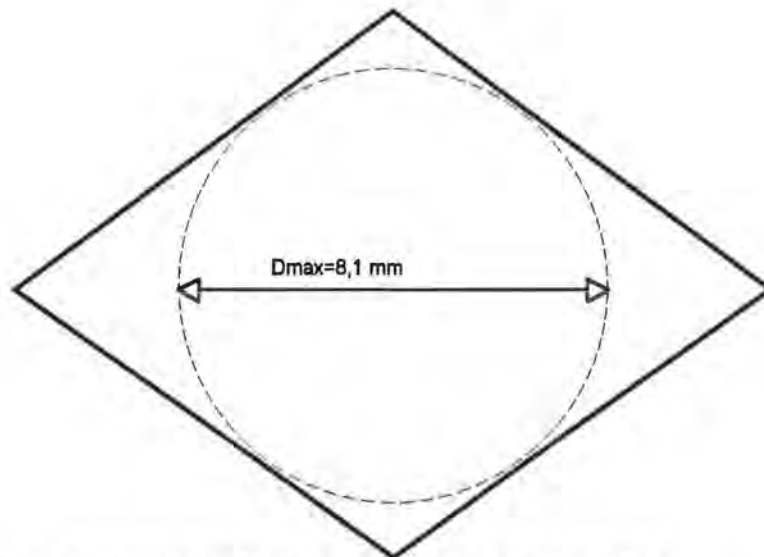
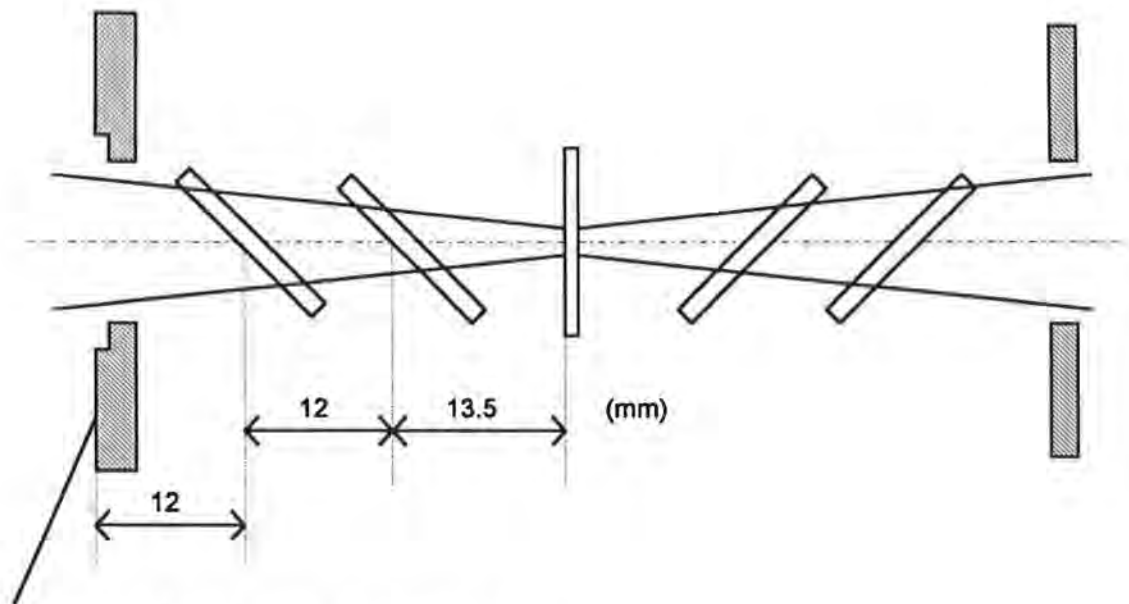


**Fig.5:** View of the first photodiode of the trap as seen from the entrance hole.

Figure 6 shows the optical path inside the trap device, unfolded. From this figure the maximum spot size and beam divergence can be deduced for each individual measurement arrangement (monochromator  $F/\#$  number etc.). The parameters for the measurements with the trap devices at the BIPM were, for example, spot size 3 mm (spot imaged on photodiode No. 3), beam divergence  $4,8^\circ$  full angle.



reference surface when dust-cap removed.

**Fig.6:** Optical path inside the trap.

The housing of each of the original 50 photodiodes for the comparison was marked with the letter  $F$  and a number between 1 and 50. Each of the 15 trap detectors was marked with the letter  $P$  and a number between 1 and 15. The detectors were then grouped in sets in the following way: after measurements of the uniformity of sensitivity of the photodiodes had been made, the five least uniform diodes were

excluded from the lot, leaving 45 detectors divided among 15 sets. The sets themselves were marked 1 to 15 on the wooden box described above. The first photodiode of each set had the same number as the set itself, except for set #15 which had photodiode F16, because F15 had been excluded for reasons described above. The other two photodiodes and the trap detector were assigned randomly to the sets. The sets were then themselves distributed at random to the laboratories. The distribution was as follows:

Batch	diode 1	diode 2	diode 3	trap	laboratory
1	1	42	30	12	INM
2	2	23	41	14	NIM
3	3	35	27	4	NPL
4	4	49	29	2	BIPM
5	5	37	40	6	CSIR
6	6	44	36	8	OMH
7	7	43	31	13	CSIRO
8	8	38	24	9	NRC
9	9	28	48	11	IRL
10	10	34	33	15	CSMU
11	11	25	20	10	KRISS
12	12	18	19	3	NIST
13	13	45	26	7	ETL
14	14	47	39	5	PTB
16	16	32	21	1	VNIIOFI

**Table 3:** Assignment of detectors to the laboratories for the first round.

The four participants in the second round received batches which had been to one of the other laboratories before. These were:

<i>batch</i>	<i>laboratory</i>
3	IENGF
5	SP
7	VSL
9	IOM

**Table 4:** Assignment of detectors to the laboratories for the second round.

### ***PROTOCOL FOR THE COMPARISON***

Following the discussions of the working group the protocol of the comparison was established as follows: In the ultra violet (UV) calibrations were carried out at the following Hg emission line wavelengths:

248,3 nm (or 253,7 for laboratories not using a high-pressure arc)  
 302,2 nm  
 365,5 nm (on the maximum of the group)  
 404,7 nm  
 435,8 nm

Starting from 450,0 nm, wavelengths at regular spacings of 50 nm were used up to 1000 nm making a total of 17 wavelengths. To assist BIPM internal procedures, it was proposed to the laboratories that measurements also be made at the two laser wavelengths 476,24 nm and 647,09 nm using the monochromator.

The following parameters were used at the BIPM and it was recommended that laboratories would work with parameters as close as possible to these, although this was not obligatory.

spot:	circular, 5 mm diameter (except for traps).
max. power:	150 $\mu$ W.
temperature:	(21,5 $\pm$ 0,5) $^{\circ}$ C ,
bandwidth:	3,5 nm approximately
beam divergence:	8 $^{\circ}$ full angle (except for traps).

The surface of the photodiode was aligned to be perpendicular to the optical axis with the spot centred on this surface. All detectors were used without a bias voltage.

### ***EXPERIMENTAL ARRANGEMENT***

The experimental arrangement used at the BIPM for the measurement of relative spectral responsivity is shown in Fig. 7.

Calibrations at wavelengths of 248,3 nm, 302,2 nm, 365,5 nm, 404,7 nm and 435,8 nm were made using the emission lines of a high pressure 200 W mercury arc. The light emerging from the arc was imaged at the entrance slit of the monochromator using a F/3,5 condenser and a lens. Holographic gratings optimised for 280 nm were used for the UV measurements.

Measurements from 450 nm to 1000 nm were made using a 400 W quartz tungsten halogen (QTH) lamp. The filament of the lamp was imaged with unit magnification at the entrance slit of the monochromator. For both arc and QTH sources, the F-number of the incident light and that of the monochromator were closely matched. Ruled

measurements of detector responsivity were made. It is important however for the BIPM absolute spectral responsivity scale.

### SHUNT RESISTANCE

The circuit diagram for the measurement of the shunt resistance is shown in Fig.9.

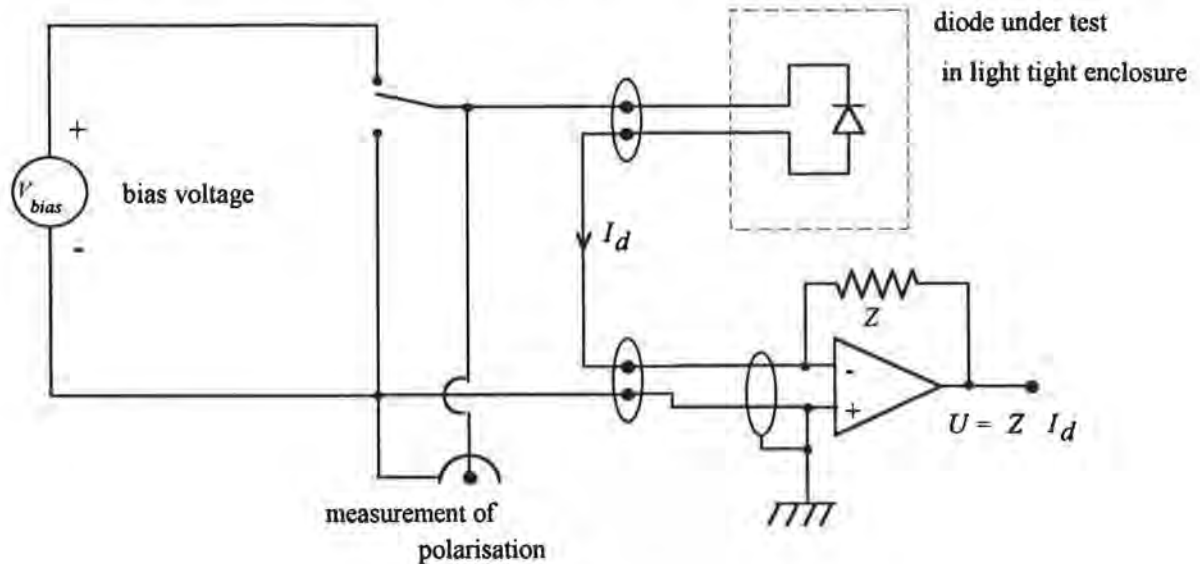


Fig.9: Circuit diagram for the measurement of shunt resistance.

In the photodiode equivalent circuit, the shunt resistance  $R_{sh}$  is the leakage resistance associated with the current generator. A high  $R_{sh}$  value is usually correlated with linear response and good overall performance.

For bias voltages in the range of  $V_{bias} = \pm 10$  mV, the dark-current vs. voltage curve is approximately linear. The slope of the line is the  $1/R_{sh}$  value.  $R_{sh}$  was obtained by measuring the dark current  $I_d$  with a small (-10 mV) bias applied to the photodiode.

$$R_{sh} = \frac{V_{bias}}{I_d}$$

As the current to be measured was very small, a high-gain two-stage amplifier was used, the amplifier's input offset voltage, temperature stability, offset nulling and the influence of bias voltage were checked. The relative uncertainty in the measurement of  $R_{sh}$  was estimated to be 3%.

The average value of  $R_{sh}$  for a test batch of 15 photodiodes at  $(20,5 \pm 0,5$  °C) was 346 M $\Omega$ . The dispersion, estimated by the standard deviation, was 25 M $\Omega$ . The shunt

The uncertainty<sup>3</sup> [3] in the stability of the reference diode due to the instability of air humidity in the laboratory (5%) is estimated to be 4 parts in  $10^5$ . The influence of temperature on the comparison is negligible because the prime reference and the diodes of the comparison are of the same type and have very similar temperature coefficients. The overall drift of the prime reference, as derived from the measurements with the four additional references, is estimated to be zero, but the uncertainty in the knowledge of an eventual drift is about 1,5 parts in  $10^4$ .

### ***RELATED MEASUREMENTS***

A number of related measurements were made on some of the detectors to give a more complete characterization of the ensemble. These included measurements of the temperature coefficient and linearity. They were made over a small sub-sample of the photodiodes used in the international comparison, because of the very small differences of these parameters over the whole set. The measurement of uniformity of the sensitivity over the active surface was also made on a sub-set of the detectors, except for the wavelength of 365 nm, at which the non-uniformity was considerable and all detectors were measured.

### ***AMPLIFIER CALIBRATION***

The four photodiodes mounted on the turntable (see Fig.7) are connected to four amplifiers of the same type. These consist of a current-voltage converter followed by a voltage amplifier. The time constant of the latter is set to 1 second.

The amplifier attached to the reference photodiode is referred to as the reference amplifier. Each of the others was compared to this reference amplifier to obtain a correction factor used to compensate for slight differences in gain. The comparison was made by permutation of the photodiodes connected to the reference amplifier and to the amplifier under test. The procedure was periodically repeated for all amplifiers and all gain settings. The correction factors are very close to 1, with a relative uncertainty estimated at 4 parts in  $10^5$ .

On occasion, the relative calibration was followed by an absolute calibration of the reference amplifier against a current standard. This is a way of checking for any drifts. However, this absolute calibration does not appear in the results, as only relative

---

<sup>3</sup>A table summarising the uncertainties of the comparison of two detectors is given later. All uncertainties stated in this report are relative standard uncertainties (coverage factor  $k=1$ ).

An example showing the stability of the prime reference with respect to one of the additional references is shown in Fig.8. For clarity only three of the wavelengths are shown.

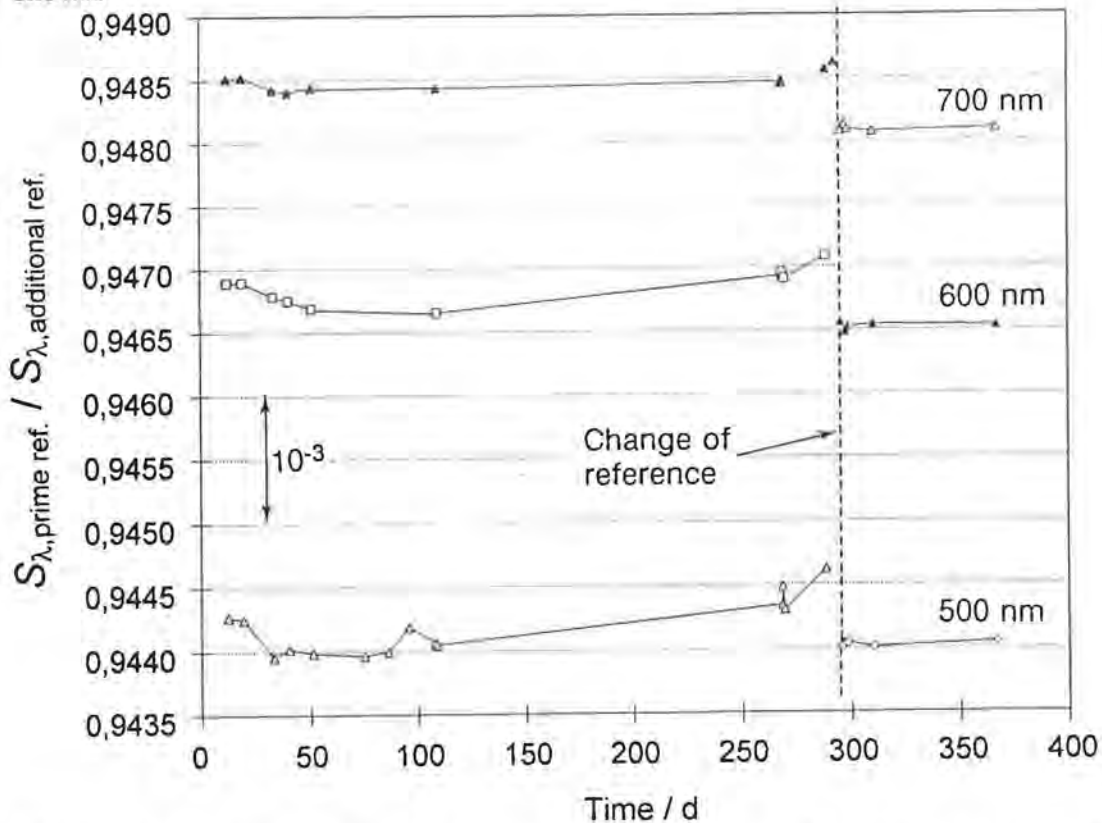


**Fig.8:** Ratio of the output prime reference photodiode to that from one of the additional references for three out of seventeen wavelengths over a period of about one year.

The stability of the prime reference diode checked by comparison with the average of the additional references was initially good (1-2 parts in  $10^4$ ) although a small, but significant drift was present, especially at the shorter wavelengths. It was planned to study this effect at the end of the comparison when the behaviour had been observed over a very long period. Unfortunately however, at the beginning of the repeat measurements after the first detector sets had been returned by the participating laboratories, something happened to the prime reference diode and its responsivity changed significantly by a sudden step of almost 1 part in  $10^3$ . This change was present in the ratios with all the additional references, clearly indicating that the problem was with the prime reference itself. Because it was feared that such a change could happen again, the prime reference was replaced by one of the additional references. The ratio of spectral responsivities between the 'new' prime reference and the 'old' prime reference was known from previous measurements and all the ratios of the diodes in the comparison could be adjusted to the new prime reference without significantly increasing the uncertainties of the data. At the same time, two additional references were added to the set for safety reasons. It was never discovered what had happened to the original prime reference diode. No damage could be observed on visual examination.

The measurement sequence was as follows: for each source the detectors were measured symmetrically first in an ascending and then descending order of wavelengths. At each wavelength the sequence of detectors on the turntable was 'reference' - A B C - C B A - 'reference'. This symmetric scheme corrects for linear source drifts when averaging the signal for each detector and wavelength.

### *METHOD OF THE COMPARISON*

It is of vital importance in a comparison such as this, that a reference scale be maintained at the BIPM over the whole period of the comparison with uncertainties no larger than the estimated uncertainties of the scales to be compared. Fortunately, however, it is not necessary to maintain an absolute scale with these small uncertainties, as this would require the pilot laboratory to maintain a scale better than those of the participants. It was necessary merely to maintain a suitably stable relative spectral responsivity scale over the whole period of the comparison (approximately 3 years).

As a result of the experience with detectors gained at the BIPM since 1988 it was decided that all the photodiodes of the comparison should be compared with a photodiode (hereafter called the 'prime reference') and that the stability of this reference should be checked regularly against a set of three additional reference diodes at all wavelengths used in the comparison.

The photodiode used as prime reference was of the same type as those in the comparison, except that it was windowless and had served at the BIPM for a number of years. This decision was taken, because the behaviour of windowed photodiodes over such a long period and at such small uncertainties was not known sufficiently well at the start of the comparison, whereas the stability of windowless photodiodes under carefully controlled environmental conditions had previously been demonstrated at the BIPM [2]. It was considered that a photodiode which had already served many times was likely to be stable as any ageing should have occurred before the comparison started.

The three additional reference detectors consisted originally of four photodiodes, also of the Hamamatsu S1337-1010 type, two with quartz windows and two without. Later two further photodiodes of this type were added to the set, because of the failure of the prime reference. As an additional check, a QED-200 was used for stability checks.

gratings with a blaze angle optimised for 1000 nm were used for the visible (VIS) and infrared (IR) measurements. After each change of the gratings, the wavelength calibration of the monochromator was checked using low pressure spectral lamps.

Because the BIPM regularly does absolute spectral responsivity measurements at the two Kr laser wavelengths 476,24 nm and 647,09 nm, these wavelengths were included in the measurement scheme. These two wavelengths were measured with both sources (QTH and arc) and matching gratings, in order to provide an overlap between the different sources. No significant difference was found between the measurements made with different sources or gratings.

The monochromator used was a Jobin & Yvon HR2, double grating type with a focal length of 600 mm. The output slit of the monochromator has been replaced by a circular hole of 5 mm diameter (3 mm for the traps). The monochromatic light emerging from the hole was imaged using a slightly inclined spherical mirror onto the detectors. A plane mirror in the path served only to bend the beam. A small part of the beam was diverted by a quartz beam splitter and imaged onto another photodiode referred to as the monitor. The detector to be calibrated and the monitor were connected to different amplifiers and voltmeters and were triggered simultaneously. This method enabled corrections to be made for noise and drift of the source. Additionally, a shutter allowed the measurement of the dark current of the photodiodes and a filter wheel with band-cut filters was used to prevent higher order wavelengths from the monochromator to reach the detectors.

Stray light, i.e. light of different wavelength from that selected with the monochromator, was measured using either a laser as a source in front of the monochromator or using narrow band interference filters. In the latter case measurements were done using the monochromator, first with, and then without an interference filter centered on the monochromator set wavelength. In the double monochromator configuration the stray-light to signal ratio was found to be zero within the uncertainty of the measurement, that is to within 1 part in  $10^5$ .

The three detectors of each set were mounted on a turntable together with another detector which served as a reference for all the detectors of the set. The turntable could be rotated to position the detectors in turn at the image of the output of the monochromator. The whole system was controlled by a personal computer (PC). The PC controlled and read the monochromator wavelength setting, the filter used, the position of the turntable, the shutter drive and the scanning digital voltmeters.

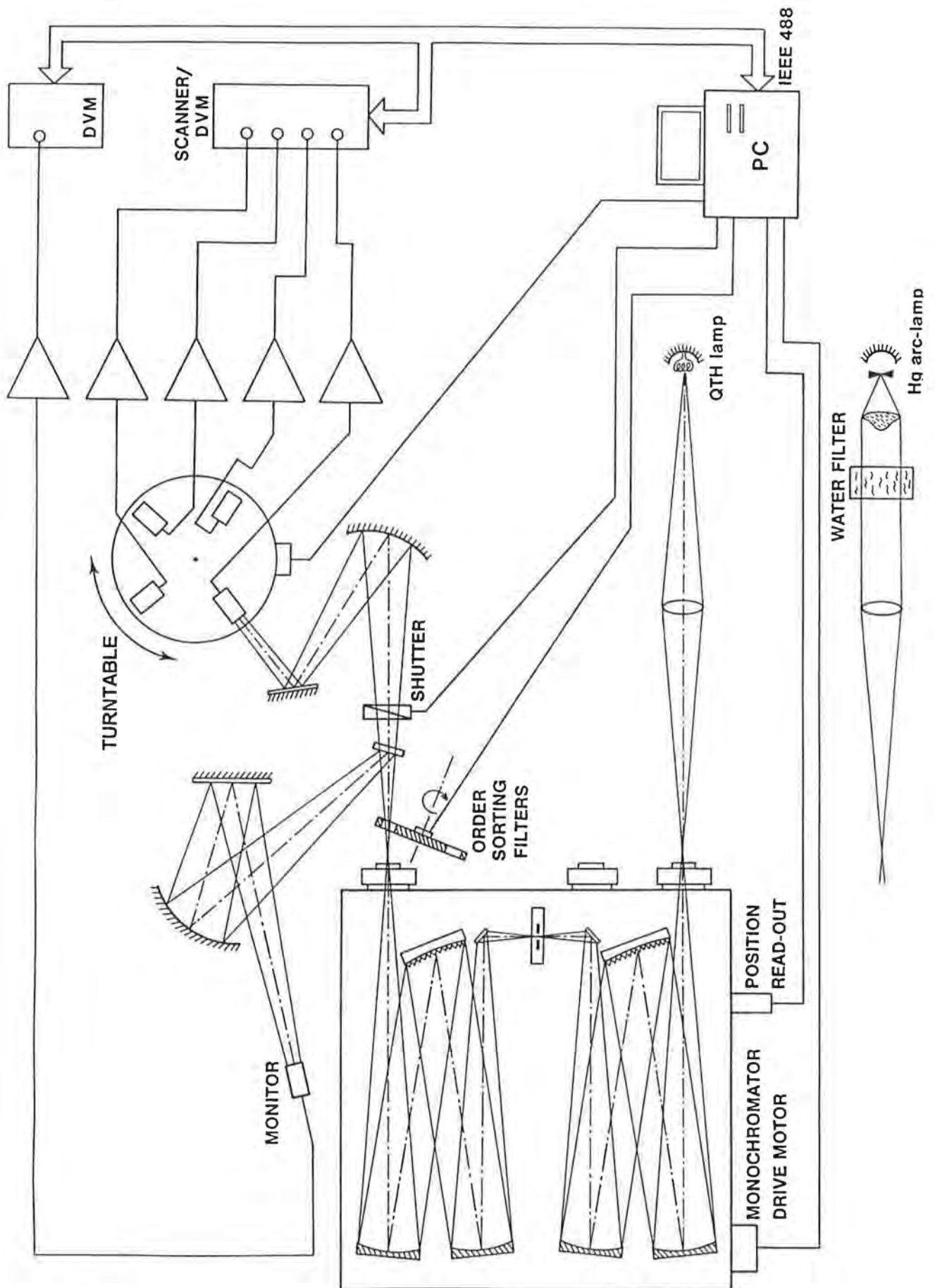


Fig.7: The experimental arrangement for the relative spectral responsivity measurement (not to scale).

resistance of all photodiodes was uniformly high, so that all detectors were judged to be of sufficient quality for use in the comparison.

### LINEARITY

The linearity of the photodiodes was measured using the exit of the single monochromator in order to have a sufficiently high power level (see Fig.10). The output slit of the single monochromator was replaced by a 5 mm diameter circular hole. A beam splitter (BS) close behind this output port divided the radiation into two approximately equal intensity beams. In each beam the output port of the monochromator was imaged using spherical mirrors and plane mirrors to give unit magnification on the detector under test. Each of the two beams could be separately obstructed with a shutter (SH). The signal from the detector was recorded first with only beam 1 incident on it and then with only beam 2. After that, both shutters were opened and the signal was again recorded. Finally, the dark current of the detector was measured with both shutters closed. This was repeated for all wavelengths of interest. The linearity is then defined as:

$$L(\lambda) = \frac{I(\Phi_1 + \Phi_2)}{I(\Phi_1) + I(\Phi_2)}$$

which is unity for a perfectly linear detector.

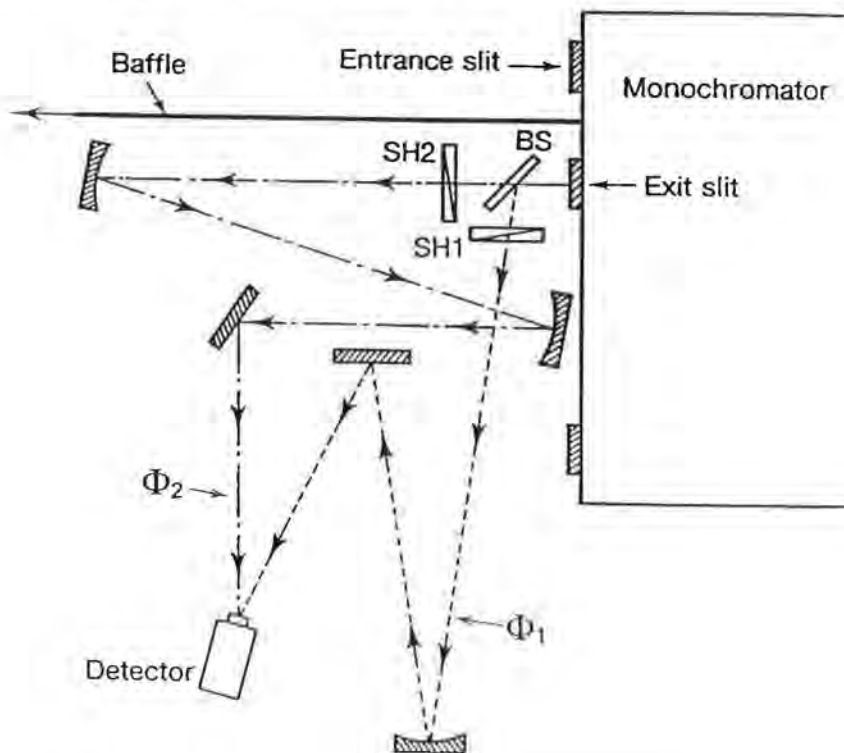


Fig.10: Experimental arrangement of the linearity measurement.

Linearity measurements were made for three wavelengths between 550 nm and 950 nm up to an optical power of 100  $\mu$ W. No deviation from linearity could be detected for any of the detectors within the uncertainties of the measurement ( $<1$  part in  $10^4$ ). This value is consistent with measurements published elsewhere [4]. The noise inherent in the arc measurements did not allow the linearity to be checked in the UV.

The uncertainty on the linearity contributes one additional part in  $10^5$  to the uncertainty in the comparison of two photodiodes.

### **TEMPERATURE COEFFICIENT**

The temperature coefficient of the detectors was measured for a sub-set of detectors at 7 wavelengths. For this, the detector, together with the housing used for normal measurements, was placed inside a copper block through whose walls flowed water at a stabilized temperature (Fig.11). The detector housing was pressed firmly against the inner walls of the copper block to ensure good thermal contact.

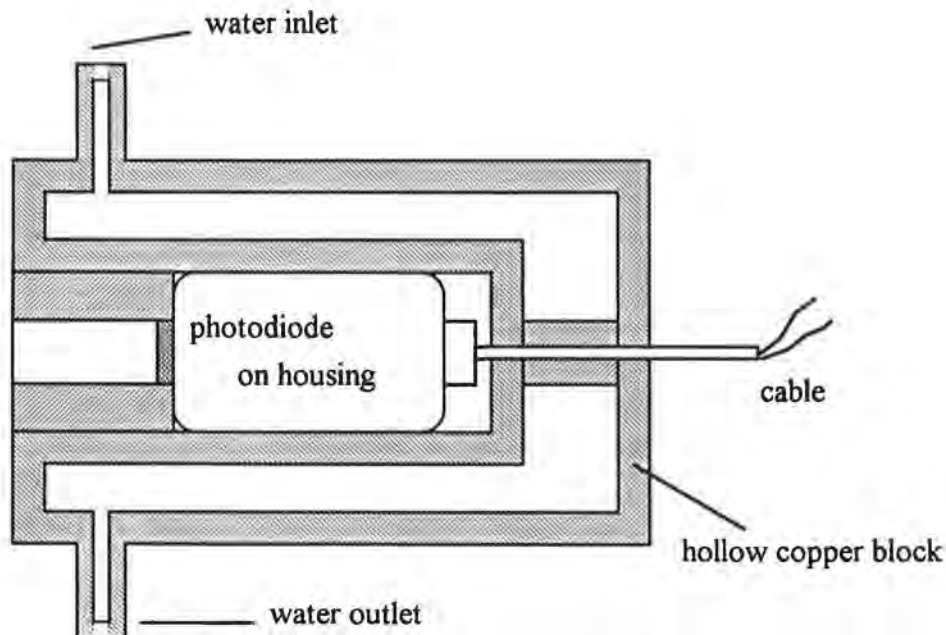


**Fig.11:** Copper block for temperature control of a photodiode to measure its temperature coefficient.

The ratio of the signal of the photodiode to that of the monitor detector (see Fig.7) was recorded over about 30 minutes with the temperature of the water fixed at 20° C. The water temperature was then changed to 30° C and the ratio was again recorded until it stabilized. After this the temperature was again set to 20° C (Fig. 12).

A straight line was fitted as base line through the values at 20° C to correct for drift. (Note that the drift between the first and the second sequence of points corresponding

to 20° C is of order of one part in  $10^4$ .) A correction for the slope of the line was then subtracted from all points and the temperature coefficient was calculated from the ratio of the averages of the points corresponding to each temperature.

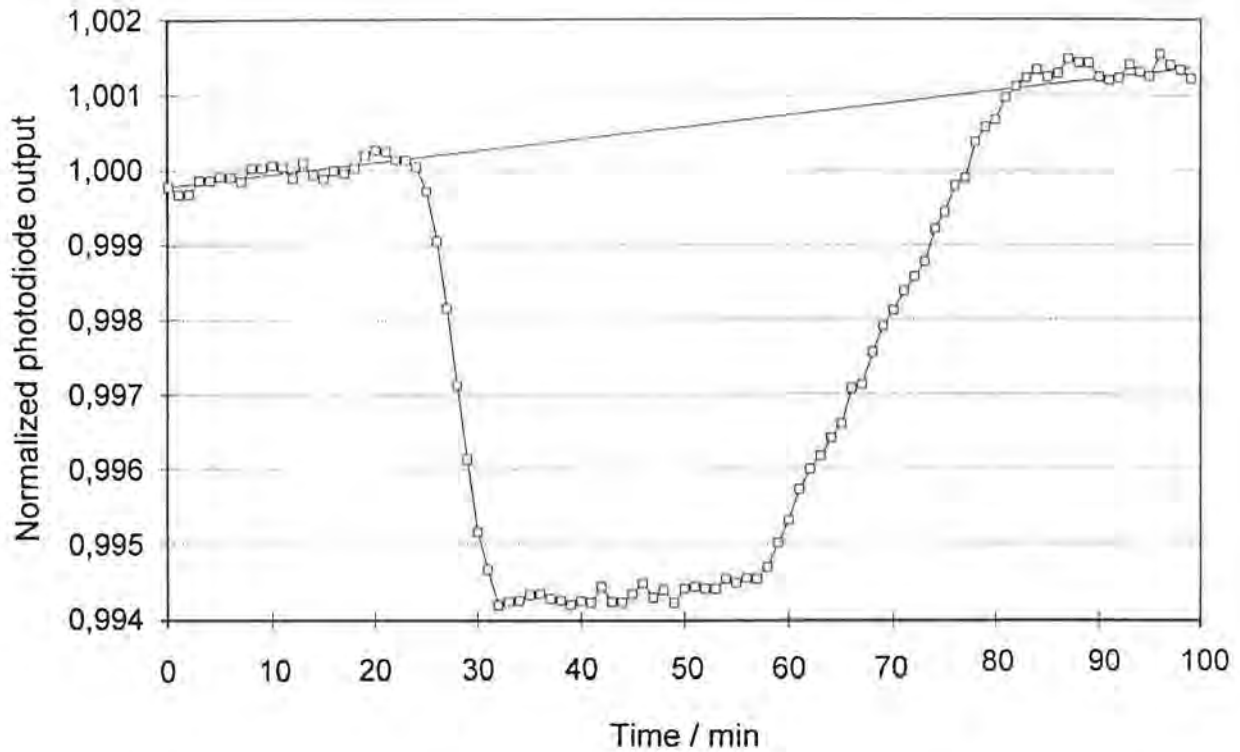


**Fig.12:** Photodiode output current (normalized to average at first temperature), example for 550 nm, temperature originally 20° C, then raised to 30° C and again 20° C. The straight line is a linear fit through the values at 20° C.

This measurement was repeated for 7 wavelengths over the range used in the comparison. The temperature coefficient found is small (generally a few times  $10^{-5}/^{\circ}\text{C}$ ) except for very short and very long wavelengths and particularly for 1000 nm (Fig.13).

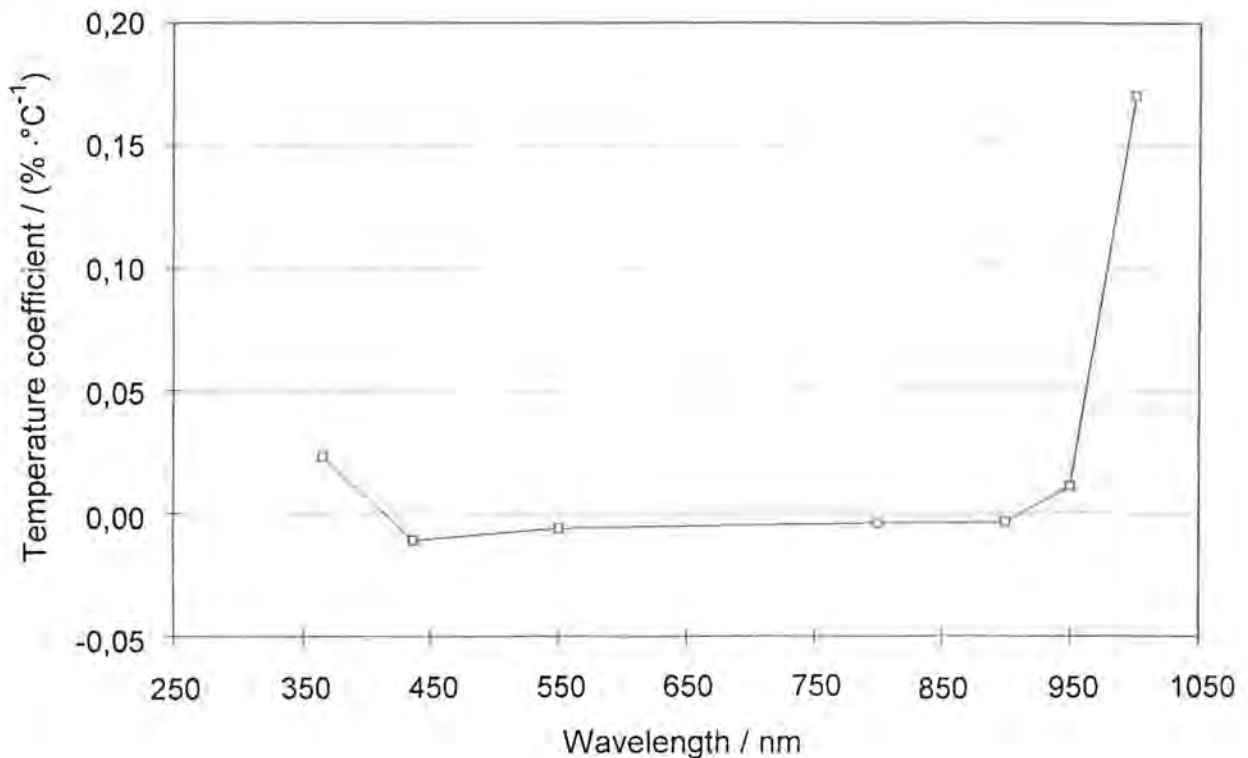


**Fig.13:** Temperature coefficient of the diodes used as a function of wavelength (ratio of photodiode responsivity per degree difference from 20° C).

As the temperature coefficient is small, and is very similar for the reference diode and the detector being measured, the influence of the temperature coefficient on the total uncertainty of the comparison is estimated to be negligible.

## ***UNIFORMITY***

### ***1) PHOTODIODES***

For the measurement of the uniformity of the responsivity of the photodiodes, the output slit of the monochromator was replaced by a hole of approximately 1 mm diameter. This hole was then imaged on the detector, with unit magnification. The detector itself was mounted on two, orthogonal, linear stepper motors controlled by the PC used for the other measurements.

The surface was scanned as follows: before the start of a scan and at the end of each scan, measurements were taken at the geometric center of the detector. These two values were used to correct intermediate data for drift and to normalise the results.

A typical result is shown in Fig. 14, for four different wavelengths. Note that the scales are enlarged to show only the top 2% of the available responsivity, i.e. it shows values above 98%. The same scale is used for all four plots.

Originally it was planned to carry out this measurement only on a sub-set of the batch. The non-uniformity in the UV however, was found to be relatively large (see Fig. 14) and it was decided to measure all photodiodes of the batch at 365.5 nm. From the fifty diodes purchased for the comparison, only forty-five were needed to make the fifteen batches. The worst five photodiodes were subsequently excluded from the comparison.

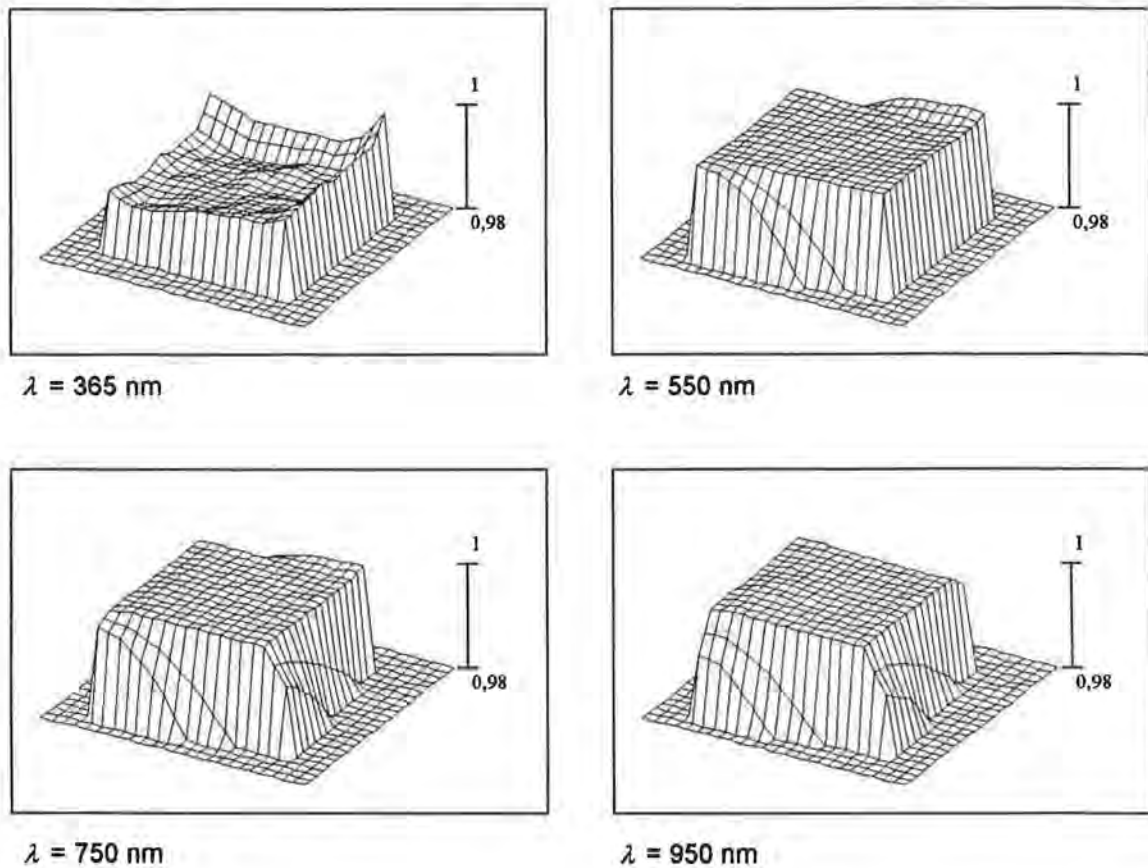


**Fig.14:** Measured uniformity of the spectral responsivity of the photodiodes for different wavelengths. The scale is enlarged to show only the top 2% of the available sensitivity.

The longest wavelength used for that measurement was 950 nm. The uniformity for this wavelength is excellent, as can be seen from Fig. 14. No measurements were made at 1000 nm because the data was expected to be very similar to that found at 950 nm. Later information shows that the photodiodes used in the comparison are very non-uniform at 1000 nm [5].

## 2) TRAP DETECTORS

The uniformity of the trap detector was measured in the same way as for the photodiodes. A typical result for 365,5 nm is shown in Fig.15

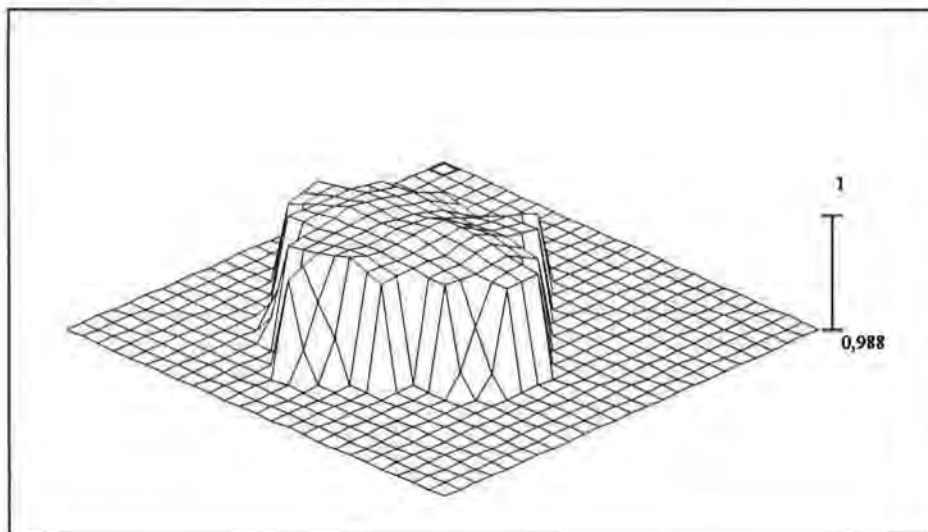


**Fig.15:** Uniformity of sensitivity of the trap detector at 365,5 nm. The scale is enlarged to show only the top 1,2% of the available sensitivity.

## 3) SPOT IMAGED ONTO THE DETECTORS

For the measurement of the intensity distribution in the spot a detector with a small aperture was scanned in front of the beam. The distribution was measured for both the QTH source and the mercury arc for most of the wavelengths used in the comparison. Figure16 shows a typical example for  $\lambda = 700$  nm.

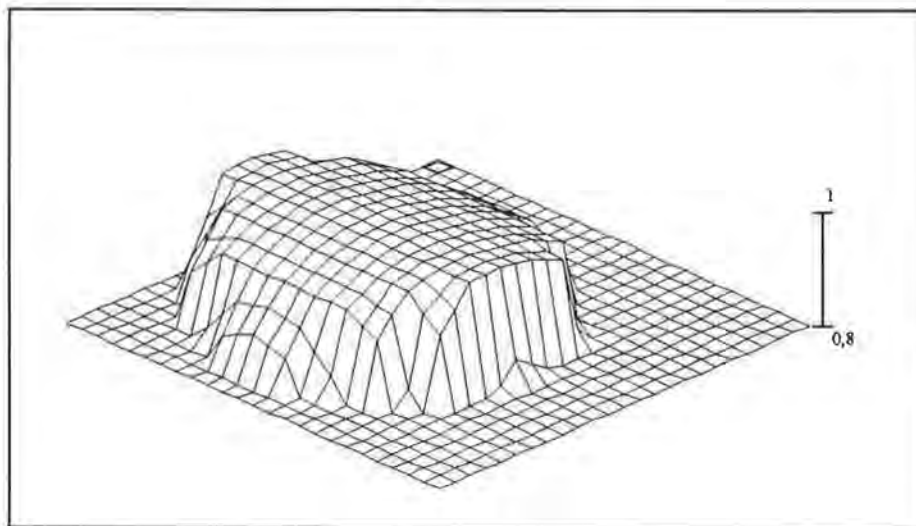


**Fig.16.** Intensity distribution over the spot at  $\lambda=700$  nm (QTH source). The scale is enlarged to show only the top 20% of the available intensity.

### ***UNCERTAINTIES ARISING FROM THE NON-UNIFORMITIES***

Knowledge of the intensity distribution in the spot and of the uniformity of the detectors allowed calculation of the influence of detector re-positioning on the repeatability of the measurements. The size of this influence, estimated by a simulation program, was confirmed experimentally on a subset of traps and photodiodes by measuring the relative variations of signal output as a function of detector displacement. As a result, it was estimated that an uncertainty in the detector position of 0,2 mm contributes additional uncertainties of 4 parts in  $10^5$  to the relative uncertainties in the sensitivity measurements in the visible and IR regions, and 8 parts in  $10^4$  in the UV region.

The uncertainty due to the use of a non-uniform spot was estimated using the same type of simulation program that was used to examine the non-uniformity of the sensitivity.

### ***MONOCHROMATOR***

The bandwidth of the double monochromator depends slightly on wavelength and has been measured, using low pressure spectral lamps or lasers, to be about 3,5 nm.

The accuracy of the wavelength calibration of the monochromator was estimated to be 0,15 nm, the wavelength repeatability being 0,05 nm. As the spectral responsivities of the photodiodes and the reference are very similar, these uncertainties when combined contribute 2 parts in  $10^6$  to the total uncertainty of the comparison.

### ***SUMMARY OF UNCERTAINTIES OF THE COMPARISON***

The uncertainties of the comparison of relative spectral responsivity, as developed in the preceding sections, are summarised in Table 5.

WAVELENGTH AND SOURCE TYPE	$\lambda = 365,5 \text{ nm}$ (source: Hg arc)		$\lambda = 650 \text{ nm}$ (source: QTH)	
	type A	type B	type A	type B
	$10^4 \times$ Relative uncertainty			
<b>NON UNIFORMITY OF SENSITIVITY (*):</b>				
position diode ( $\pm 0,2 \text{ mm}$ )		0,7		0,3
position reference diode ( $\pm 0,2 \text{ mm}$ )		0,4		0,2
<b>NON UNIFORMITY OVER THE SPOT (*):</b>		0,4		0,0
<b>NON LINEARITY OF DETECTORS:</b>		0,1		0,1
<b>STABILITY OF REFERENCE:</b>				
humidity (5% relative)		0,37		0,37
correction of long term drift		1,5		1,5
<b>TEMPERATURE:</b>		0,0		0,0
<b>CALIBRATION OF AMPLIFIERS:</b>		0,4		0,4
<b>MONOCHROMATOR (*):</b>				
wavelength calibration (0,15 nm) and wavelength repeatability (0,03 nm)		0,04		0,02
stray light		0,0		0,0
<b>SOURCE (*):</b>				
short term instabilities	1,0		0,3	
<b>COMBINED (A and B) (*)</b>	<b>2,1</b>		<b>1,7</b>	

**Table 5.** Uncertainties for the comparison of relative spectral responsivities of the detectors in parts of  $10^4$  ( $1 \sigma$ ) for the two different sources used during the comparison. Values marked with a (\*) are wavelength dependent and typical values are given here.

Table 5 specifies the uncertainty budget at two wavelengths: the overall estimated spectral dependence of the uncertainties is given in Table 6.

wavelength /nm	$10^4 \times$ Relative uncertainty
248	10
302.2	5
365.5	2,1
404.2	2,1
450 - 950	1,7
1000	2,5

**Table 6.** Spectral dependence of the uncertainties for the comparison of two detectors.

A verification of the estimation of some of these uncertainties (short term instabilities, diode and monochromator repositioning) can be obtained by analysing the results of series of measurements on the same detectors. In Figure 17 the relative standard deviation of measurements of relative spectral responsivity for four detectors are

shown as a function of wavelength. Here a subset of four diodes has been measured several times over a period of 5 months using both sources.

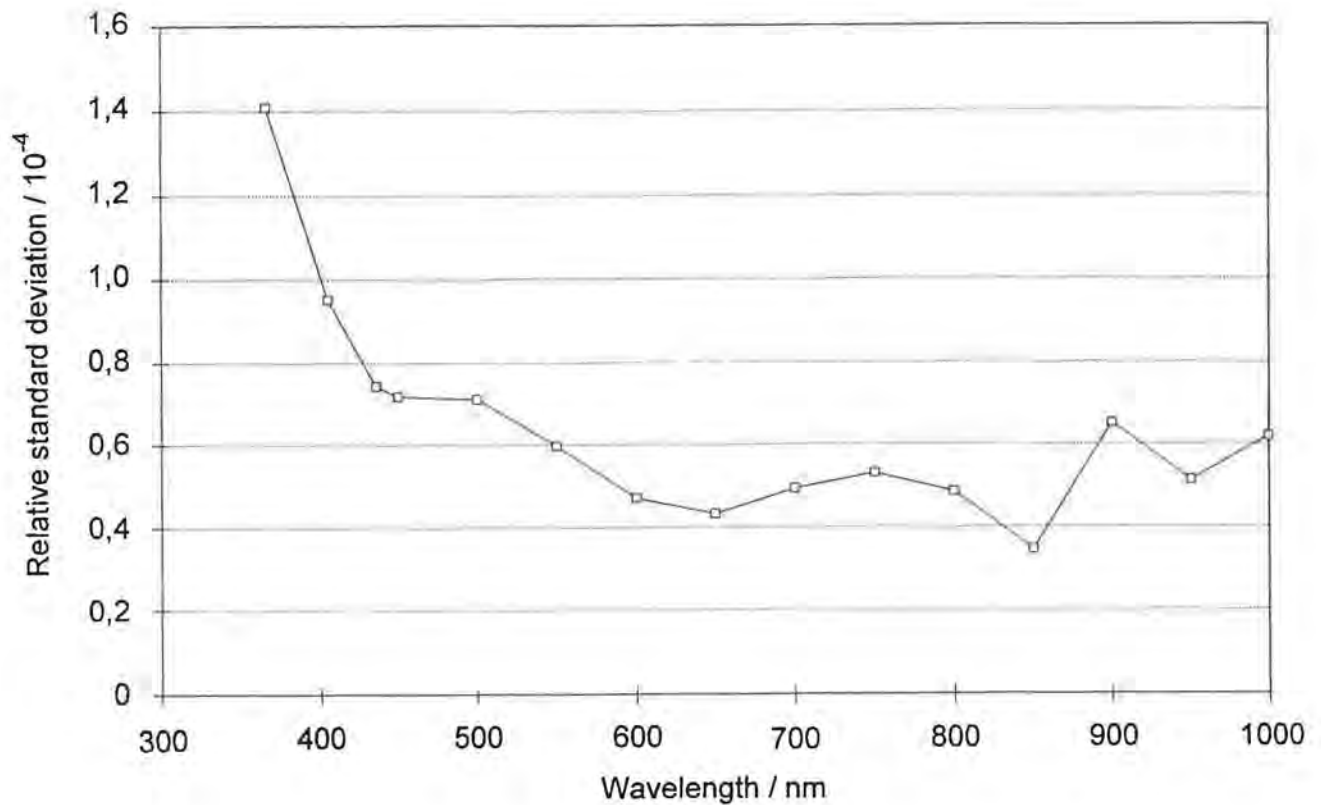


**Fig.17:** Relative standard deviation of measurements on a set of photodiodes over a period of five months at the BIPM (see text).

### ***UNCERTAINTIES IN THE ABSOLUTE SCALES***

It is interesting to compare the uncertainties for the relative spectral responsivity measurements (diode-diode comparisons) from Table 5 and Fig.17 with the uncertainties of absolute spectral responsivities of the same detectors as given by the other laboratories (Fig.18).

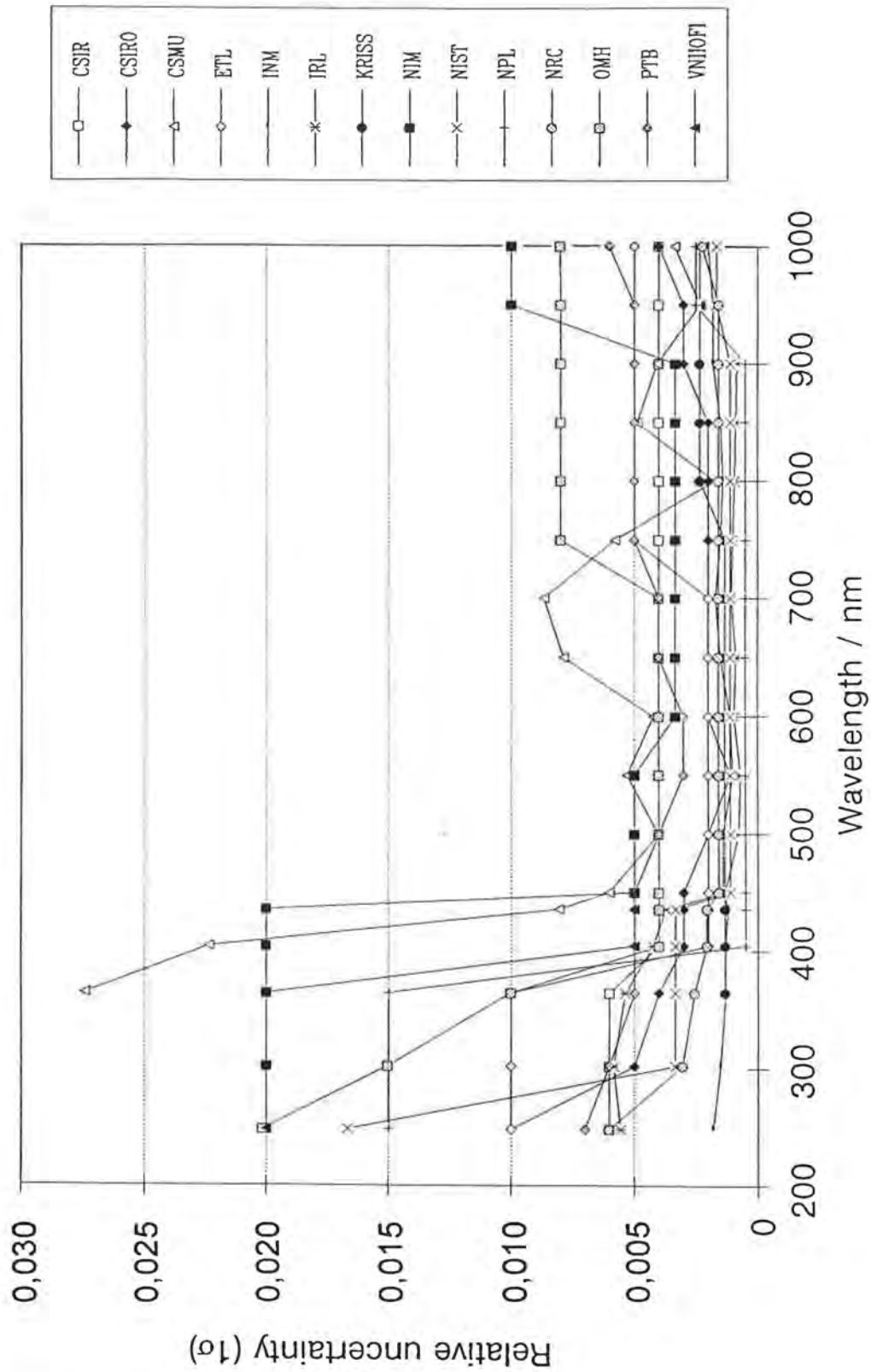


**Fig.18:** Relative uncertainties of the absolute spectral responsivity measurements as a function of wavelength, as stated by the participating laboratories.

It can be seen that the absolute scales of the laboratories can be compared at the BIPM with uncertainties that are generally smaller by a factor of ten than the uncertainties with which the scales are themselves defined. This is a very satisfactory situation.

### *MEASUREMENT OF RELATIVE SPECTRAL RESPONSIVITY*

After completion of the measurements described above, the quartz window of each detector was cleaned using optical lens cleaning paper and ethanol. A week was allowed for the detectors' responsivities to stabilise, before the responsivity measurements began. From then on the detectors were cleaned only by blowing dry, dust-free air over their surfaces. It was suggested that the participants also clean the detectors only with dry air.

The spectral responsivity of each detector was measured twice relative to the reference detector with the QTH source in the visible and near IR. Figure 19 shows the ratio of the responsivities as a function of wavelength, measured in two different runs using the same detectors. The measurements for each detector were made at intervals of two weeks and the detectors were placed at different positions on the turntable for each run. The maximum difference in responsivity found between the two runs does not exceed  $\pm 1$  part in  $10^4$  with a standard deviation of 4,7 parts in  $10^5$ , showing the excellent repeatability of the measurements and the stability of the detectors.

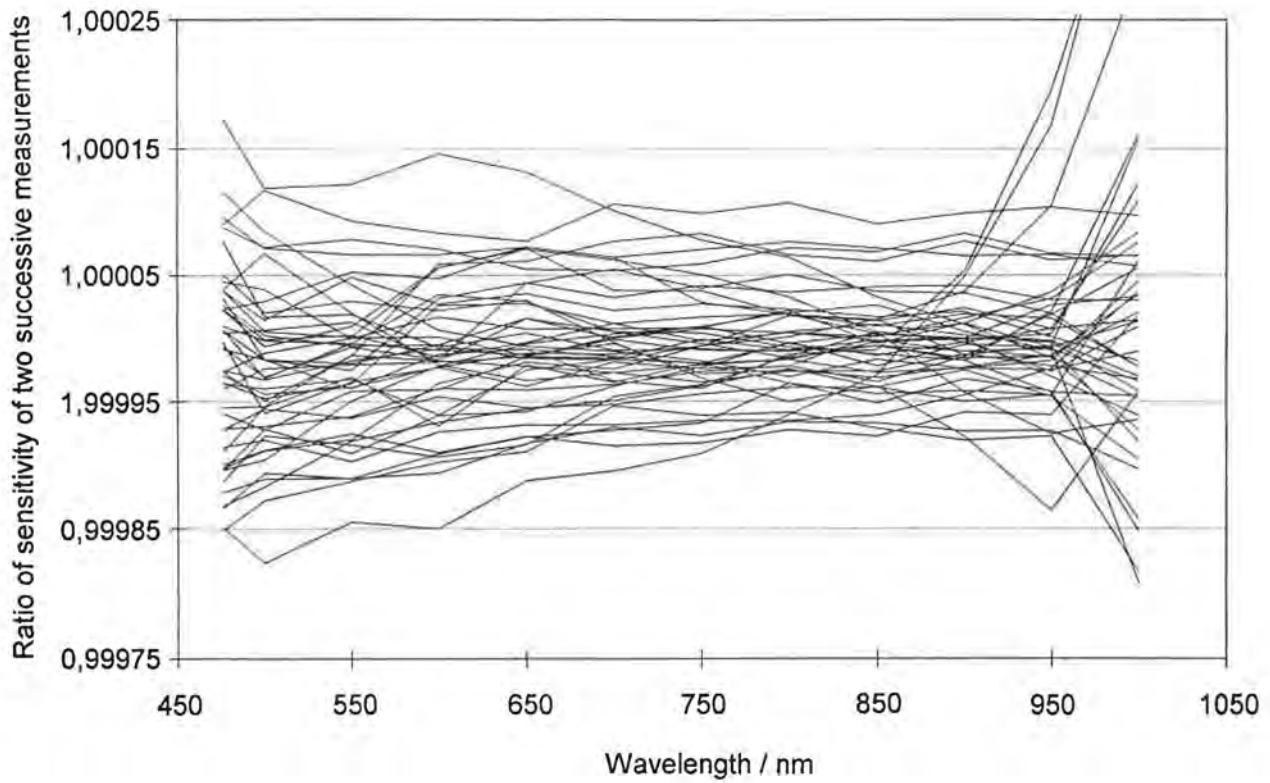


**Fig.19:** Ratio of sensitivities measured with an interval of two weeks using the QTH lamp.

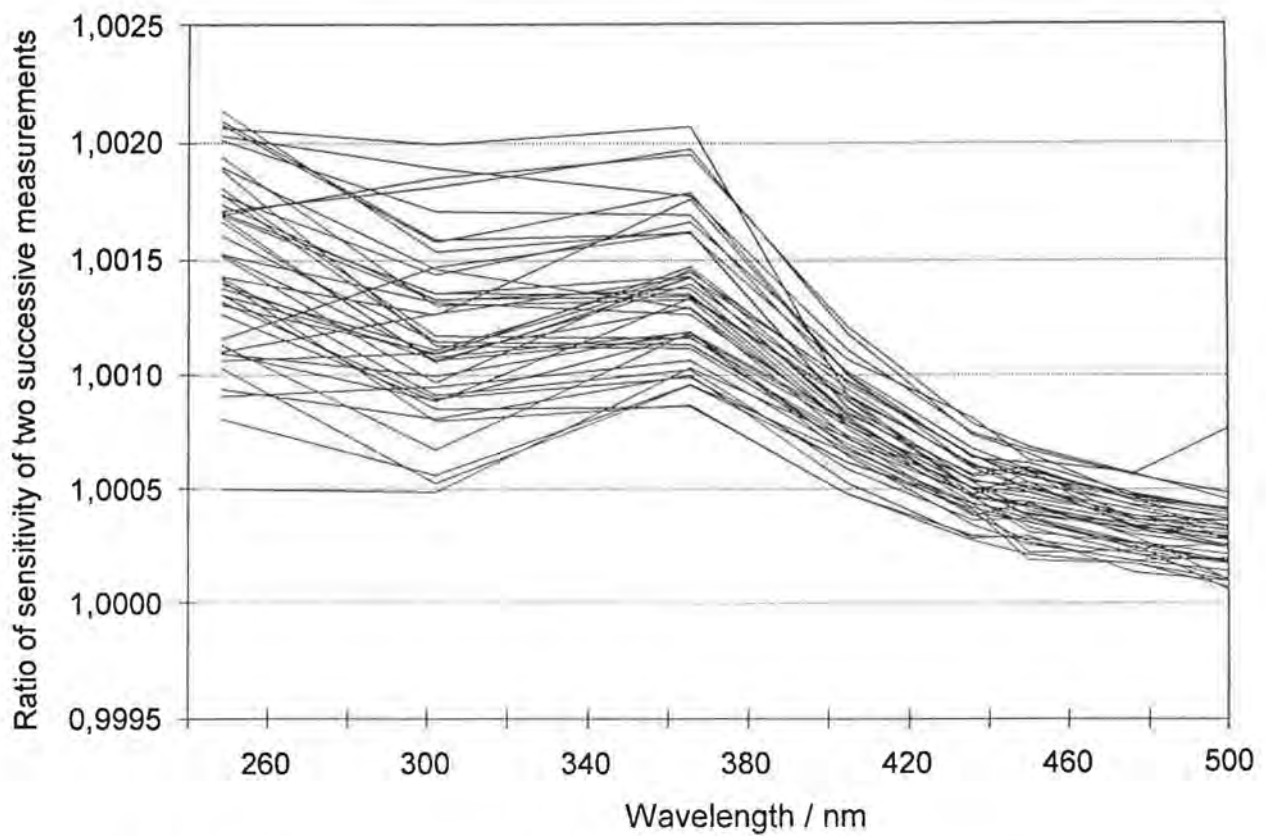


**Fig.20:** Ratio of sensitivities measured with an interval of two weeks using the arc lamp.

After the measurements with the QTH, the detectors were measured twice in the UV. The values found during the two arc measurements were quite different from one another. Their ratio is shown in Fig.20. Two independent effects can be observed:

1. A systematic structure is common to all photodiodes when the responsivities measured during the second calibration are compared with those obtained during the first. This indicates an ageing effect due to passage in front of the UV beam.
2. The over-all distribution around that systematic structure is more spread out than the noise in the QTH measurements. The diodes probably do not all age in the same way. Furthermore, the noise inherent in the arc has not been completely compensated by the monitor.

The change in spectral responsivity observed after the arc measurements was judged to be too large for the comparison, and it was decided to investigate the problem further (see next chapter) and then to repeat the measurements with the QTH lamp for all the photodiodes. However, it was found that the behaviour of all the detectors was very similar and only half of them were re-measured over the whole range from 450 nm to 1000 nm. From Fig.21 it can be seen that the change declines as a function of wavelength in a quasi-exponential way up to about 700 nm, beyond which it was no longer significant. For this reason it was decided that it was sufficient to measure the second half of the set of detectors only up to 700 nm.

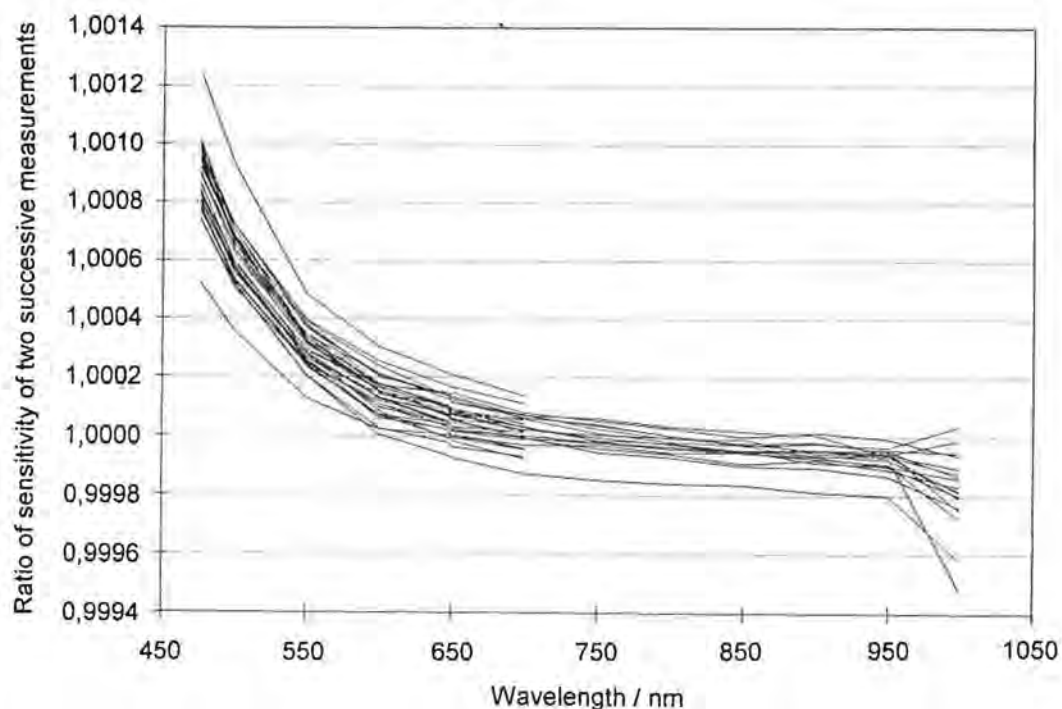


**Fig.21:** Evolution of the QTH measurements after passing the diodes in front of the arc.

### ***EFFECTS OF UV RADIATION***

The curious behaviour of the diodes after exposure to UV was investigated further. A number of photodiodes were measured several times using the Hg arc lamp and their change in sensitivity was recorded. During these measurements, the additional reference detectors showed a stable behaviour compared to the prime reference diode.

Further experiments showed that, for the whole set, sensitivity slightly decreased (1 to  $2 \cdot 10^{-4}$ ) for wavelengths above 600 nm, but increased (up to  $2,5 \cdot 10^{-3}$ ) for shorter wavelengths. Sensitivity changes immediately after UV exposure, as can be seen in Fig.22, but reaches a new stable value after two series. Each series needs an 80 second exposure per point, leading to a total of 320 seconds per series.

As the stability of the new values seemed to be compatible with the estimated uncertainties in the UV region, it was decided to keep the values obtained in the last UV run, and to repeat all the comparisons in the 450 nm - 1000 nm range as described above.

These earlier measurements were made before the UV measurements of the trap detectors started, which allowed some checks before starting the series. The effect of UV on trap detectors is of the same magnitude as that for the photodiodes. Figure 23 shows a typical trap behaviour: the values are normalised to the results of the first UV run.

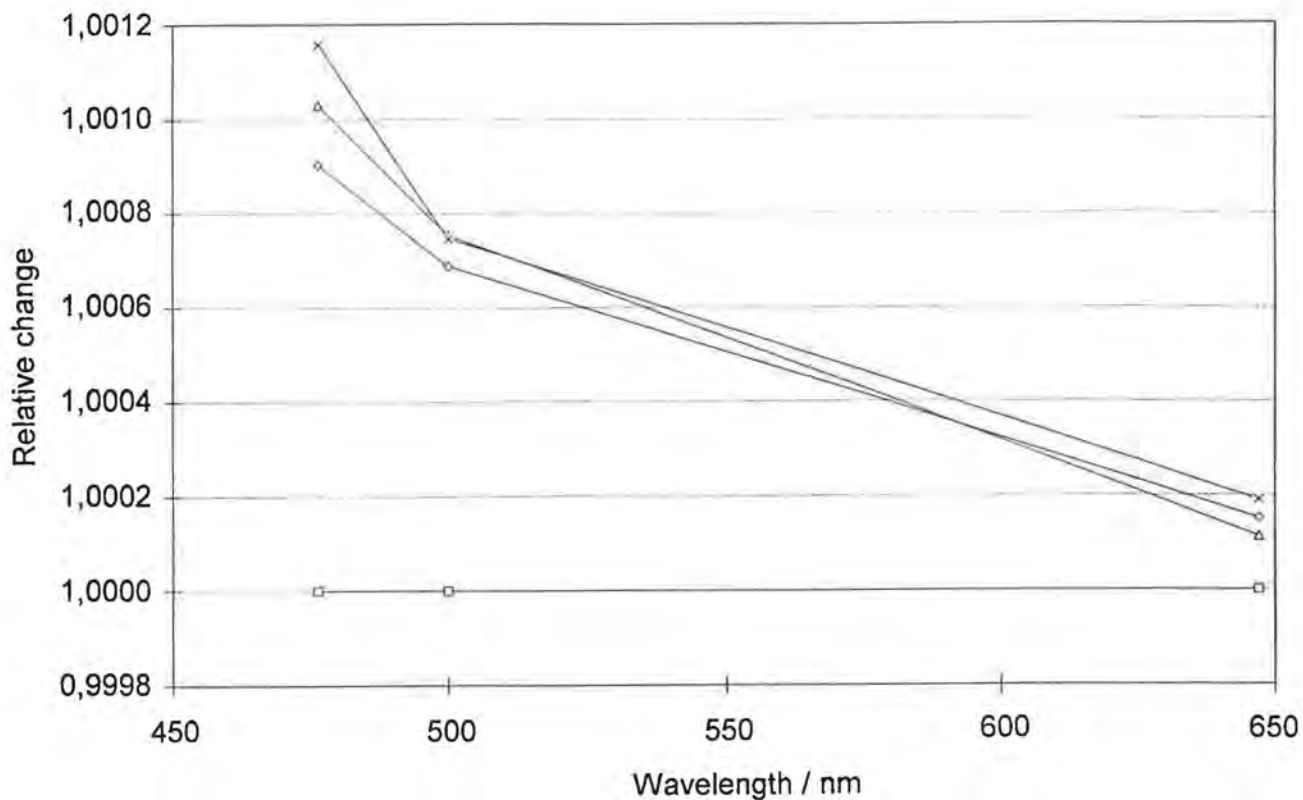


**Fig.22:** Relative change in spectral sensitivity after exposure to UV (diodes). *Squares:* First measurement (before UV exposure, normalized to unity), *Diamonds, Triangles, Crosses:* successive measurements normalized to first one.

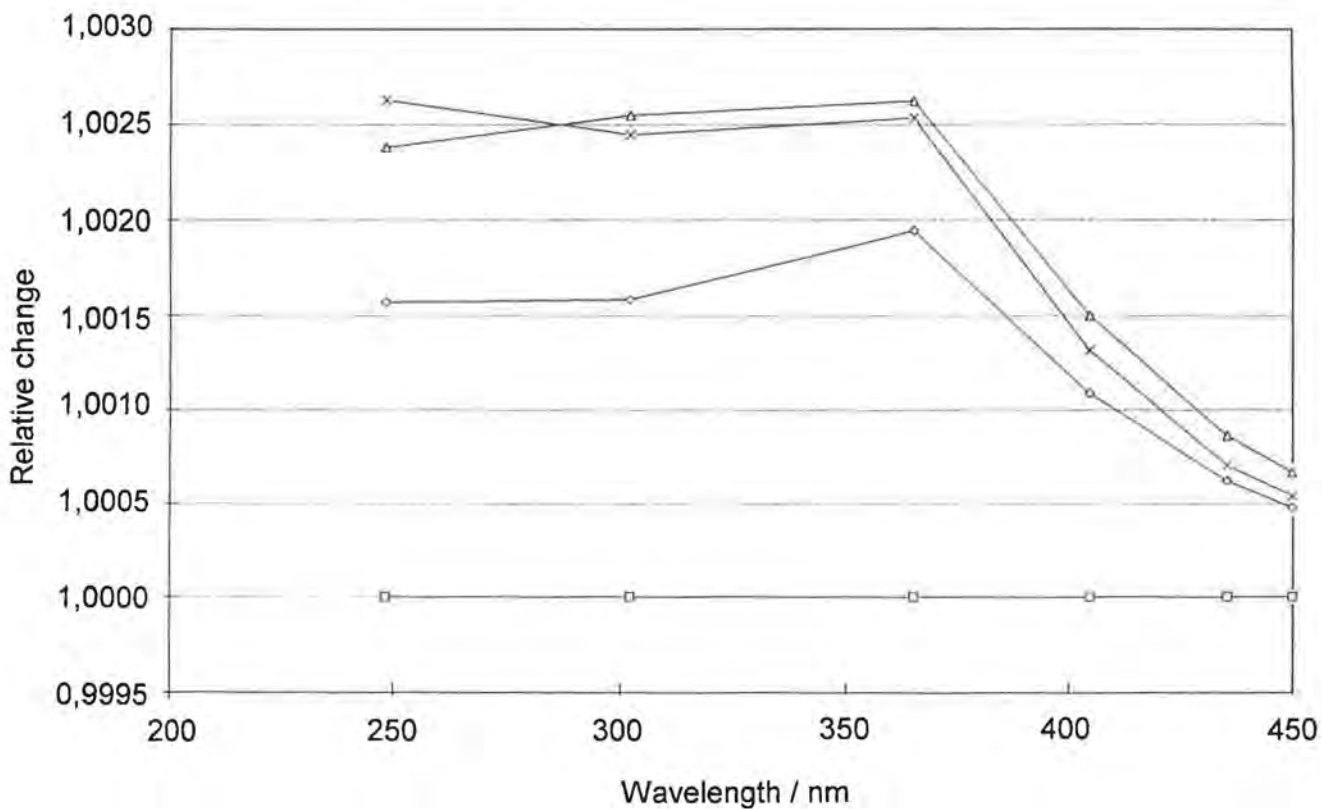


**Fig.23:** Relative change in spectral sensitivity after exposure to UV (traps). *Squares:* First measurement (first UV exposure, normalized to unity), *Diamonds, Triangles, Crosses:* successive measurements normalized to first one.

As a consequence, it was decided to "age" the traps by exposing them to UV radiation: 248 nm (15  $\mu$ W) and 302 nm (130  $\mu$ W), 200 seconds each time. Measurements were then made in the UV and the visible and IR measurements were repeated.

This UV-effect seems to be related to the age of the photodiodes. The BIPM additional reference diodes are insensitive to it, and we also tested photodiodes of the same type (with and without windows), taken from a batch four years older. They were used in the visible but never exposed to UV, and exhibited negligible variations after UV exposure.

Complementary experiments were made with traps and with windowless photodiodes taken from the batch used to build the traps. They indicate that the origin of these variations lies in the modification of the internal quantum efficiency rather than in a change of reflectivity.

### ***MEASUREMENTS AFTER RETURN OF THE DETECTORS***

All detectors were measured again after their return to the BIPM, with both QTH and Hg arc lamps in exactly the same way as they had been measured before they left the BIPM. Each batch was re-measured as soon as possible after its return. More than three months elapsed between the return of the first and the last detector sets and, as an additional check on drift, the first set returned was re-measured several times along with newly returned batches and the batch been retained at the BIPM throughout the comparison.

All the photodiodes aged between the last measurements before they left the BIPM and the first measurements after their return (Fig.24). The drift however, is uniform within the batch, except in the UV.

The trap detectors were much more stable during their absence from the BIPM. All were very stable except for the trap which had been to the NIM. It is not known what has happened to this trap. No measurement results for it were communicated to the BIPM. On visual inspection it seemed to be undamaged.

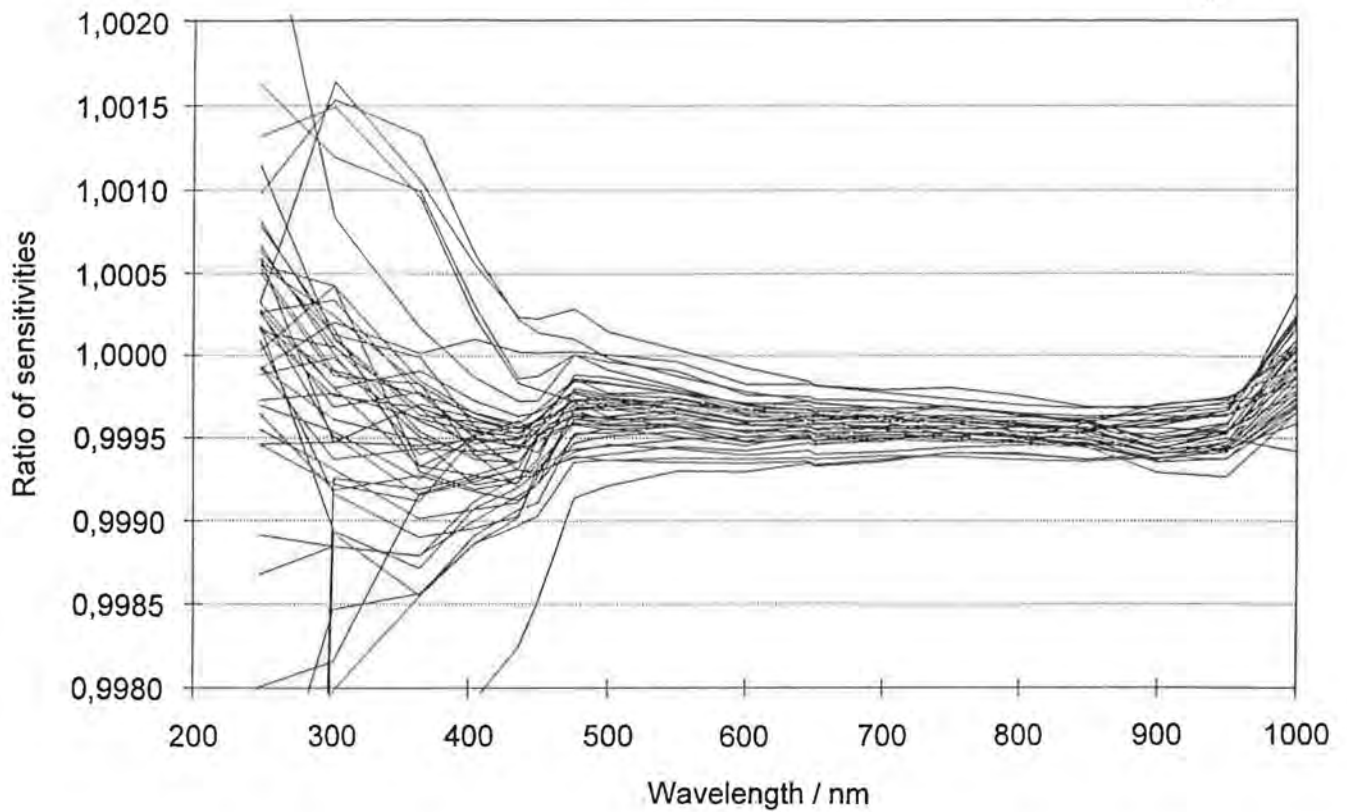


**Fig.24:** Change in spectral responsivity of diodes: Ratio of diode sensitivity after return from the participant to that found before sending to participant.

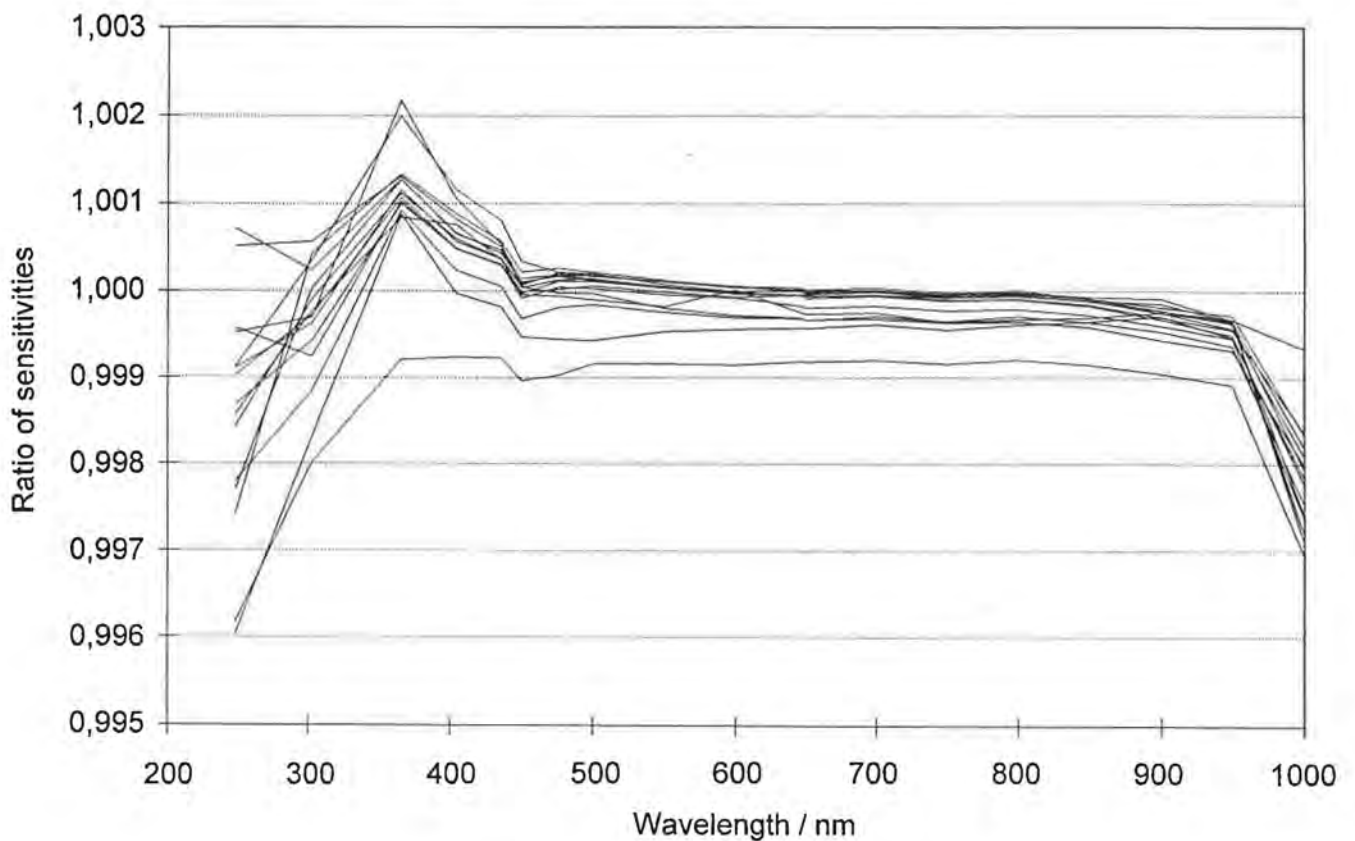


**Fig.25:** Change in spectral responsivity of traps: Ratio of trap sensitivity after return from the participant to that found before sending to participant.

**NATIONAL SCALES*****CSIR (Pretoria, South Africa)***

At the CSIR only the photodiodes were calibrated and not the traps. Measurements were made at 365 nm and from 500 nm to 1000 nm every 100 nm. For 365 nm an UV-A lamp was used in connection with interference filters. The other wavelengths were measured using two different single grating monochromators (depending on wavelength). All measurements were made using the CSIR-designed absolute radiometer (ESR).

Spot size:	7 mm x 2,5 mm or round (5 mm), respectively
Temperature:	(23,5 ± 0,5) °C
Beam divergence (full angle):	≈ 6°
Bandwidth:	≈ 8 nm
Radiant power:	≈ 100 μW

***CSIRO (Lindfield, Australia)***

At the CSIRO the photodiodes were measured at 5 nm intervals in the range from 240 nm to 800 nm and at 10 nm intervals from 800 nm to 1000 nm. The sources used were an argon arc for the UV and a tungsten halogen lamp for the visible and IR, combined with a single grating monochromator with prism pre-disperser. Responsivities for wavelengths corresponding to the Hg lines were obtained by spline interpolation. The absolute calibration was obtained by silicon self-calibration on working standards, which was then transferred to gold-black bolometers. The traps were measured for a number of laser lines only.

Spot size:	6 mm diameter
Temperature:	(21 ± 1) °C
Beam divergence (full angle):	≈ 7°
Bandwidth:	≈ 4 nm
Radiant power:	≈ 0,2 μW - 2,4 μW

***CSMU (Bratislava, Czechoslovakia)***

At the CSMU all detectors were measured at all wavelengths above 365 nm (inclusive). The source was a grating monochromator in combination with a halogen

lamp or a low pressure mercury lamp. The detectors were compared directly with a QED-200 (365 nm - 800 nm) and an absolute pyro-electric radiometer Laser Precision Rs 3964 (800 nm -1000 nm).

Spot size:	6 mm diameter
Temperature:	(21 ± 1) °C
Beam divergence (full angle):	≈ 5°
Bandwidth:	5 nm
Radiant power:	10 μW (max.)

### ***ETL (Tsukuba-Shi, Japan)***

At the ETL both the photodiodes and the trap were measured at all wavelengths. The absolute spectral responsivity scale was based on the silicon self-calibration method in the range from 400 nm to 740 nm. Above and below this region three different radiometers were used (thermocouple, thermopile and pyro-electric detector). The scale was maintained using a group of silicon photodiodes as a working standard. The sources used were halogen or deuterium lamps in connection with a prism/grating monochromator.

Spot size:	5 mm diameter for photodiodes, 3 mm x 1 mm for trap
Temperature:	21 °C - 22 °C
Beam divergence (full angle):	4,2 °
Bandwidth:	≈ 3,5 nm
Radiant power:	2,8 μW max.

### ***INM (Paris, France)***

At the INM the photodiodes were measured at all wavelengths and the trap at three laser wavelengths only. The light sources were a xenon-mercury arc for the UV, a xenon arc for the visible and a quartz halogen lamp for the infrared. A double grating monochromator, with different sets of gratings depending on the spectral range, was used. The absolute spectral responsivity detector was either a QED-200 or a cryogenic radiometer. The relative spectral responsivity was measured using a thermal cavity detector.

Spot size:	7 mm diameter
Temperature:	(21 ± 1) °C

Beam divergence (full angle):	6,5 °
Bandwidth:	≈ 3 nm - 6 nm (depending on grating)
Radiant power:	2,4 μW- 75 μW (Xe-Hg arc), 4,2 μW- 35 μW (QTH lamp)

### ***IRL (Lower Hutt, New Zealand)***

At the IRL both trap and photodiodes were measured from 240 nm to 900 nm. Below 400 nm, data were taken every 10 nm. The scale was obtained by fitting the internal quantum efficiency of traps and predicting the external quantum efficiency in the wavelength range from 400 nm to 900 nm. Below 400 nm a spectrally flat detector was used to measure relative spectral responsivity. The mercury line wavelengths are interpolated values from sources with a continuous spectrum.

Spot size:	3 mm - 5 mm diameter
Temperature:	No information given
Beam divergence (full angle):	No information given
Bandwidth:	≈ 3 nm
Radiant power:	No information given

### ***KRISS (Taejon, Republic of Korea)***

At the KRISS both the photodiodes and the trap detector were measured at all wavelengths above 365 nm (inclusive). Absolute standards used were a QED-200 (360 nm - 750 nm), silicon self-calibration (800 nm - 850 nm) and ESR (900 nm - 1000 nm)

Spot size:	5 mm diameter
Temperature:	(21,5 ± 0,5) °C.
Beam divergence (full angle):	5,7 °.
Bandwidth:	3 nm - 5 nm
Radiant power:	100 μW (max.).

### ***NIM (Beijing, China)***

At the NIM the photodiodes were measured above 302 nm (inclusive) for all wavelengths and the trap was measured only at 633 nm using a laser. The source was a quartz halogen lamp in combination with a prism-grating monochromator. The

absolute spectral responsivity scale was deduced using silicon self-calibration at 633 nm and transferred to a pyro-electric detector as a working standard.

Spot size:	5 mm diameter
Temperature:	$(27 \pm 1) ^\circ\text{C}$
Beam divergence (full angle):	F/6,8
Bandwidth:	$\approx 3,5 \text{ nm}$
Radiant power:	10 $\mu\text{W}$ (max.)

### *NIST (Gaithersburg, USA)*

At the NIST the photodiodes were measured between 200 nm and 1100 nm at 5 nm intervals and the trap from 350 nm to 1100 nm at the same intervals. Values corresponding to the Hg lines were interpolated. An argon arc is used in the UV and a quartz halogen lamp in the visible and IR connected to a double monochromator. The primary standard was a cryogenic radiometer. Trap detectors (of NIST design) were used as transfer devices to a group of silicon working standards. The absolute spectral response of the trap detectors was modeled from 400 nm to 900 nm. Above and below this region a pyro-electric detector was used to determine the relative spectral responsivity of the working standards.

Spot size:	1,1 mm diameter (visible), 1,5 mm (UV)
Temperature:	$(23,8 \pm 0,5)^\circ\text{C}$ .
Beam divergence (full angle):	F/9 (visible and IR), F/5 (UV)
Bandwidth:	$\approx 4 \text{ nm}$
Radiant power:	0,1 $\mu\text{W}$ - 0,6 $\mu\text{W}$ (350 nm - 1100 nm) 1,0 $\mu\text{W}$ - 4,0 $\mu\text{W}$ (200 nm - 400 nm)

### *NPL (Teddington, UK)*

At the NPL all detectors were measured at all wavelengths proposed. The sources used were a tungsten lamp or a Hg arc lamp connected to a double grating monochromator. Trap detectors, which were directly calibrated against the NPL cryogenic radiometer, were used as working standards from 400 nm to 940 nm. Outside this range silicon photodiodes calibrated against thermal detectors were used.

Spot size:	5 mm
Temperature:	$(21,5 ^\circ\text{C} \pm 0,5) ^\circ\text{C}$ .
Beam divergence (full angle):	quasi collimated beam.

Bandwidth:	3,5 nm
Radiant power:	0,03 $\mu$ W - 0,46 $\mu$ W (Hg source) 0,45 $\mu$ W - 3,15 $\mu$ W (QTH source)

### *NRC (Ottawa, Canada)*

At the NRC all detectors were measured at all wavelengths proposed. However a vignetting problem was encountered with the traps, because of the angular divergence of the monochromator radiation. NRC therefore asked that their results for these detectors be excluded from the comparison. After discussions between NRC and the BIPM, it was agreed that it would be useful to include NRC's trap measurements in the comparison. The inclusion of this data may help to understand eventual problems of other laboratories with these detectors.

The source for the measurements was a single grating monochromator used in conjunction with a xenon arc (250 nm - 500 nm) or a tungsten halogen lamp (500 nm - 1000 nm). Silicon photodiodes were used as working standards, they were calibrated using NRC ESR type absolute radiometers.

Spot size:	3 mm diameter
Temperature:	$\approx (22,5 \pm 1,0) ^\circ\text{C}$
Beam divergence (full angle):	$10^\circ$
Bandwidth:	10 nm FWHM
Radiant power:	15 $\mu$ W to 450 $\mu$ W (Xe source), 35 $\mu$ W to 55 $\mu$ W (tungsten source)

### *OMH (Budapest, Hungary)*

At the OMH the photodiodes were measured at all wavelengths proposed. The sources used were deuterium and tungsten halogen lamps in combination with a double grating monochromator. Responsivities for wavelengths corresponding to Hg lines were obtained by interpolation. The absolute calibration was done by silicon self-calibration and extended to the IR with non-selective detectors.

Spot size:	4 mm diameter
Temperature:	$(23 \pm 1)^\circ\text{C}$
Beam divergence (full angle):	$\approx 7^\circ$
Bandwidth:	$\approx 5$ nm
Radiant power:	0,1 $\mu$ W - 50 $\mu$ W

***PTB (Braunschweig, Germany)***

At the PTB all detectors were calibrated at all wavelengths required. The source used was a high pressure mercury lamp or a quartz halogen lamp in combination with a double prism monochromator. The relative spectral responsivity was measured using a thermopile as a secondary standard. The absolute responsivity was measured at 633 nm with the PTB primary standard radiometer LM7 and then transferred to the secondary standard.

Spot size:	5 mm diameter
Temperature:	(22 ± 1) °C
Beam divergence (full angle):	0,1 rad
Bandwidth:	< 8,5 nm depending on wavelength
Radiant power:	0,1 μW - 110 μW

***VNIIOFI (Moscow, Russia)***

At the VNIIOFI all detectors were measured at all the wavelengths. A double monochromator was used but the light sources were not specified. The absolute scale was based on the MAR-1 radiometer and a QED-200. A thermopile and a cavity non-selective detector were used for the relative spectral responsivity scale.

Spot size:	rectangular 3 mm x 2 mm
Temperature:	(21 ± 1) °C
Beam divergence (full angle):	4,6 °
Bandwidth:	3,25 nm
Radiant power:	100 μW (max.)

***COMPARISON OF THE NATIONAL SCALES***

Individual national scales were compared by first being related to the prime reference diode. As explained above, all detectors aged slightly between the time they left the BIPM and the time of the measurements after their return. The relative spectral responsivities of the detectors after their return was used in calculation of the scales, because it was assumed that the diodes aged the most just after they left the BIPM. This assumption is supported by the following observations:

The batches which returned to the BIPM were all re-measured for the first time not more than one week after their return to the BIPM. The first batch (#8, NRC) was measured regularly between its arrival and the arrival of the last batch. Only a small drift (1 part in  $10^4$  of the sensitivity) was observed over this period (4 months). This indicates that the ageing was probably still due to the first UV measurements and decreased in its magnitude with time until the detectors became stable. The BIPM batch, which had not been measured at all when the others were away aged exactly as the other sets. This suggests that a further use of the detectors, including in the UV, did not provoke a further ageing process.

The ratio of the relative spectral responsivity of the prime reference diode to that of each individual detector was calculated first. This ratio was then multiplied by the absolute spectral responsivity assigned to that detector by the participant laboratory. A different calibration was thus attributed to prime reference diode by each laboratory. The values derived by the individual laboratories were then averaged.

Because of the differences between some of the scales it was not considered useful to calculate an average and show the differences of individual laboratory scales from the average. Instead, we decided to plot the ratios of the scales from each laboratory with respect to the BIPM absolute scale. (For information on how the BIPM absolute spectral responsivity scale was obtained, refer to appendix A). Any common structure in the curves when compared with the BIPM scale thus indicates a common difference and probably an error in the BIPM scale and not in all the other scales.

A difficulty was that not all laboratories used high pressure Hg lamps, and thus the UV wavelengths were not always identical. Three laboratories measured the responsivities of their detectors in the UV at short wavelength intervals. The curves are shown in Fig.26. The slight differences in the curves come from different absolute responsivities of the detectors, because the curves have not been normalized to one another. For the data analysis, only the slopes around 250 nm and 365 nm were needed. Once the slopes had been fitted, the values given by laboratories which did not carry out the measurements at the same wavelengths as the BIPM were extrapolated to these values.

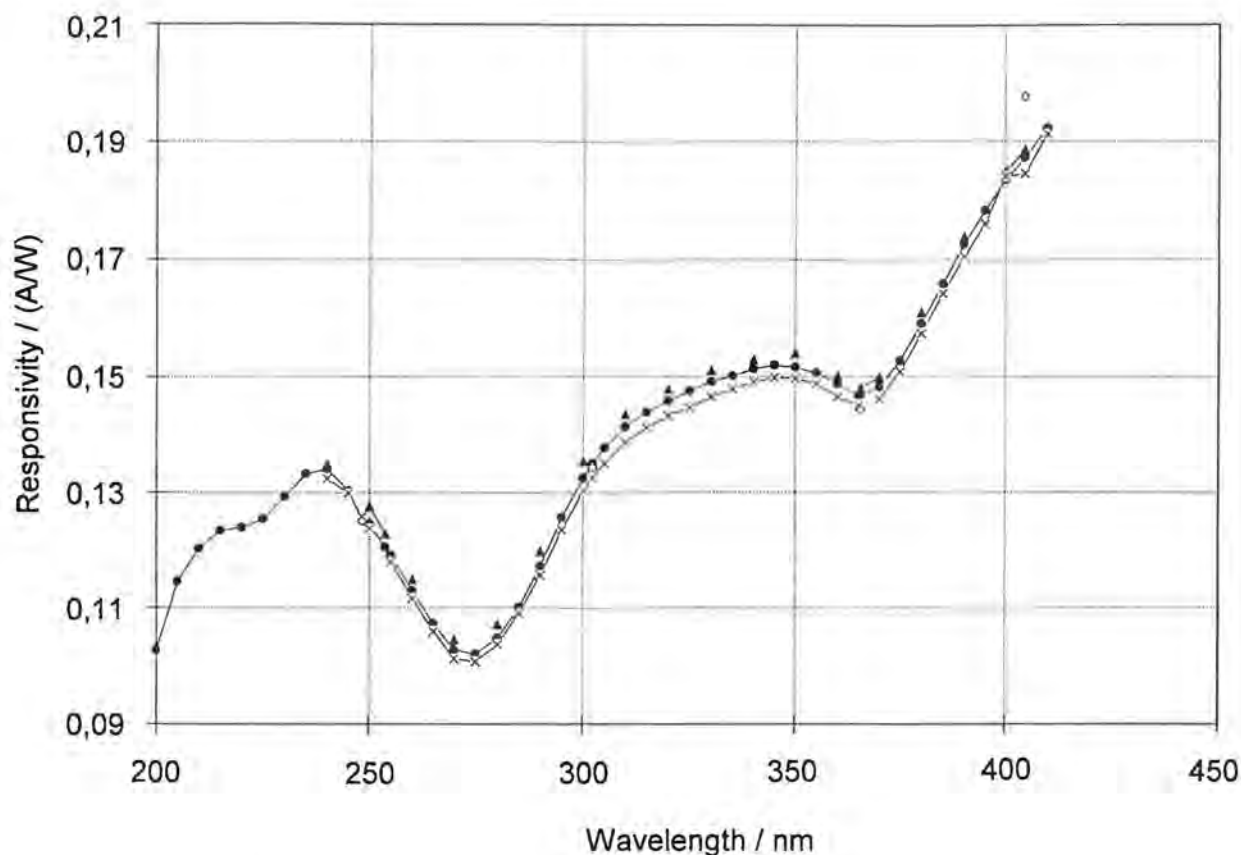
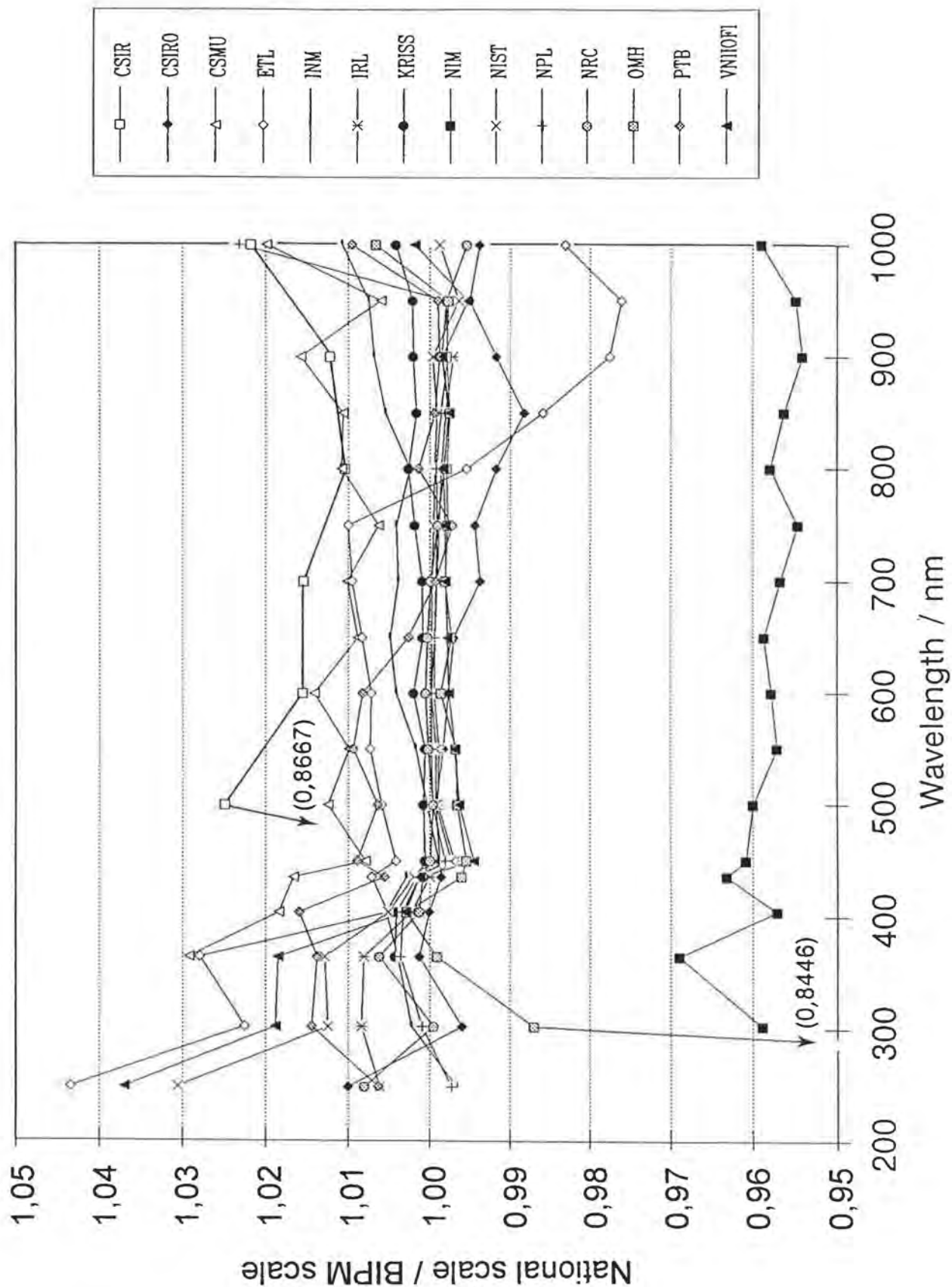


Fig.26: Absolute spectral responsivity of the photodiodes in the UV as measured by CSIRO (*crosses*), IRL (*triangles*) and NIST (*circles*).

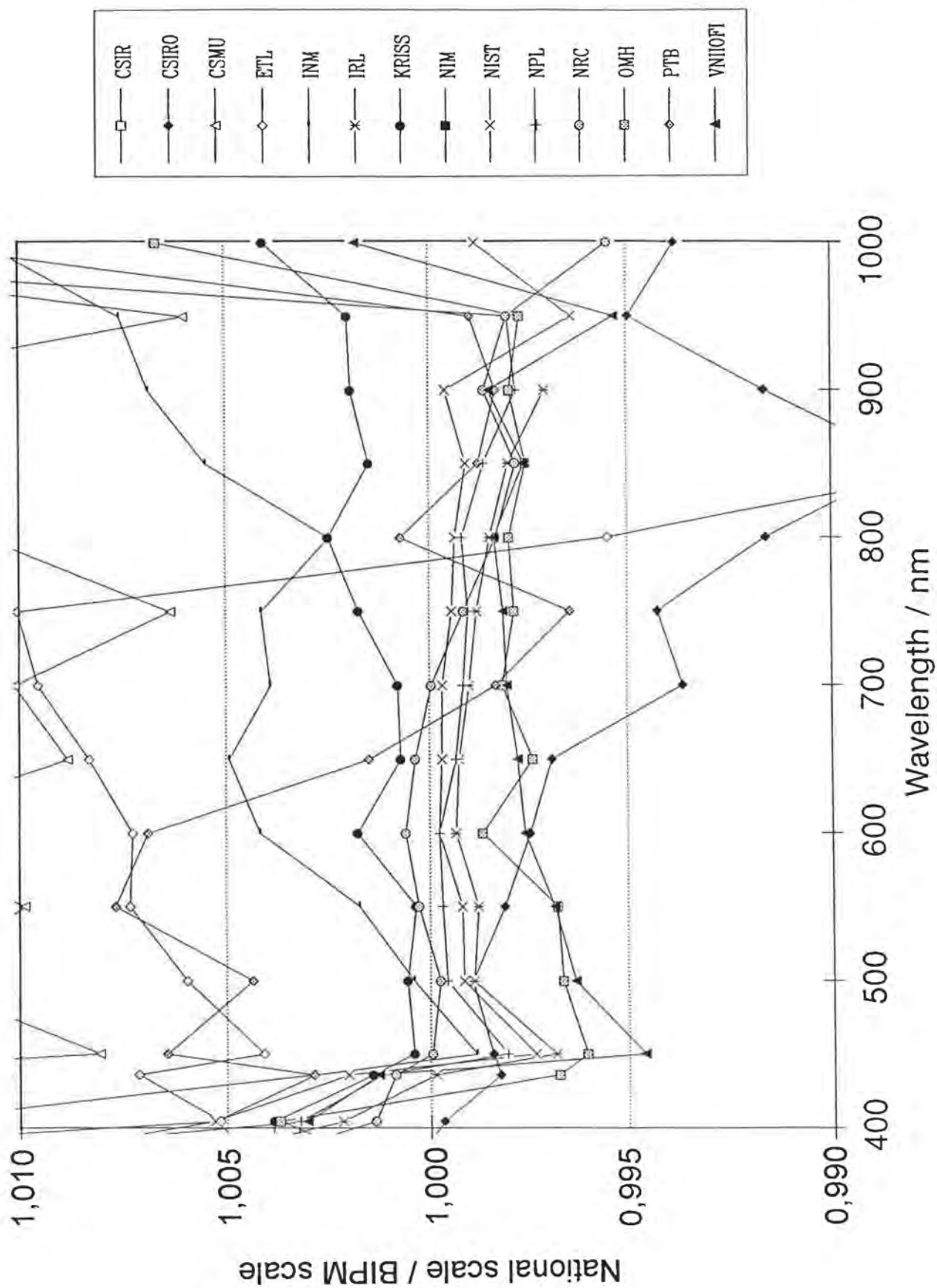
## PHOTODIODES

Figure 27 shows the ratios of the individual national spectral responsivity scales to that of the BIPM. It is obvious that a large number of laboratories are grouped very close to the BIPM, especially in the wavelength range above about 400 nm. It is also clear that some laboratories deviate considerably from this core. Two points have been omitted in Fig.27 because they were too far away from the average. Their values can be found in the curves for the individual scales (Figs.36 to 49) or in Table 7.

If the scale is expanded to include only the range of  $\pm 1\%$  around the BIPM scale and the plot is limited to wavelengths above 400 nm (Fig.28), it becomes obvious that four laboratories (NRC, NIST, NPL and IRL) are grouped very close together on curves of the same shape and slope, slightly below the BIPM scale. Two other curves (VNIIOFI and OMH) join this group for wavelengths above about 750 nm.



**Fig.27:** Comparison of the individual national scales, derived from the diodes, with the spectral responsivity scale of the BIPM.



**Fig.28:** Comparison of the individual national scales, derived from the diodes, with the spectral responsivity scale of the BIPM (zoom).

As each laboratory calibrated each of the three photodiodes individually, it is possible to estimate the spread in the absolute calibrations of individual laboratories. As the primary reference diode was calibrated against each photodiode, the spread of the three different values obtained in this way is a rough estimate of the consistency of the calibrations. The spectral dependence of this spread is shown in Fig.29, expressed as a relative standard deviation.

### ***TRAPS***

The traps were not measured by all laboratories, but the available results are shown in Fig.30. The curves are grouped much closer than those of the diodes in Fig.27. An expanded scale, as in Figure 28 (see Fig.31), shows that the general behaviour is similar to that of the diodes, but the range is smaller. Again the NIST, the NPL and the IRL are grouped closely together, but this time are joined over the whole range above 400 nm by the OMH and the VNIIOFI. The NRC lies somewhat lower, but with the same shape of curve. This behaviour reflects exactly the vignetting problem that NRC had observed with its monochromator during the measurements with the traps.

Individual differences between the scales obtained by traps compared to those obtained with diodes by one laboratory will be discussed individually if necessary (Figs.36 to 49).

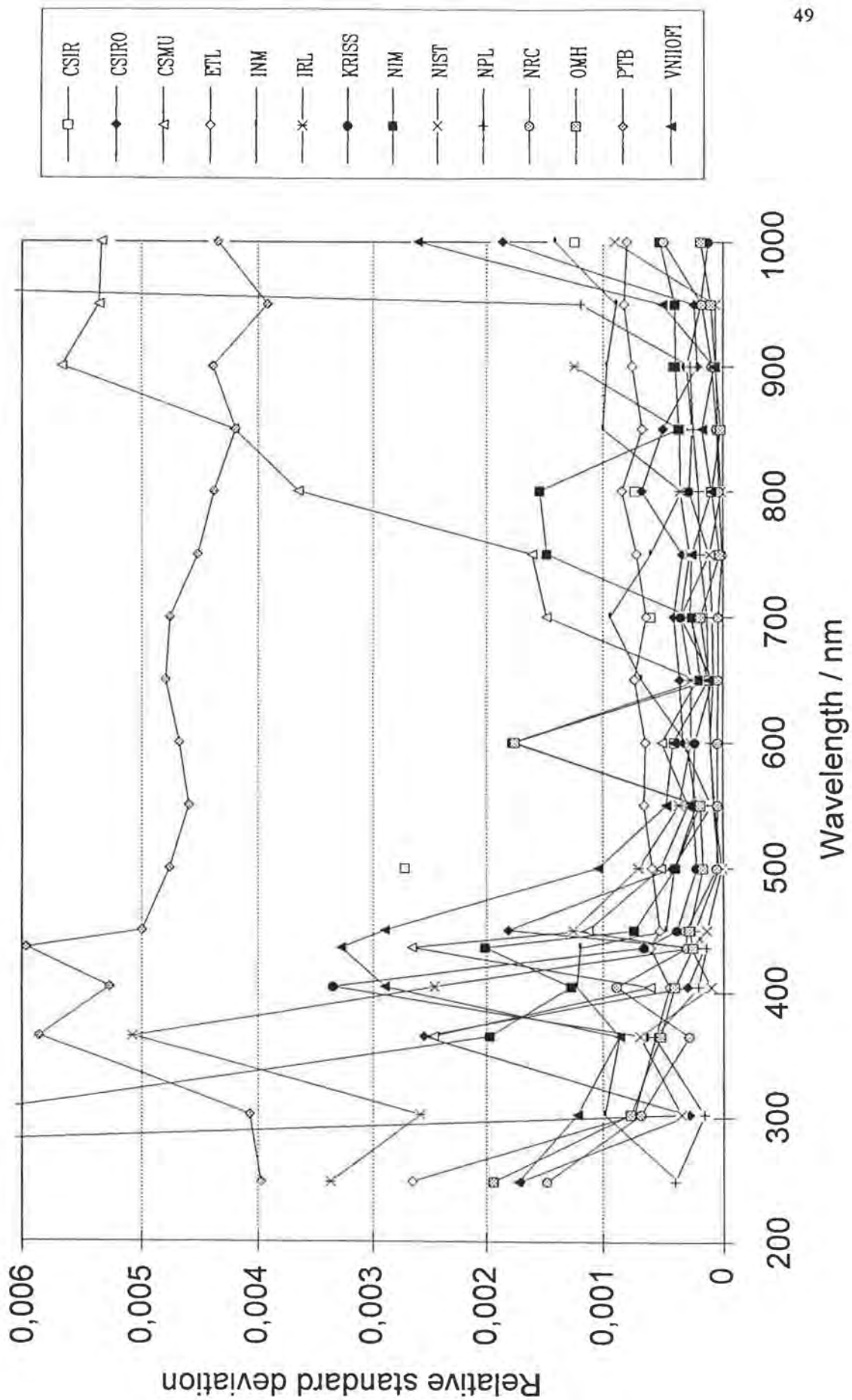


Fig.29: Spread of calibration of the three photodiodes for each laboratory.

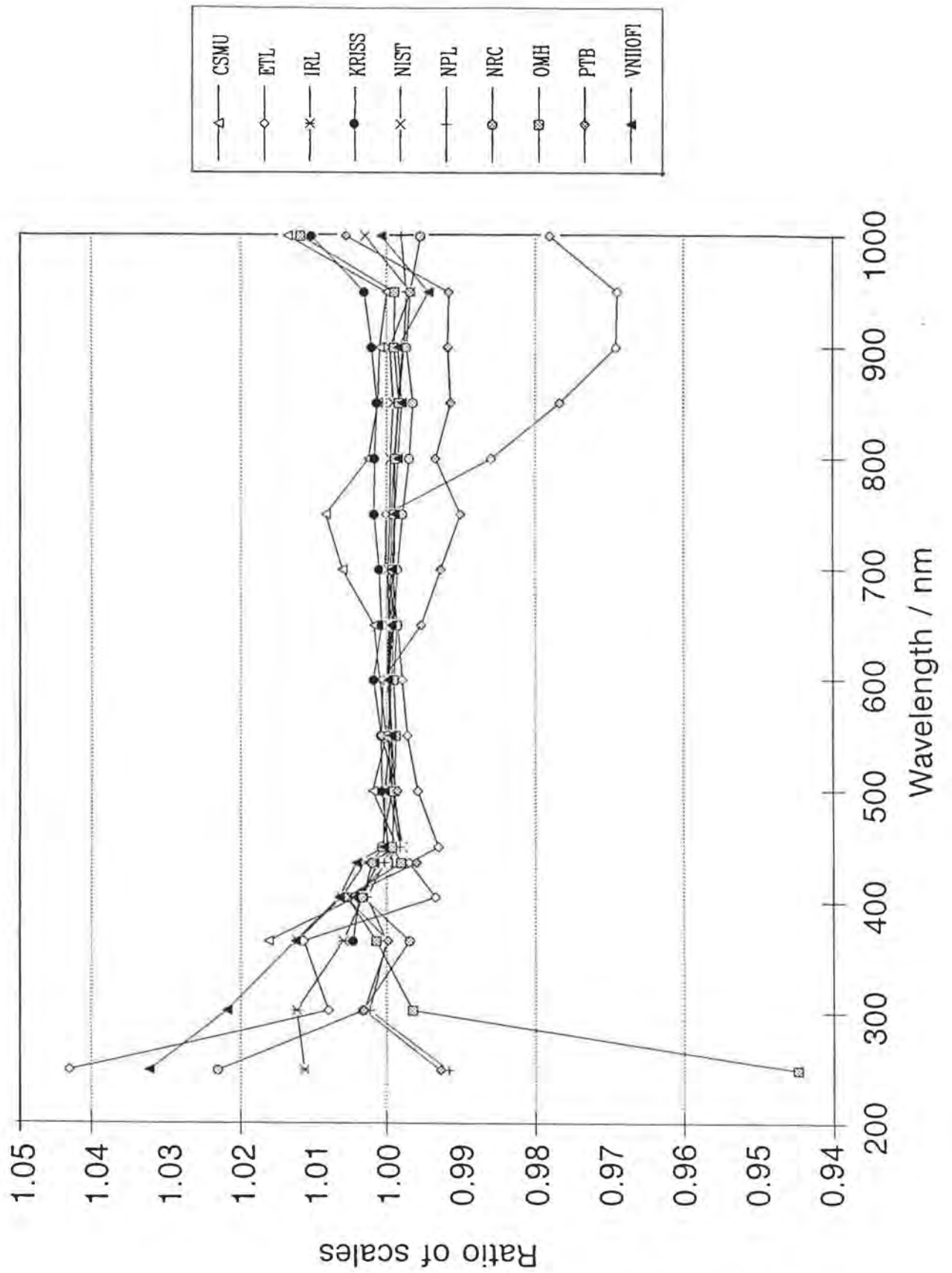
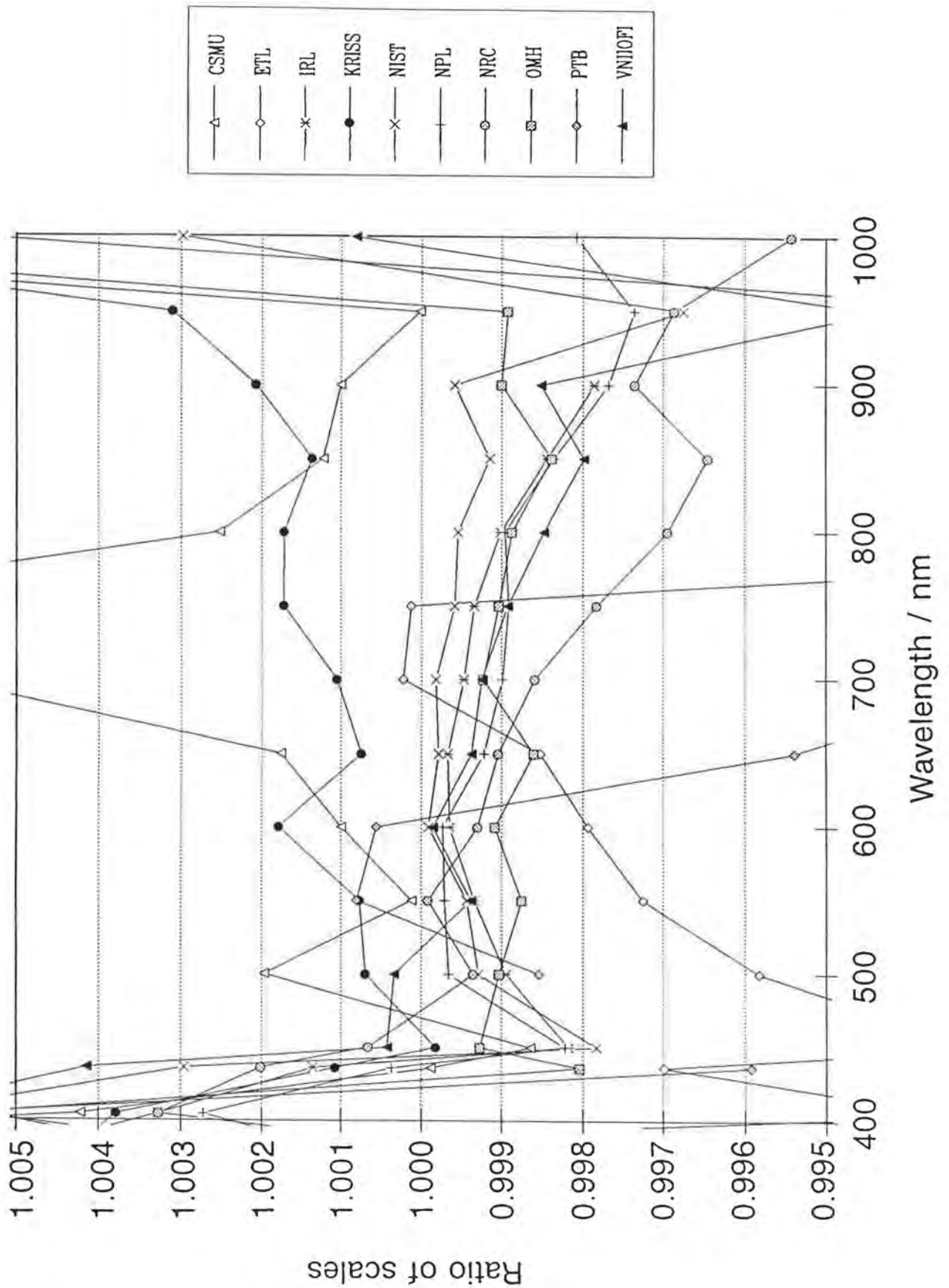


Fig.30: Comparison of the individual national scales, derived from the traps, with the spectral responsivity scale of the BIPM.

(revised)



**Fig.31:** Comparison of the individual national scales, derived from the traps, with the spectral responsivity scale of the BIPM (zoom).

(revised)

Figure 32 shows the spread between the laboratories: the standard deviations of the ratios of scales, as calculated above, are shown for each wavelength. The three curves correspond to the results obtained from the trap measurements (all laboratories which calibrated the traps), the results from the diodes for the same ensemble of laboratories, and results from diodes for all laboratories. From this figure the excellent uniformity of the different scales, when measured with the traps in the visible region is evident.

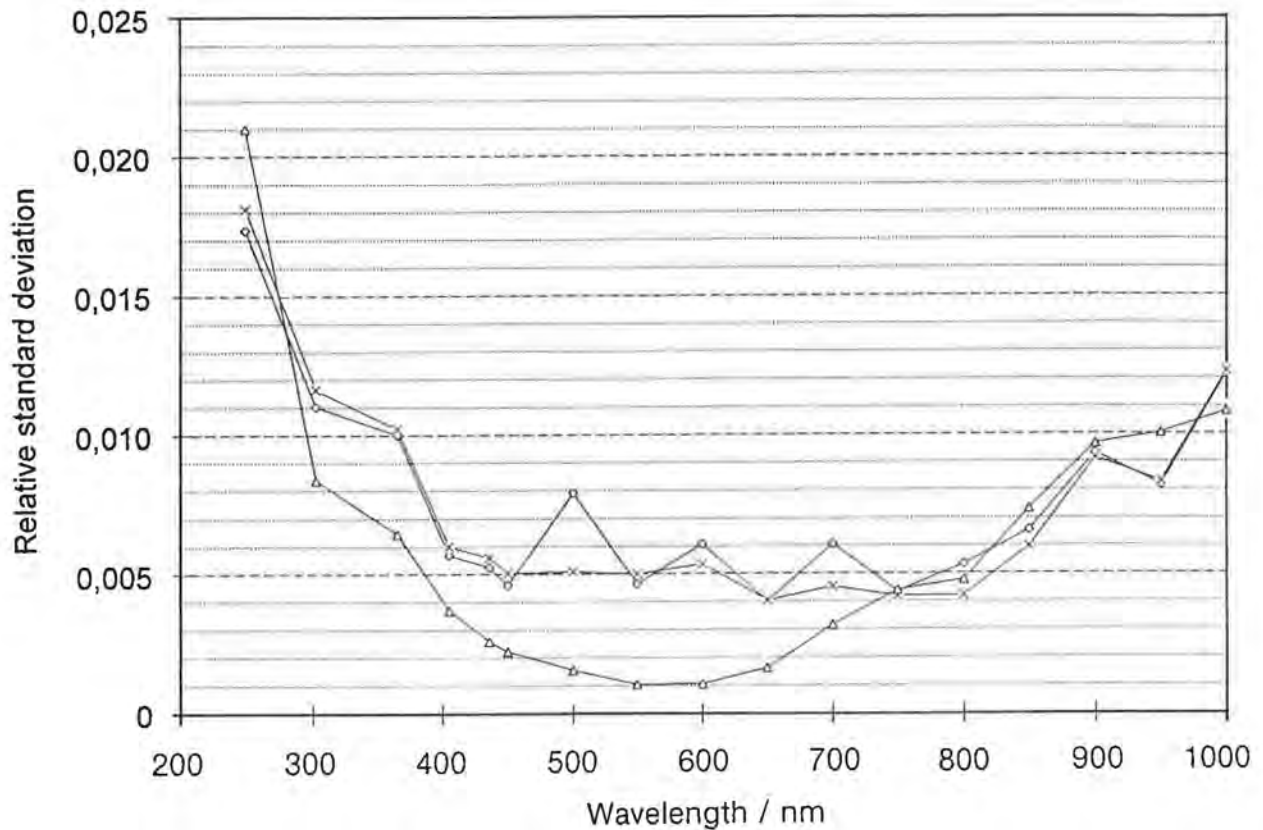


**Fig.32:** Spread (expressed as relative standard deviation) of the calibration between the laboratories. *Triangles:* measured with traps, *Crosses:* diodes, same laboratories as with traps, *Diamonds:* diodes, all laboratories.

### ***AGREEMENT OF THE NATIONAL SCALES***

The standard deviation of the measurements shown in Fig.32 shows the dispersion of the scales. It does, however, not take into account the uncertainties assessed by the laboratories. To do this, the maximum number of laboratories which agree within their mutual uncertainties were calculated for all wavelengths and for different coverage factors  $k=1-3$ . This is plotted in the Figures 33 - 35.

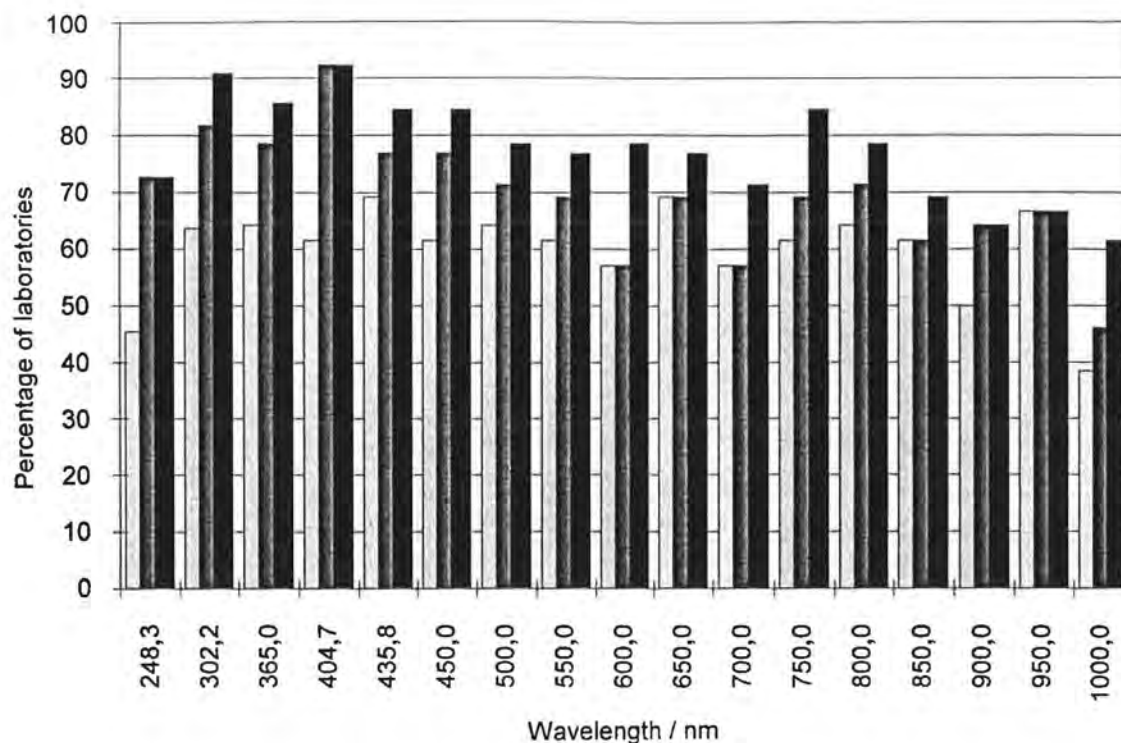


**Fig.33:** Maximum percentage of laboratories in agreement within their mutual uncertainties (diodes).  
*Light grey: coverage factor k=1, Grey: k=2, Black: k=3.*

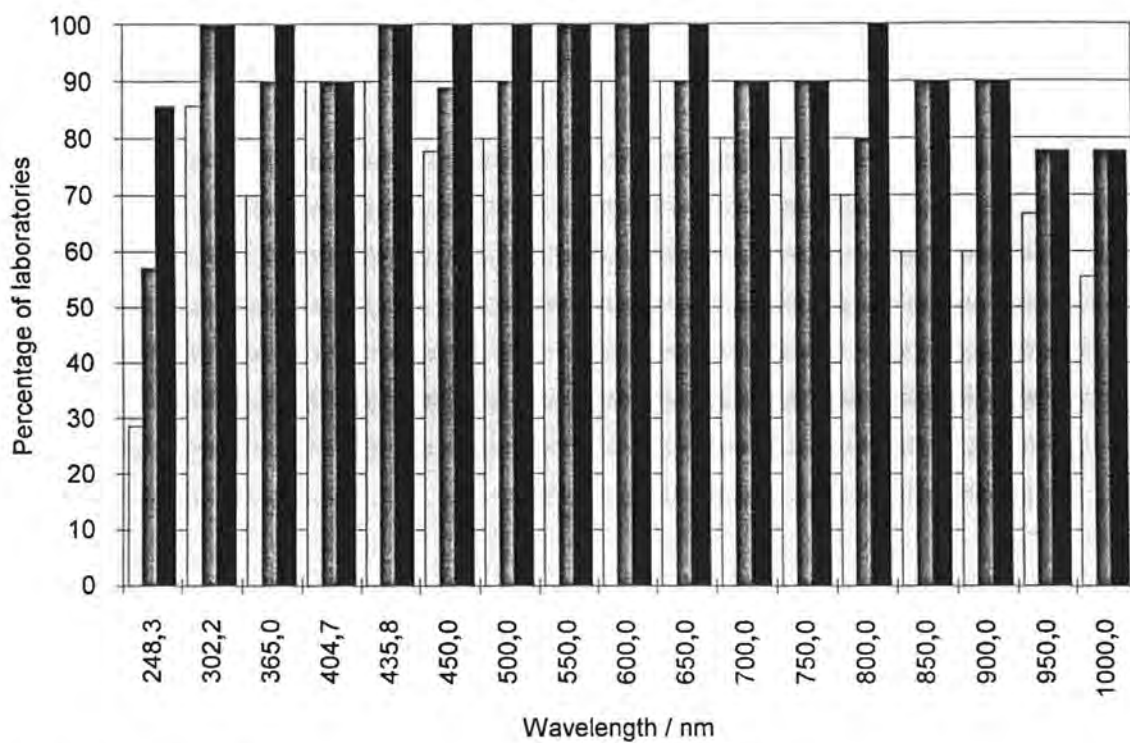


**Fig.34:** Maximum percentage of laboratories in agreement within their mutual uncertainties (traps).  
*Light grey: coverage factor k=1, Grey: k=2, Black: k=3.*

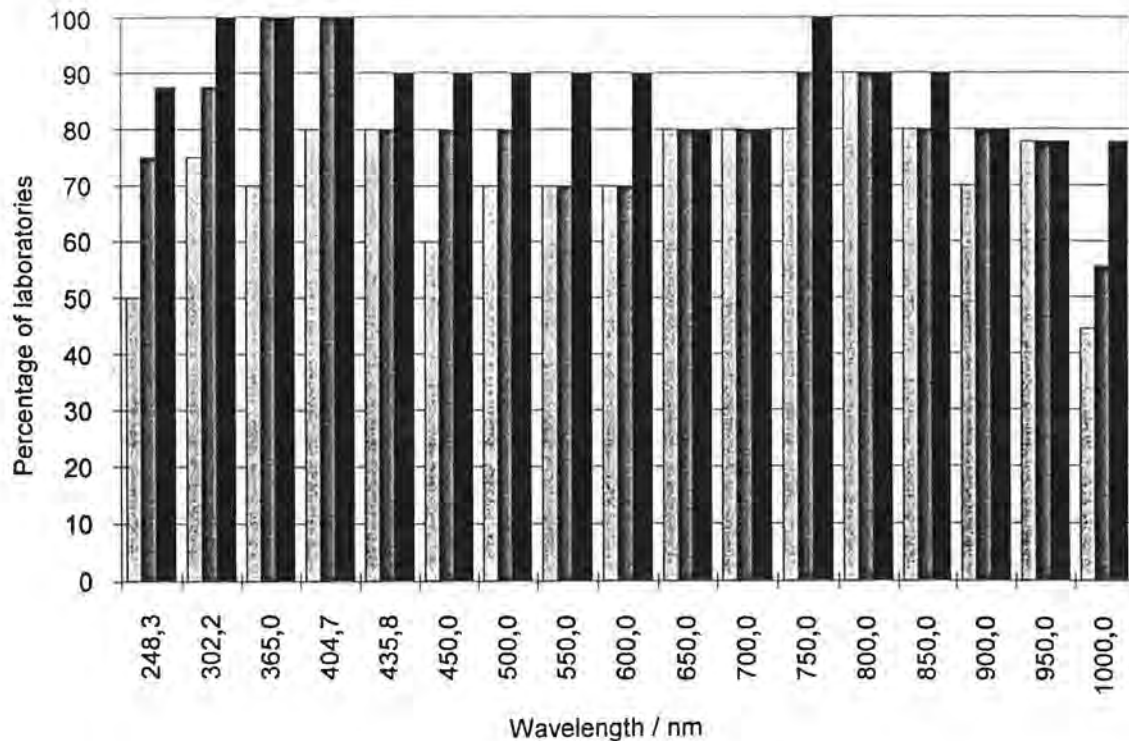


**Fig.35:** Maximum percentage of laboratories in agreement within their mutual uncertainties (diodes (same laboratories as for traps)). *Light grey:* coverage factor  $k=1$ , *Grey:*  $k=2$ , *Black:*  $k=3$ .

### ***INDIVIDUAL NATIONAL SCALES***

The fact that four laboratories (considering diodes) and six laboratories (considering traps) are above 450 nm closely grouped within their respective  $1\sigma$ -uncertainties, probably indicates that the correct scale is close to the average of this group. Additionally, the BIPM scale, although not necessary for the comparison, agrees with this average in the uncertainties over a part of the wavelength range. However, data from these laboratories lie on a curve which increases its slope above 700 nm, when compared with the BIPM scale which indicates that the BIPM scale deviates in this range (probably because of the spectral non-flatness of the pyro-electric detector above 700 nm).

Below 450 nm the ratio of values from almost every laboratory to those from the BIPM is above unity by between one and four percent, indicating non-ideal behaviour of our pyroelectric detector in the UV. The spread in national scales, however, is very large for wavelengths below 365 nm. The difference in the scales between the NIST and the NPL, for example, is about 1% at 365 nm and more than 3% at 248 nm.

National scales may be compared using the data of Table 7, in which the ratio of values from individual scales to those from the BIPM scale is listed for every wavelength. The values for the photodiodes are averages for the calibrations derived from the three diodes measured at each laboratory. Taking the ratio of any two of these values (by detector) gives the comparison of the two scales, as this eliminates the BIPM value.

Figures.36 to 49 show the results from the individual national laboratories, together with their stated  $1\sigma$ -uncertainties, relative to those from the BIPM. Shown are two curves, the scale obtained by averaging the results for the diodes, and the scale obtained from the calibration of the trap.

Some interesting conclusions can be drawn from inspection of these graphs. A number of laboratories find scales which are consistent, regardless of whether they calibrate traps or photodiodes. Other laboratories show a large and wavelength independent difference between the two types of detectors: in these cases the results for the traps are usually in closer agreement with the average of the other laboratories. This probably indicates a problem with light reflected back into the optical system, as the photodiodes have approximately 35 % reflectance, whereas the traps have only 0,2%.

Some laboratories show distinct structures in their calibration curves. For some of them, the origin can be understood from the reports of how the scales were obtained. The ETL, for example, uses a direct method between 400 nm and 750 nm and spectrally flat detectors outside this region. It is just at the junction of the two methods, that the steps in the scale appear, indicating imperfect spectral flatness in these non-selective detectors.

Table 7 National scales compared to the BPM scale.

lambda / nm	individual scale / BPM scale													
<b>PHOTODIODES</b>	CSIR	CSIRO	CSMU	ETL	INM	IRL	KRISS	NIM	NIST	NPL	NRC	OMH	PTB	VNIOFI
248,3		1,01004		1,04343	0,99671	1,00614			1,03055	0,99744	1,00805	0,84471	1,00379	1,03696
302,2		0,99565		1,02246	1,00211	1,00838		0,95909	1,01273	1,00112	0,99955	0,98876	1,00847	1,01884
365,0	0,86662	1,00069	1,02957	1,02797	1,00385	1,00800	1,00401	0,96942	1,01318	1,00347	1,00603	1,00035	1,00921	1,01880
404,7		0,99967	1,01870	1,00517	1,00527	1,00218	1,00386	0,95725	1,00530	1,00323	1,00137	1,00373	1,01278	1,00306
435,8		0,99823	1,01695	1,00712	1,00286	0,99986	1,00143	0,96323	1,00204	1,00118	1,00087	0,99674	1,00290	1,00129
450,0		0,99841	1,00806	1,00411	0,99884	0,99682	1,00040	0,96088	0,99734	0,99805	0,99995	0,99603	1,00643	0,99458
500,0	1,02476	0,99893	1,01247	1,00594	1,00040	0,99890	1,00057	0,95997	0,99915	0,99956	0,99974	0,99663	1,00436	0,99631
550,0		0,99810	1,00988	1,00732	1,00175	0,99878	1,00035	0,95708	0,99919	0,99967	1,00028	0,99677	1,00767	0,99684
600,0	1,01544	0,99745	1,01415	1,00725	1,00417	0,99934	1,00180	0,95776	0,99975	0,99975	1,00060	0,99867	1,00689	0,99758
650,0		0,99690	1,00883	1,00831	1,00492	0,99926	1,00071	0,95867	0,99969	0,99934	1,00036	0,99738	1,00151	0,99777
700,0	1,01536	0,99360	1,01012	1,00954	1,00391	0,99900	1,00078	0,95675	0,99967	0,99915	0,99995	0,99816	0,99833	0,99804
750,0		0,99423	1,00634	1,01004	1,00414	0,99880	1,00176	0,95459	0,99943	0,99902	0,99914	0,99785	0,99643	0,99812
800,0	1,01031	0,99156	1,01082	0,99548	1,00249	0,99847	1,00251	0,95791	0,99935	0,99917	0,99832	0,99797	1,00072	0,99835
850,0		0,98807	1,01064	0,98592	1,00547	0,99799	1,00150	0,95629	0,99907	0,99862	0,99781	0,99755	0,99875	0,99760
900,0	1,01214	0,99160	1,01578	0,97760	1,00685	0,99706	1,00193	0,95409	0,99958	0,99780	0,99860	0,99796	0,99831	0,99848
950,0		0,99495	1,00600	0,97616	1,00753		1,00202	0,95486	0,99639	0,99801	0,99802	0,99769	0,99895	0,99531
1000,0	1,02176	0,99379	1,01991	0,98310	1,01082		1,00407	0,95895	0,99882	1,02308	0,99548	1,00665	1,01279	1,00182
<b>TRAPS</b>														
248,3				1,04295		1,01126				0,99157	1,02309	0,94476	0,99268	1,03229
302,2	D	D		1,00800	D	1,01232		D		1,00232	1,00323	0,99646	1,00311	1,02185
365,0	E	E	1,01625	1,01141	E	1,00595	1,00463	E	1,01231	1,00000	0,99688	1,00143	0,99987	1,01254
404,7	R	R	1,00422	0,99338	R	1,00328	1,00379	R	1,00623	1,00273	1,00327	1,00547	1,00558	1,00651
435,8	U	U	0,99988	0,99699	U	1,00135	1,00107	U	1,00296	1,00037	1,00201	0,99804	0,99592	1,00415
450,0	S	S	0,99864	0,99302	S	0,99817	0,99982	S	0,99783	0,99822	1,00066	0,99927		1,00042
500,0	A	A	1,00197	0,99583	A	0,99894	1,00069	A	0,99928	0,99965	0,99935	0,99903	0,99854	1,00033
550,0	E	E	1,00012	0,99725	E	0,99934	1,00077	E	0,99943	0,99971	0,99992	0,99875	1,00081	0,99938
600,0	M	M	1,00100	0,99793	M	0,99965	1,00179	M	0,99991	0,99973	0,99930	0,99908	1,00056	0,99985
650,0			1,00176	0,99852		0,99967	1,00075		0,99979	0,99922	0,99904	0,99860	0,99539	0,99937
700,0	T	T	1,00608	1,00023	T	0,99946	1,00106	T	0,99982	0,99899	0,99859	0,99923	0,99272	0,99924
750,0	O	O	1,00840	1,00013	O	0,99934	1,00173	O	0,99958	0,99891	0,99783	0,99904	0,98999	0,99893
800,0	N	N	1,00252	0,98595	N	0,99901	1,00172	N	0,99954	0,99896	0,99695	0,99887	0,99337	0,99848
850,0			1,00123	0,97674		0,99844	1,00137		0,99915	0,99836	0,99645	0,99838	0,99135	0,99798
900,0			1,00101	0,96916		0,99786	1,00208		0,99958	0,99768	0,99736	0,99900	0,99170	0,99851
950,0			1,00002			0,00000	1,00310		0,99675	0,99736	0,99687	0,99893	0,99158	0,99435
1000,0			1,01360			0,00000	1,01035		1,00298	0,99808	0,99543	1,01182	1,00557	1,00081

The INM has three distinct regions in the curve showing the ratio of its scale to the that of the BIPM. The steps appear at the junctions of the regions where the laboratory changes the gratings of the monochromator so as to cover the whole spectral range.

The NIM scale agrees in slope and form with the other scales, but is offset by about 4%. Here, the laboratory has obtained a correct relative spectral responsivity scale, but it has attached this scale at 633 nm using coherent laser light and a photodiode which had previously been self calibrated. It is probable that the windowed photodiode used with the laser light caused the problem.

The large deviation of the point at 1000 nm for the NPL arises from just one of the three diode measurements.

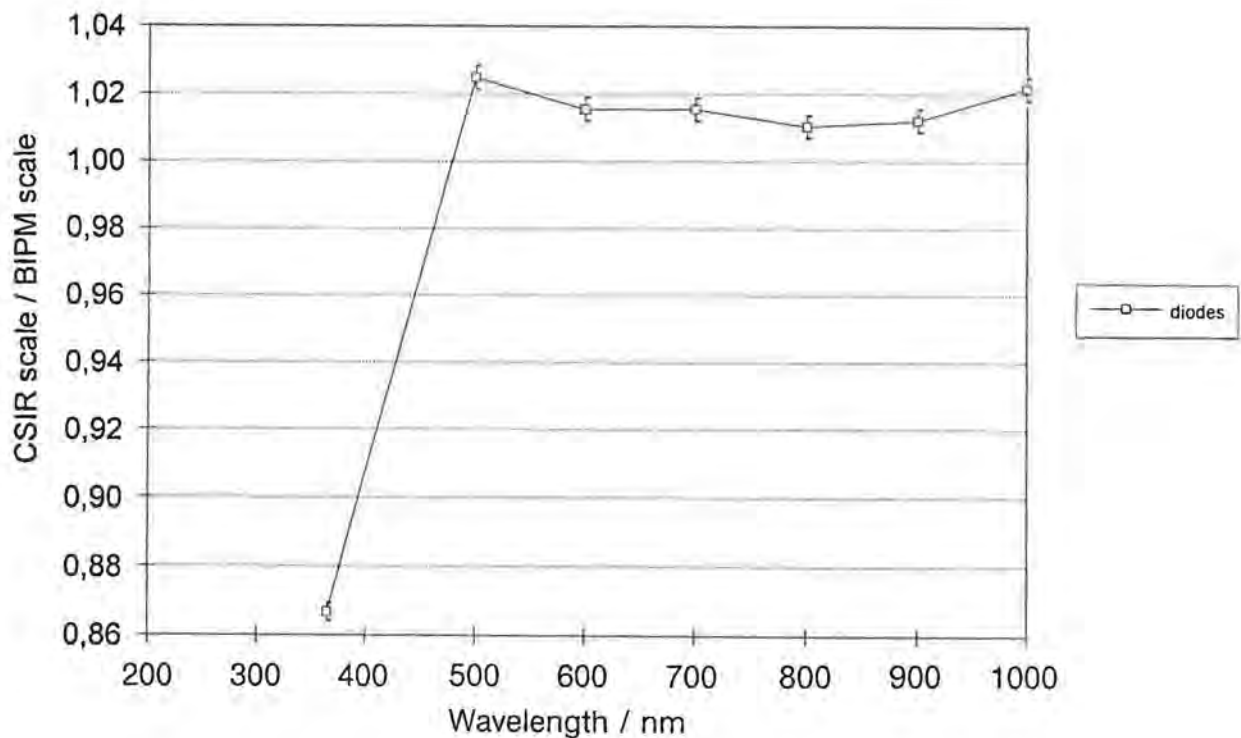
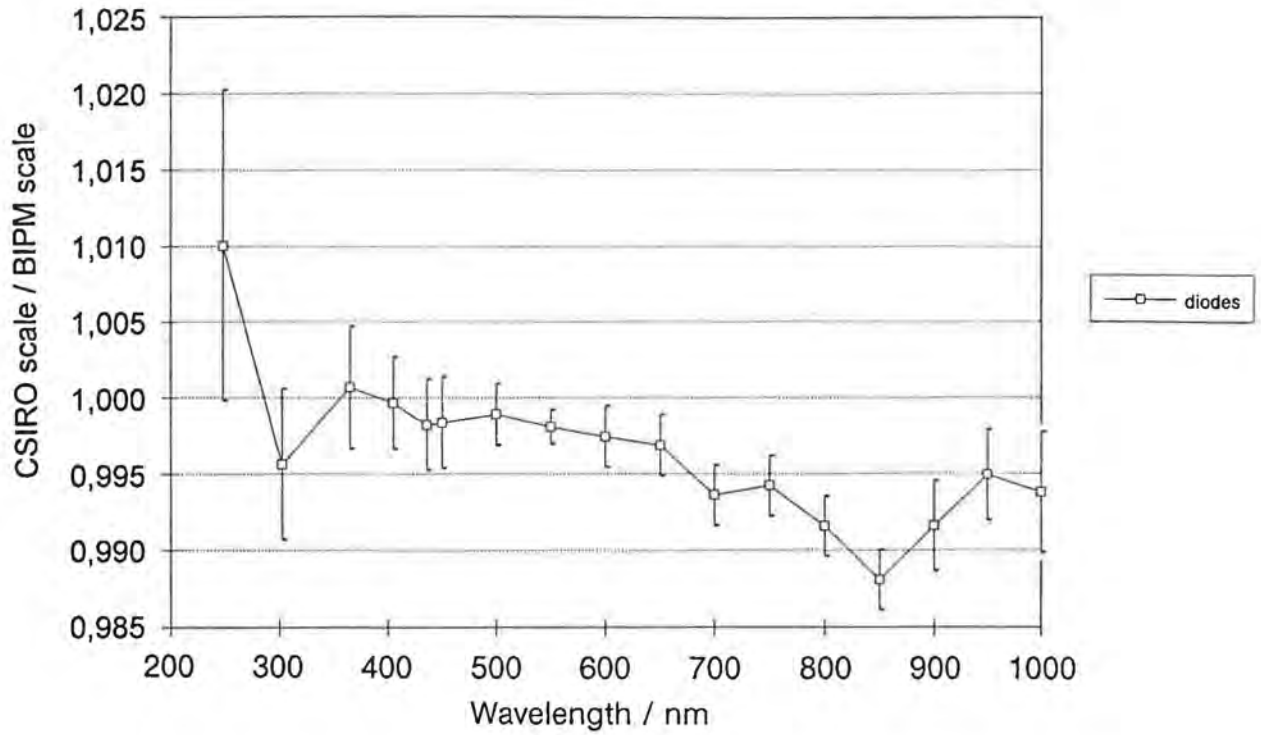
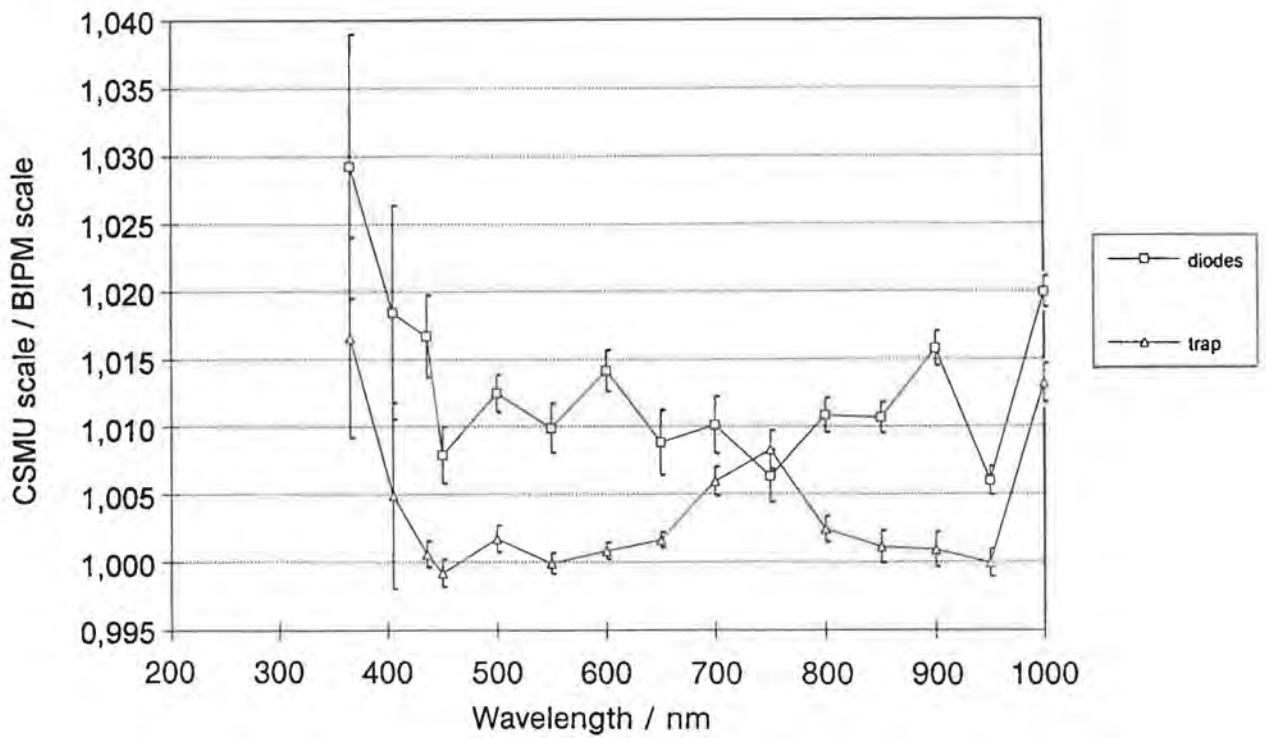


Fig.36: CSIR spectral responsivity scale compared to the scale of the BIPM.



**Fig.37:** CSIRO spectral responsivity scale compared to the scale of the BIPM.



**Fig.38:** CSMU spectral responsivity scale compared to the scale of the BIPM.

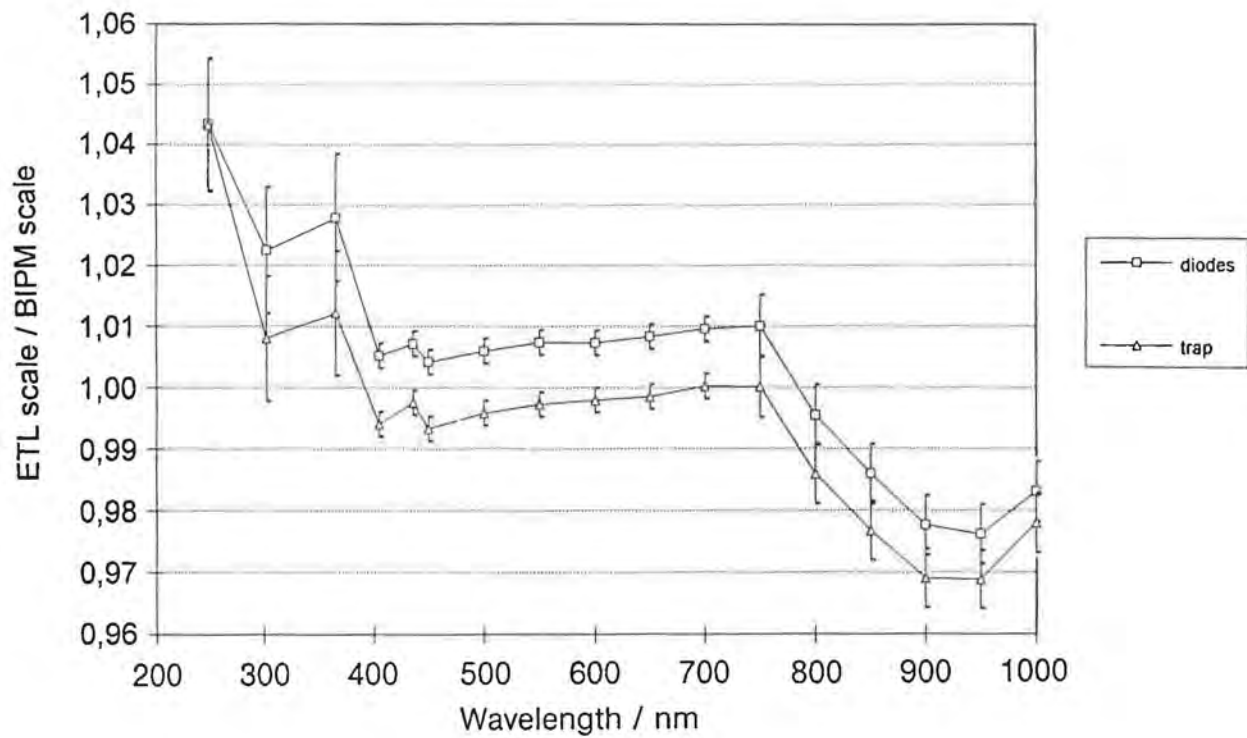


**Fig.39:** ETL spectral responsivity scale compared to the scale of the BIPM.

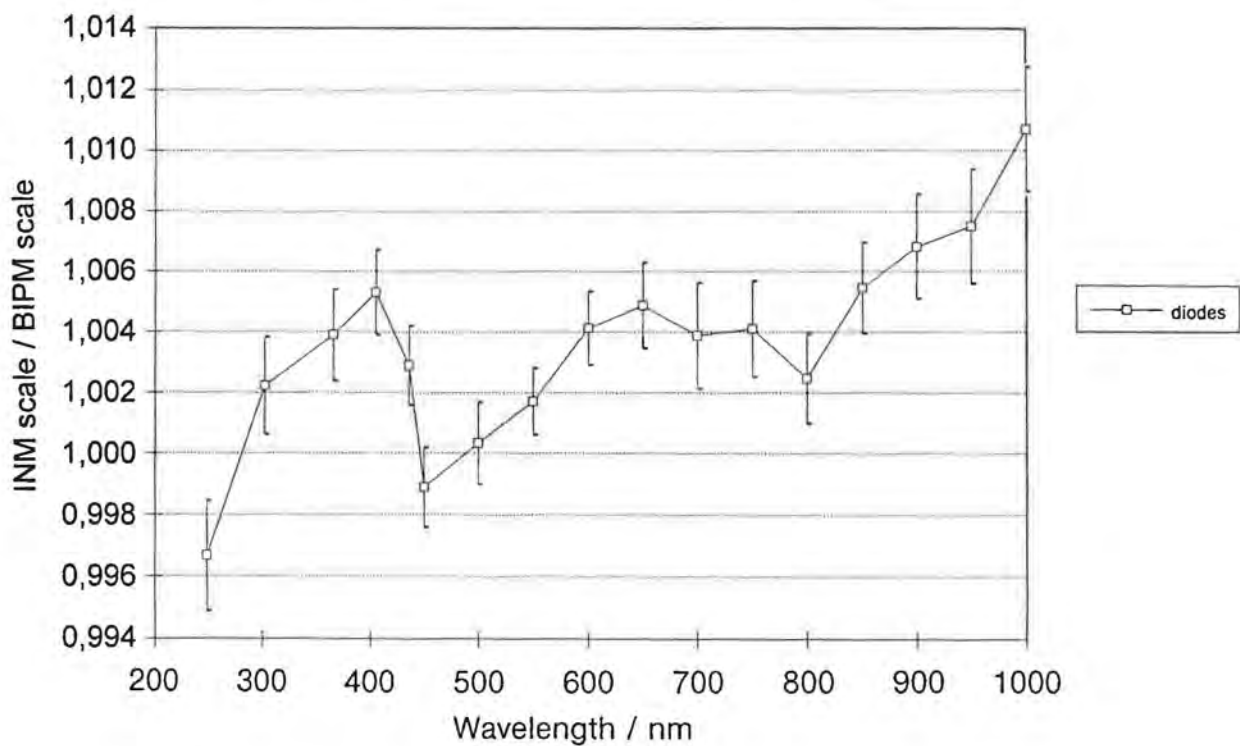


**Fig.40:** INM spectral responsivity scale compared to the scale of the BIPM.

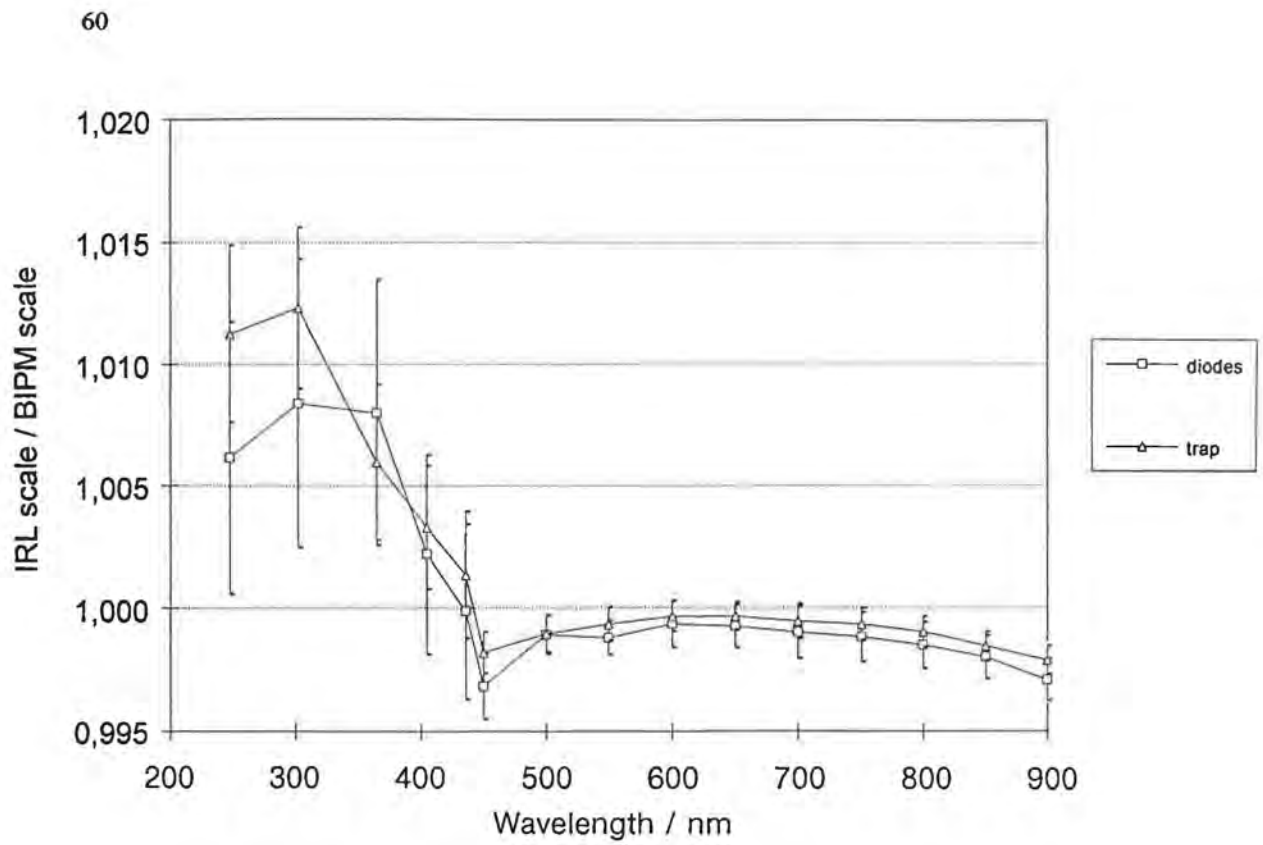


**Fig.41:** IRL spectral responsivity scale compared to the scale of the BIPM.

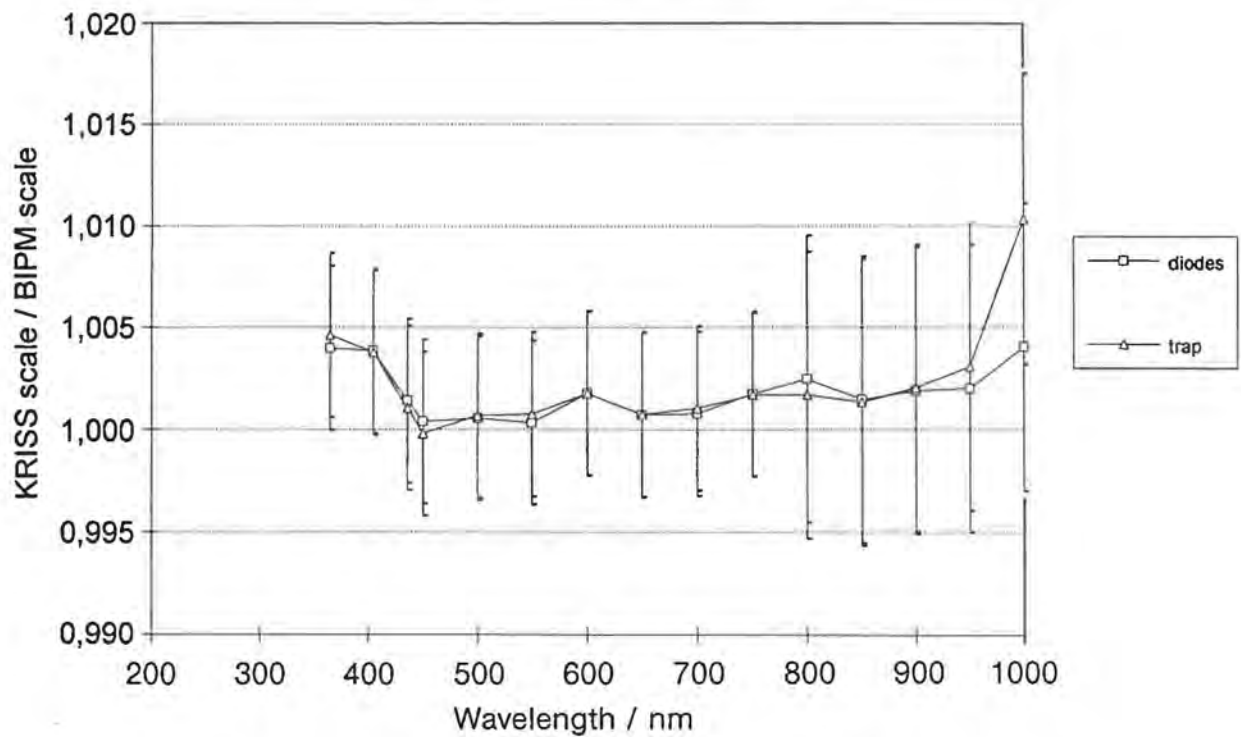


**Fig.42:** KRISS spectral responsivity scale compared to the scale of the BIPM.

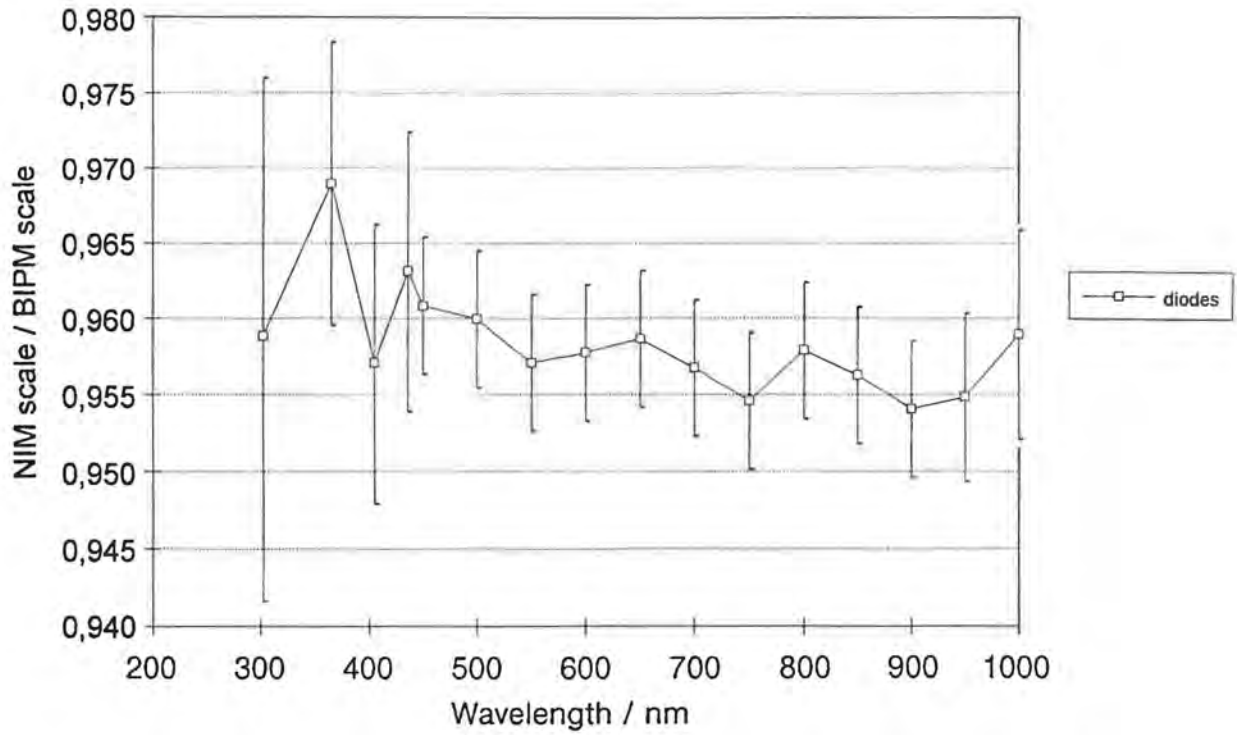


**Fig.43: NIM spectral responsivity scale compared to the scale of the BIPM.**

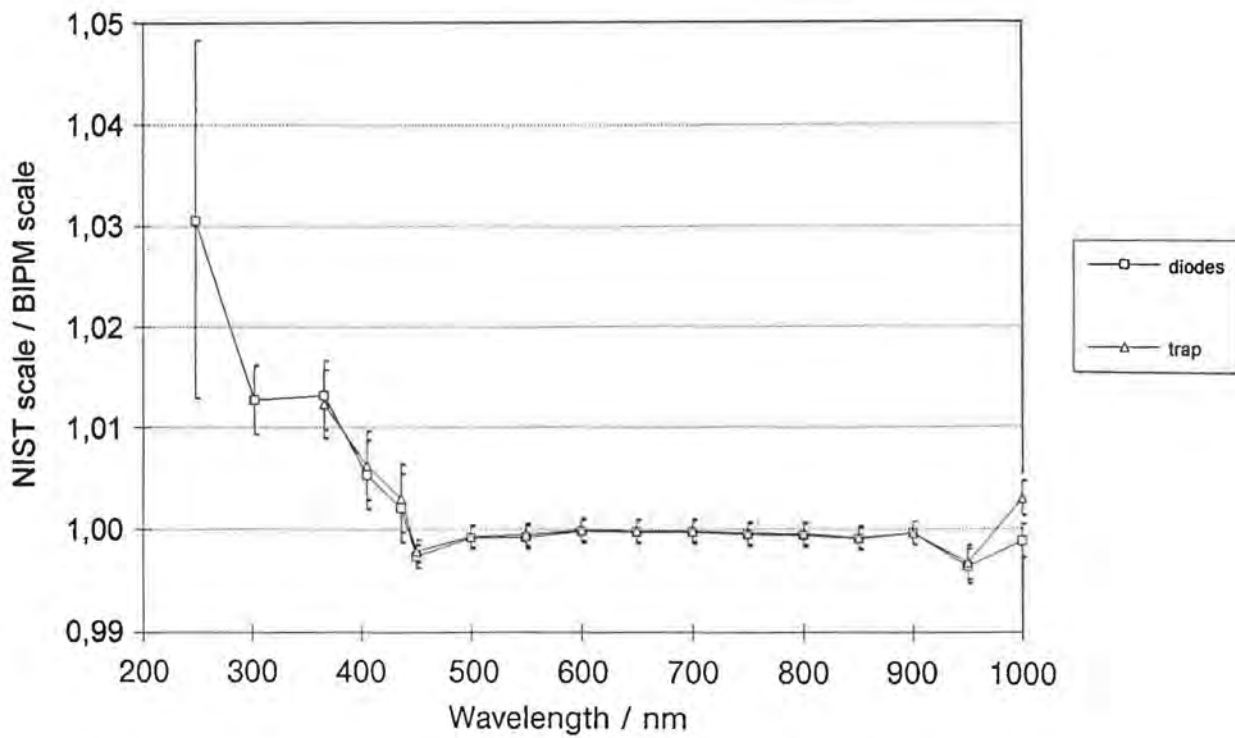


**Fig.44: NIST spectral responsivity scale compared to the scale of the BIPM.**

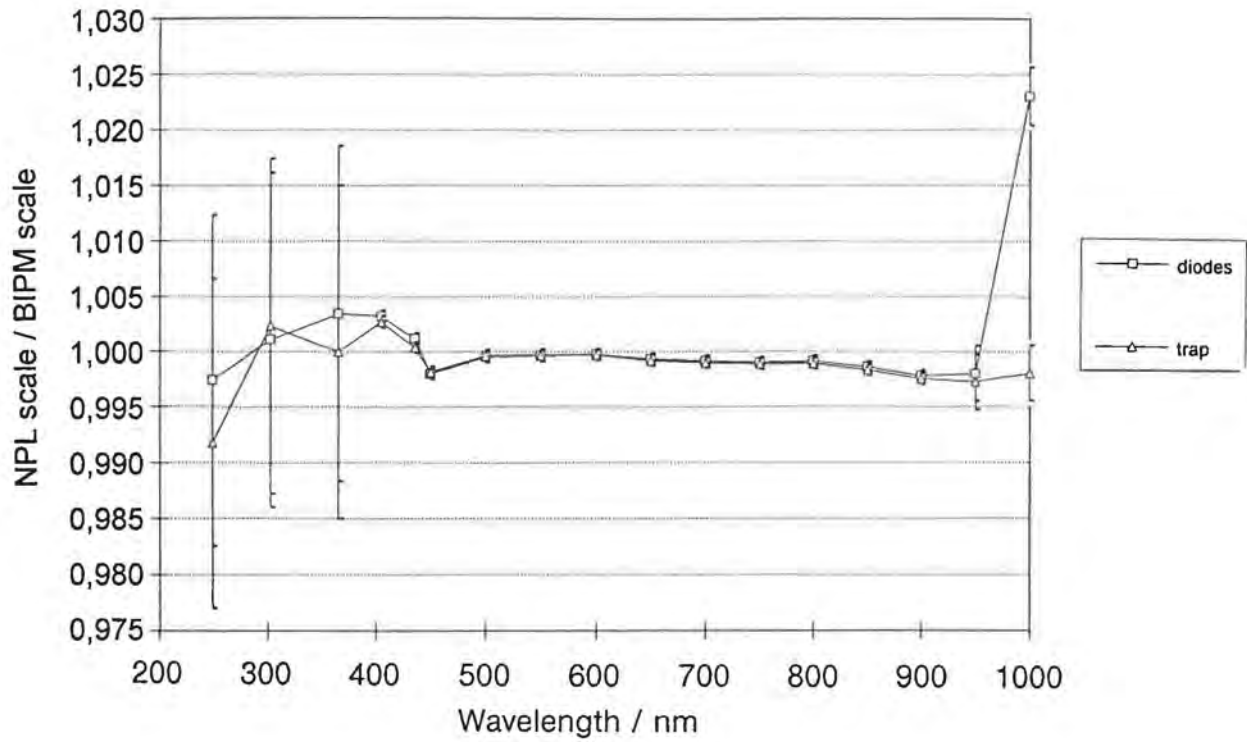


Fig.45: NPL spectral responsivity scale compared to the scale of the BIPM.

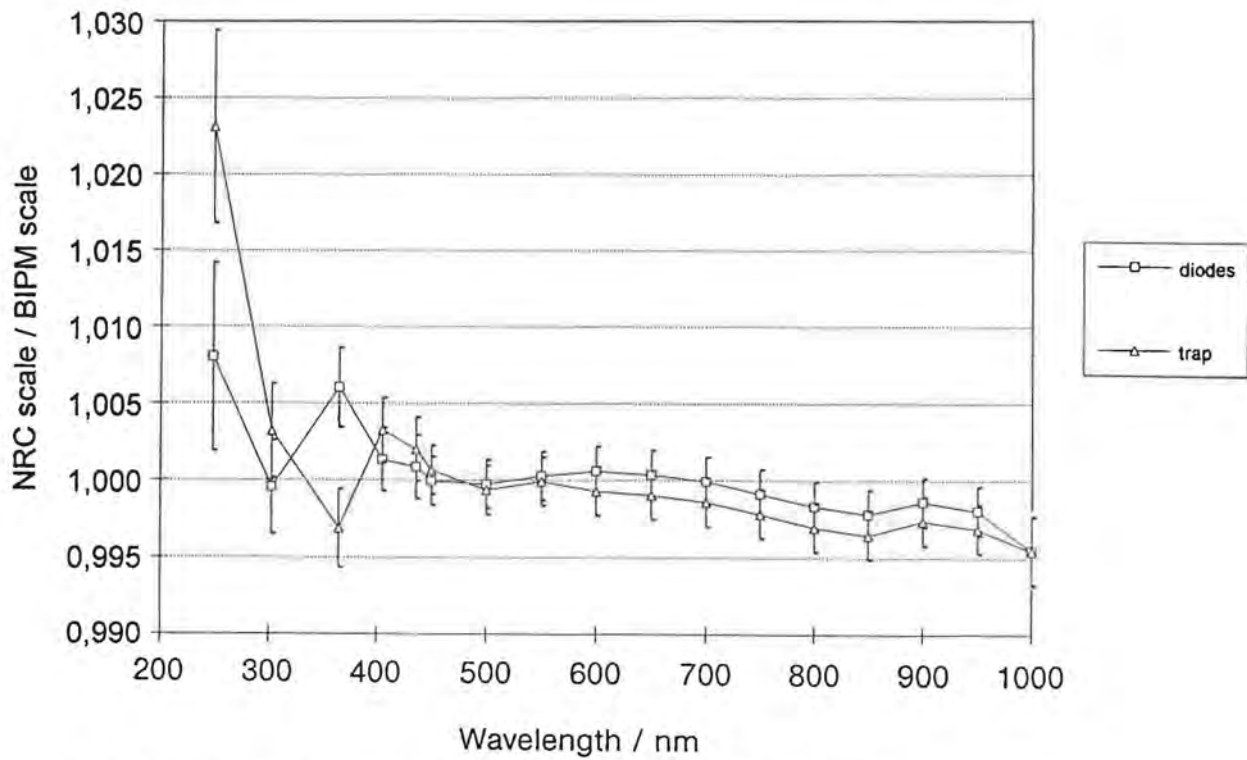


Fig.46: NRC spectral responsivity scale compared to the scale of the BIPM.

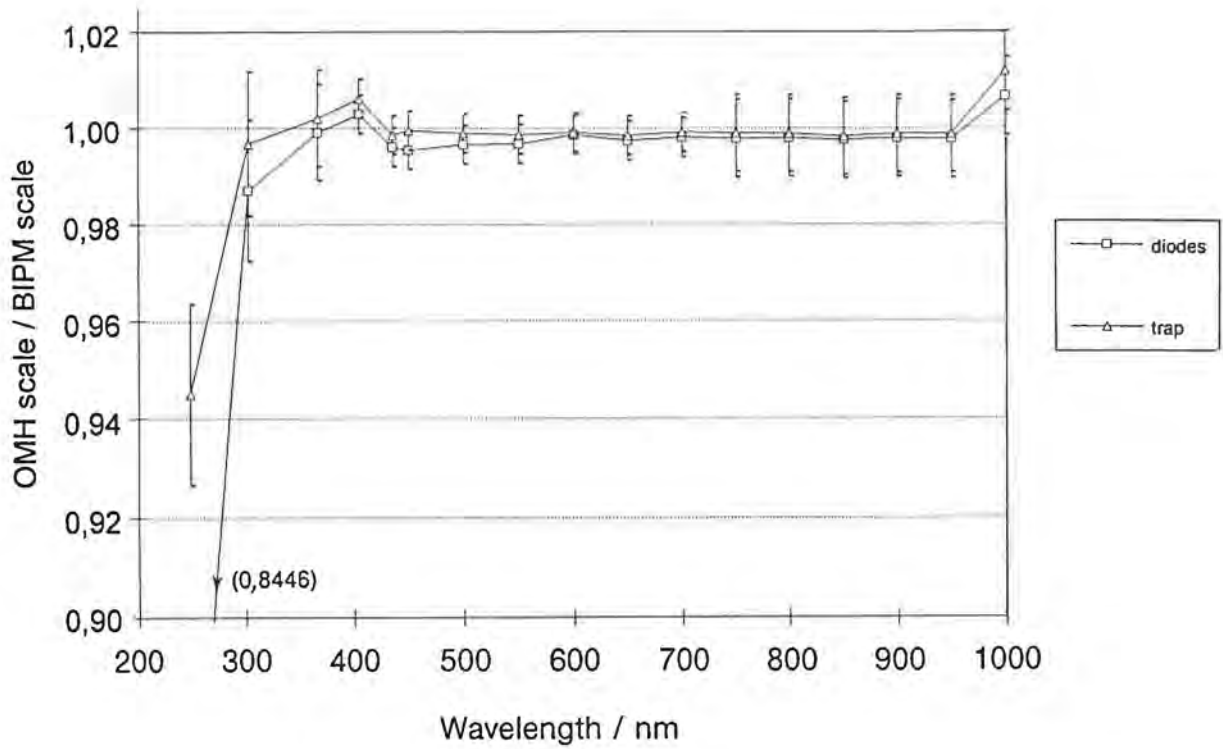


Fig.47: OMH spectral responsivity scale compared to the scale of the BIPM.

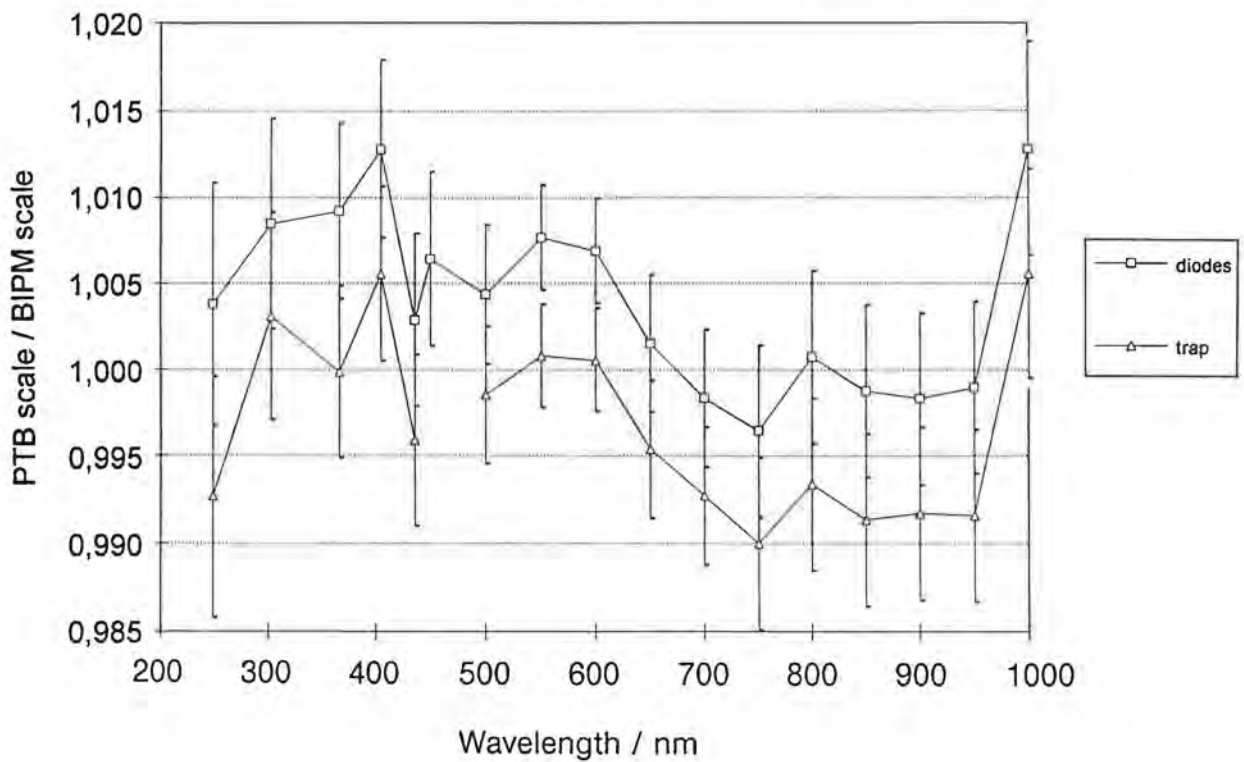


Fig.48: PTB spectral responsivity scale compared to the scale of the BIPM.

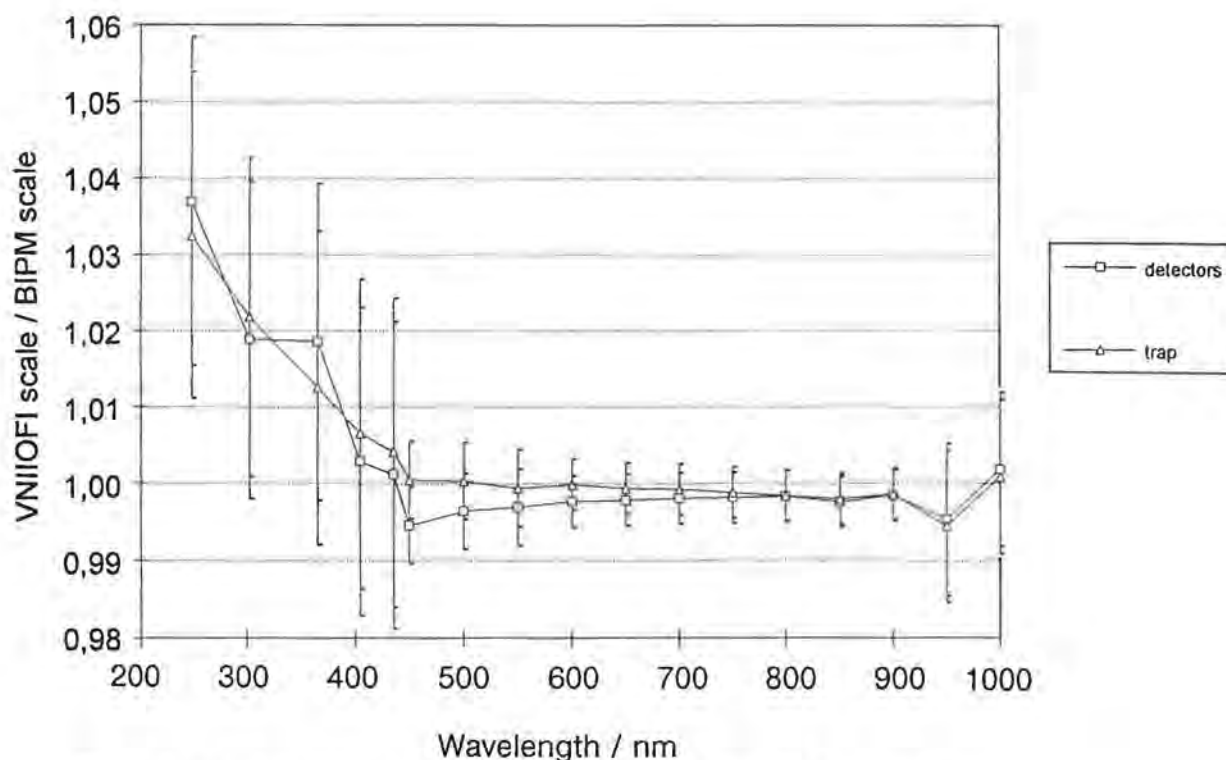
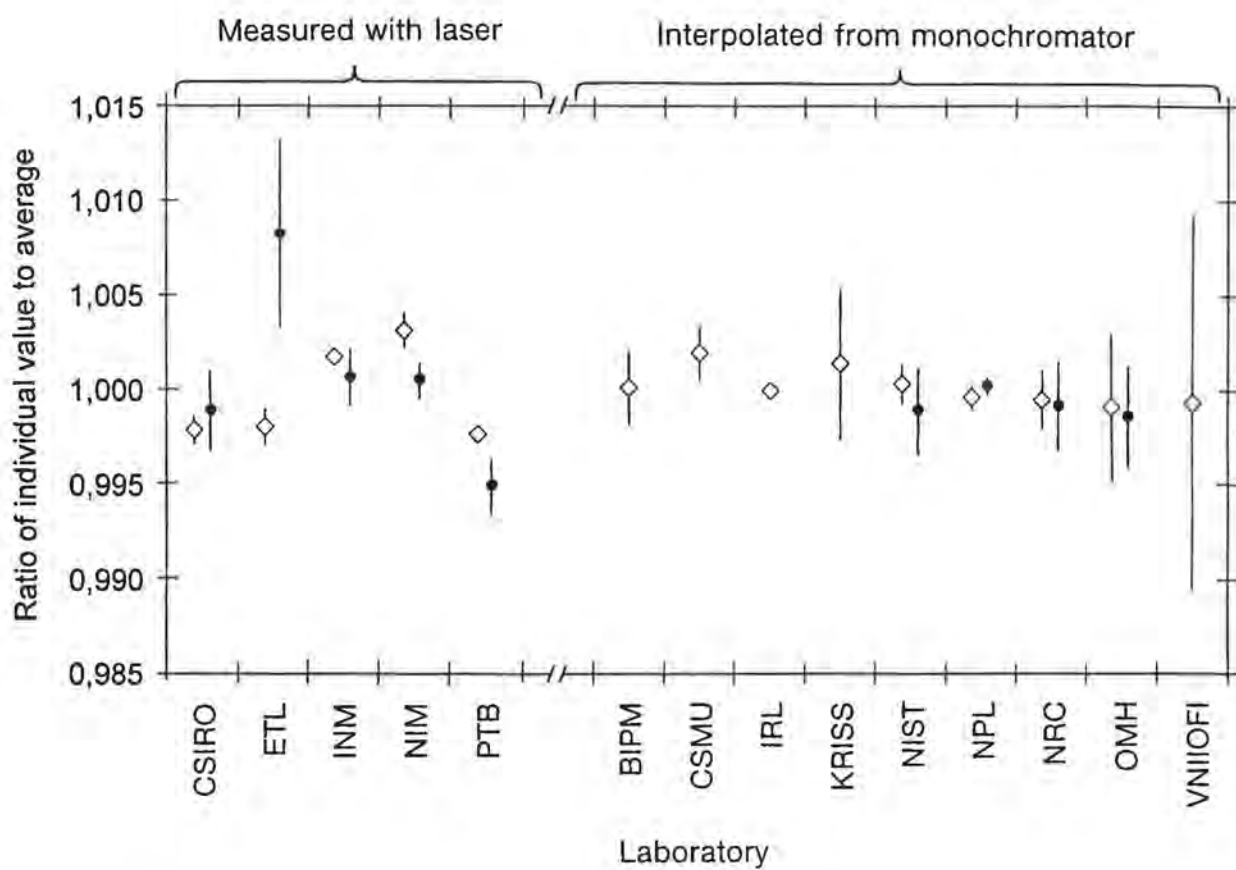


Fig.49: VNIIOFI spectral responsivity scale compared to the scale of the BIPM.

### TRAP MEASUREMENTS AT 633 nm

In the letter accompanying the detectors, the participating laboratories were invited to measure the trap detectors at as many laser wavelengths as possible. This was intended to be a test of whether absolute calibrations with traps using laser light were easier to carry out than measurements with a monochromator. Unfortunately, only a few laboratories did measurements using lasers and these measurements were almost all at 632,82 nm (He-Ne laser). Figure 50 shows the results of these calibrations. For those laboratories which measured the traps with a monochromator, the calibration of the trap at 633 nm by interpolation between 600 nm and 650 nm is displayed in Fig.50.

Included in the same figure are the results of the 1986 CCPR comparison of spectral responsivity at 633 nm [6]. The results from that comparison are given as the average between *pn* and *np* photodiodes. For this comparison the results from all laboratories were compared with the value obtained by the NIST. For the present comparison, the difference from the average is plotted.



**Fig.50.** Comparison of calibrations of the trap detector at 633 nm, using laser light or interpolation from monochromator measurements. Open diamonds: this comparison, Full circles: comparison of ref.6.

## *CONCLUSIONS*

In total, 14+4 national spectral responsivity scales were compared with the BIPM scale in the wavelength range from 250 nm to 1000 nm using silicon photodiodes and silicon trap detectors. The results from several laboratories are grouped closely together in the visible and near IR region, but data from other laboratories show large deviations from the grouped scales. The agreement in the UV region is poorer for all laboratories.

For some laboratories the deviation of the reported scale from the mean of the grouped results can be inferred from the reports submitted with the results of the comparison.

The results of the calibrations obtained with the trap detectors are generally in much better agreement than those obtained with the photodiodes. This is probably because the reflectances of the trap detectors are much lower than those of the photodiodes.

The repeated measurements of such a large batch of identical photodiodes over a wide spectral range and a long period of time, has allowed interesting conclusions to be drawn about the stability of these detectors, especially in the UV.

The comparison was concluded within the time allotted.

## *ACKNOWLEDGEMENT*

The authors are pleased to acknowledge the whole-hearted cooperation of all the participants. This allowed a great deal of useful information to be gathered during the comparison and made it possible to complete the comparison to the agreed schedule.

## APPENDIX A

### THE ABSOLUTE SPECTRAL RESPONSIVITY SCALE OF THE BIPM

The reference standards used at the BIPM are two QED-200 detectors. For radiation in the range from 450 nm to 700 nm their sensitivity can be calculated with a relative uncertainty of 0,1%. They are regularly checked by comparison with self-calibrated Si-photodiodes.

The precision of the absolute calibration procedure for photodiodes therefore depends on the wavelength range.

#### 1) Calibrations in the 450 nm - 700 nm range:

In the range 450 nm - 700 nm calibration is carried out by direct comparison with a QED. The uncertainty budget is summarized in the following table.

<i>Parameter</i>	<i>Relative uncertainty</i> <i>×10<sup>4</sup></i>	
	<i>type A</i>	<i>type B</i>
QED sensitivity		10
transfer QED / diode	2	
calibration of amplifiers		0,4
non-uniformity of source and detectors		0,4
monochromator wavelength calibration at 500 nm		3,6
<b>quadratic sum</b>	<b>11</b>	

**Table 8:** Uncertainty budget of the BIPM absolute responsivity scale (relative uncertainties, 1  $\sigma$ ), 450 nm - 700 nm.

#### 2) Calibrations in the 248 nm - 450 nm and 700 nm - 1000 nm ranges:

For the ranges 248 nm - 450 nm and 700 nm - 1000 nm, the calibration is carried out in two steps.

First, in the range 248 nm - 1000 nm, the relative spectral sensitivity of the photodiode is determined by comparison with that of a detector whose sensitivity is assumed to be not wavelength-dependent. The sensitivity of the spectrally flat detector need not be known, but it must be stable during the comparisons with the photodiode.

Second, this relative curve is attached to absolute points determined by comparison with the QED in the 400 nm - 700 nm range. After that, the photodiode is used as a working standard.

The spectrally flat detector used at the BIPM is a pyroelectric detector, which is used in conjunction with a mechanical light-chopper and a lock-in amplifier. When the signal from the pyroelectric detector is measured, the chopper is pushed into the beam by means of an automated translation table.

The pyroelectric detector is of commercial type: its sensor is cavity shaped and has a sensitive surface of  $1 \text{ cm}^2$  (Laser Precision RKP 575).

<i>Parameter</i>	<i>Relative uncertainty</i> $\times 10^4$	
	<i>type A</i>	<i>type B</i>
<b><i>Absolute calibration:</i></b>		
QED sensitivity		10
transfer QED / diode	2	
calibration of amplifiers		0,4
non-uniformity of detectors		0,4
<b><i>Quadratic sum</i></b>		10
<b><i>Interpolation</i></b>		
transfer pyroelectric detector diode (depending on wavelength)	4 - 40	
spectral non-flatness of pyr. detector		10
non-uniformities of pyr. detector and source		30
non-uniformity of diode		1
wavelength calibration		1,5 - 6
linearity lock-in amplifier		1
calibration of amplifiers		1
stray light		0
<b><i>Quadratic sum</i></b>		<b>32 - 51</b>
<b><i>Total uncertainty</i></b>		<b>34 - 52</b>

**Table 9:** Uncertainty budget of the BIPM absolute responsivity scale (relative uncertainties,  $1 \sigma$ ), below 450 nm and above 700 nm.

**APPENDIX B**  
**LIST OF ACRONYMS**

CSIR	Council for Scientific and Industrial Research, Division of Product Technology, Pretoria (South-Africa)
CSIRO	Commonwealth Scientific and Industrial Research Organisation, Division of Applied Physics, Lindfield (Australia)
CSMU	Ceskoslovensky Metrologicky Ustav, Bratislava and Prague (Czechoslovakia)
ETL	Electrotechnical Laboratory, Tsukuba (Japan)
FWHM	Full Width at Half Maximum
INM	Institut National de Métrologie, Paris (France)
IENGF	Istituto Elettrotecnico Nazionale Galileo Ferraris, Turin (Italy)
IOM	Instituto de Optica Dazs de Valdés, Madrid (Spain)
IR	Infra Red
IRL	Industrial Research Limited, Measurement Standards Laboratory of New Zealand, Lower Hutt, (New Zealand), formerly DSIR
KRISS	Korean Research Institute of Standards and Science, Taejon, (Republic of Korea)
NIM	National Institute of Metrology, Beijing (Peoples Republic of China)
NIST	National Institute of Standards and Technology, Gaithersburg (USA)
NPL	National Physical Laboratory, Teddington (Great Britain)
NRC	National Research Council, Ottawa (Canada)
OFMET	Eidgenössisches Amt für Messwesen, Wabern (Switzerland)
OMH	Országos Mérésügyi Hivatal, Budapest (Hungary)
PTB	Physikalisch Technische Bundesanstalt, Braunschweig (Germany)
QED	Quantum Efficiency Detector
QTH	Quartz Tungsten Halogen (lamp)
SP	Statens Provningsanstalt, Borås (Sweden)
UV	Ultra Violet
VSL	Van Swinden Laboratorium, Delft (The Netherlands)
VNIIOFI	All Russian Research Institute for Optophysical Measurements (Russia)
WRC	World Radiation Center, Davos (Switzerland)

**LIST OF FIGURES**

Fig.1 Photodiode assembly .....	9
Fig.2 Trap detector (schematic).....	10
Fig.3 Trap detector (3-D arrangement).....	10
Fig.4 Trap assembly drawing .....	11
Fig.5 View of first photodiode in trap.....	12
Fig.6 Optical path inside the trap detector .....	12
Fig.7 Experimental arrangement .....	16
Fig.8 Stability of the prime reference.....	19
Fig.9 Circuit diagram for the measurement of shunt resistance.....	20
Fig.10 Experimental arrangement of the linearity measurement .....	21
Fig.11 Temperature control of the photodiode.....	22
Fig.12 Measurement of the temperature coefficient .....	23
Fig.13 Temperature coefficient as function of wavelength .....	24
Fig.14 Uniformity of the photodiode.....	25
Fig.15 Uniformity of the trap detector .....	26
Fig.16 Intensity distribution over the spot.....	26
Fig.17 Relative standard deviation of measurements of photodiodes .....	29
Fig.18 Uncertainties in absolute calibrations per laboratory .....	30
Fig.19 Ratio of sensitivities using the QTH lamp.....	32
Fig.20 Ratio of sensitivities using the arc lamp.....	32
Fig.21 Evolution of QTH after arc measurements .....	33
Fig.22 Relative change in spectral sensitivity after exposure to UV (diodes) .....	35
Fig.23 Relative change in spectral sensitivity after exposure to UV (traps) .....	35
Fig.24 Spectral responsivity change of the diodes .....	37
Fig.25 Spectral responsivity change of the traps .....	37
Fig.26 Absolute spectral responsivity of the photodiodes in the UV .....	45
Fig.27 Individual scales compared to the BIPM scale (diodes).....	46
Fig.28 Individual scales compared to the BIPM scale (diodes), zoom .....	47
Fig.29 Spread of photodiode calibrations for each laboratory .....	49
Fig.30 Individual scales compared to the BIPM scale (traps) .....	50
Fig.31 Individual scales compared to the BIPM scale (traps), zoom.....	51
Fig.32 Spread of calibration between laboratories .....	52
Fig.33 Agreement of scales (diodes).....	53
Fig.34 Agreement of scales (traps) .....	53
Fig.35 Agreement of scales (diodes, same laboratories as for traps) .....	54
Fig.36 Comparison of the CSIR and the BIPM scales .....	57
Fig.37 Comparison of the CSIRO and the BIPM scales .....	58
Fig.38 Comparison of the CSMU and the BIPM scales.....	58
Fig.39 Comparison of the ETL and the BIPM scales .....	59
Fig.40 Comparison of the INM and the BIPM scales .....	59
Fig.41 Comparison of the IRL and the BIPM scales .....	60
Fig.42 Comparison of the KRISS and the BIPM scales.....	60
Fig.43 Comparison of the NIM and the BIPM scales .....	61
Fig.44 Comparison of the NIST and the BIPM scales.....	61
Fig.45 Comparison of the NPL and the BIPM scales .....	62
Fig.46 Comparison of the NRC and the BIPM scales.....	62
Fig.47 Comparison of the OMH and the BIPM scales.....	63
Fig.48 Comparison of the PTB and the BIPM scales .....	63
Fig.49 Comparison of the VNIIOFI and the BIPM scales .....	64
Fig.50 Comparison of calibrations of the trap detector at 633 nm .....	65

**LIST OF TABLES**

Tab.1 List of participants in the first round .....	7
Tab.2 List of second round participants.....	8
Tab.3 Assignment of detectors to the laboratories for the first round.....	13
Tab.4 Assignment of detectors to the laboratories for the second round .....	13
Tab.5 Uncertainties of the comparison .....	28
Tab.6 Spectral dependence of the uncertainties.....	28
Tab.7 National scales compared to the BIPM scale.....	56
Tab.8 Uncertainty budget BIPM scale, 450 nm - 700 nm.....	67
Tab.9 Uncertainty budget BIPM scale, below 450 nm and above 700 nm.....	68

**References**

- 1 International Lighting Vocabulary, CIE publication No.17.4, 1987
  
- 1 N.P. Fox, "Trap detectors and their properties", Proceedings of the Conference on New Developments and Applications in Optical Radiometry III, Davos, Switzerland 1990, published in: Metrologia, **28**, 197, 1991.
  
- 2 R. Köhler, R. Goebel, R. Pello, J. Bonhoure, "Effects of Humidity and Cleaning on the Sensitivity of Si Photodiodes", Proceedings of the Conference on New Developments and Applications in Optical Radiometry III, Davos, Switzerland 1990, published in: Metrologia, **28**, 211, 1991.
  
- 3 ISO, "Guide to the Expression of Uncertainty in Measurement", First Edition, 1993.
  
- 4 F. Lei, J. Fischer, "Characterization of Photodiodes in the UV and Visible Spectral Region Based on Cryogenic Radiometry", Metrologia **30**, 297, 1993.
  
- 5 G. Eppeldauer, private communication.
  
- 6 D.B. Thomas, "An International Comparison of Absolute Radiant Power Measurement Capabilities", J. Res. of Natl. Inst Stand. Technol, **95**, 525 (1990).

28 July, 1994

*Rapport BIPM-94/9 (a)*  
*document CCPR / 94 - 2 (a)*

***ANNEX TO THE REPORT ON THE INTERNATIONAL  
COMPARISON OF SPECTRAL RESPONSIVITY OF  
SILICON DETECTORS***

**R. Köhler, R. Goebel, R. Pello**

*Bureau International des Poids et Mesures, Pavillon de Breteuil, 92312 Sèvres,  
Cedex, France*





## **TABLE OF CONTENTS**

Abstract .....	5
Introduction .....	6
Participating laboratories .....	6
Time schedule .....	6
Detector sets.....	6
Protocol of the comparison .....	7
Ageing of the detectors.....	7
The national scales.....	9
IENGF .....	9
IOM .....	9
SP .....	9
VSL.....	10
Comparison of the national scales .....	10
Photodiodes .....	10
Traps.....	14
Individual national scales .....	17
New data.....	19
Conclusions .....	22
List of figures.....	23
List of tables.....	23



***ABSTRACT***

The spectral responsivity scales of 14 national standards laboratories have been compared within the wavelength range from 250 nm to 1000 nm using two different types of silicon photodetectors. The results of this comparison have been compiled in a BIPM report (BIPM-94/9, also a CCPR working document: CCPR / 94 -2). After distribution of the draft version of the report BIPM-94/9 to the participants, two of them communicated new values for their calibration data. This new data is given in this annex to the report.

In a second round of the comparison four more laboratories participated. The results of the comparison for these laboratories are also given here.

## ***INTRODUCTION***

This report is only an annex to the main report BIPM-94/9. It thus does not go into technical details about the preparation of the detectors or the experimental procedures, as they were exactly as for the first group of participants. It has to be read together with the main report.

## ***PARTICIPATING LABORATORIES***

The participants in this second round of the comparison are listed in Table 1

IENGF	Italy
IOM	Spain
SP	Sweden
VSL	The Netherlands

**Table 1A:** Participants in the second round.

## ***TIME SCHEDULE OF THE COMPARISON***

The detectors were dispatched at the end of April 1993 to the participants. As for the first group, a period of five months was given for the return of the detectors to the BIPM, the deadline being 1 October 1993.

## ***DETECTOR SETS USED***

The detector sets for the second round were sets which had already been used in the first round. The assignment was as follows, shown also is the laboratory at which the detectors had been during the first round of the comparison:

Batch	diode 1	diode 2	diode 3	trap	laboratory 2nd round	laboratory 1st round
3	3	35	27	4	IENGF	NPL
5	5	37	40	6	SP	CSIR
7	7	43	31	13	VSL	CSIRO
9	9	28	48	11	IOM	IRL

**Table 2A:** Assignment of detectors to the laboratories for the first and second round.

## ***PROTOCOL OF THE COMPARISON***

The protocol for the comparison was exactly as for the first round, all parameters (e.g. spotsize, wavelengths etc.) were kept the same. The laboratories of the second round did not have any supplementary information which was not available to participants in the first round, especially the results of the first round comparison.

## ***AGEING OF THE DETECTORS***

Similar to what was done for the first round, the detectors' spectral responsivities before they were sent to the participants were compared to the one measured directly after they had returned to the BIPM. The same prime reference as in the first part was used as the reference detector for the observation of an eventual change in responsivity. Again, it was monitored against a group of secondary references.

The results are shown in Figs. 1A (photodiodes) and 2A (traps). The diodes show an excellent stability above 400 nm, except for two cases, both had been at the VSL. On visual inspection traces of possibly bad cleaning could be observed on these two devices, explaining the drift in responsivity before and after the laboratory.

The traps show a somewhat poorer stability with a change in responsivity of 3 parts in  $10^4$  above 450 nm.

The data of the relative spectral responsivity measurements done at the BIPM after return of the detectors were used to compare the national scales to the BIPM absolute responsivity scale.

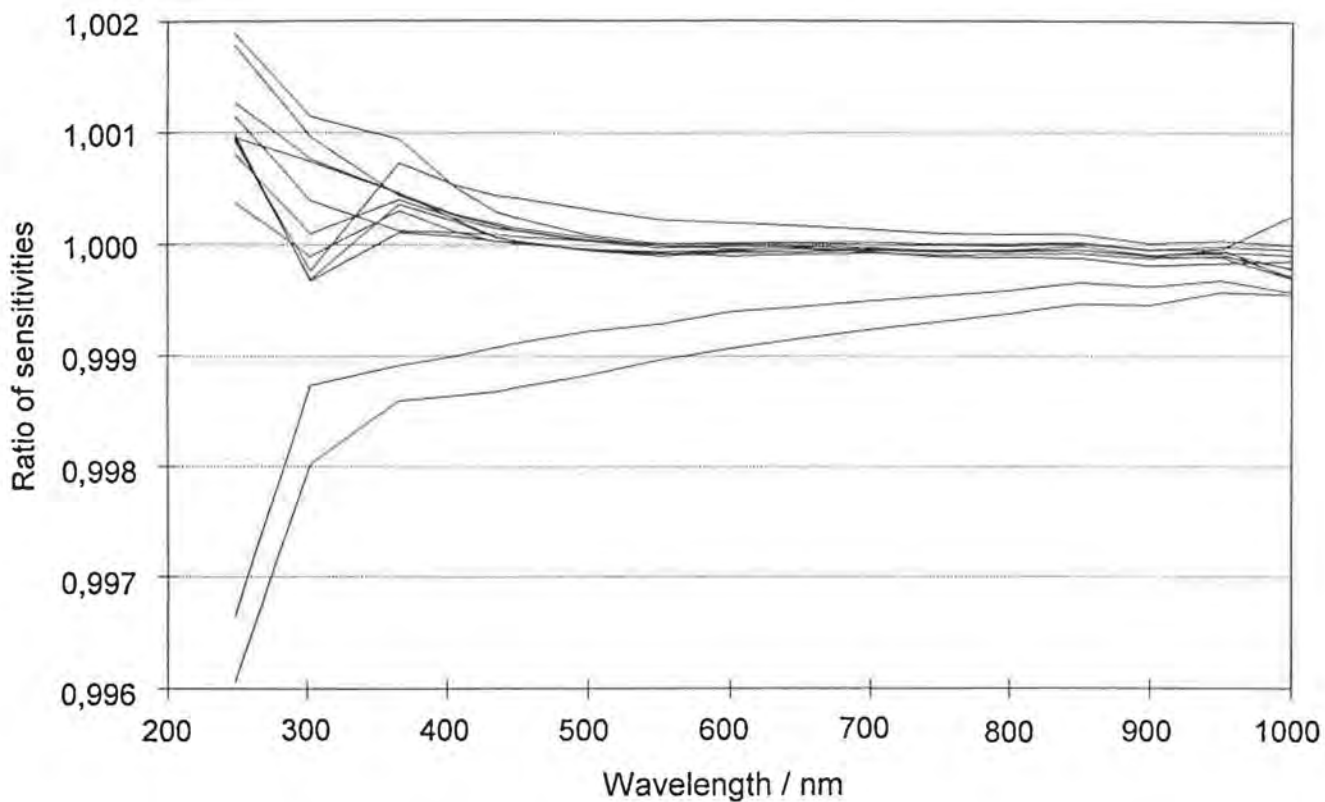


**Fig.1A:** Change in spectral responsivity of diodes: Ratio of diode sensitivity after return from the participant to that found before sending to participant.

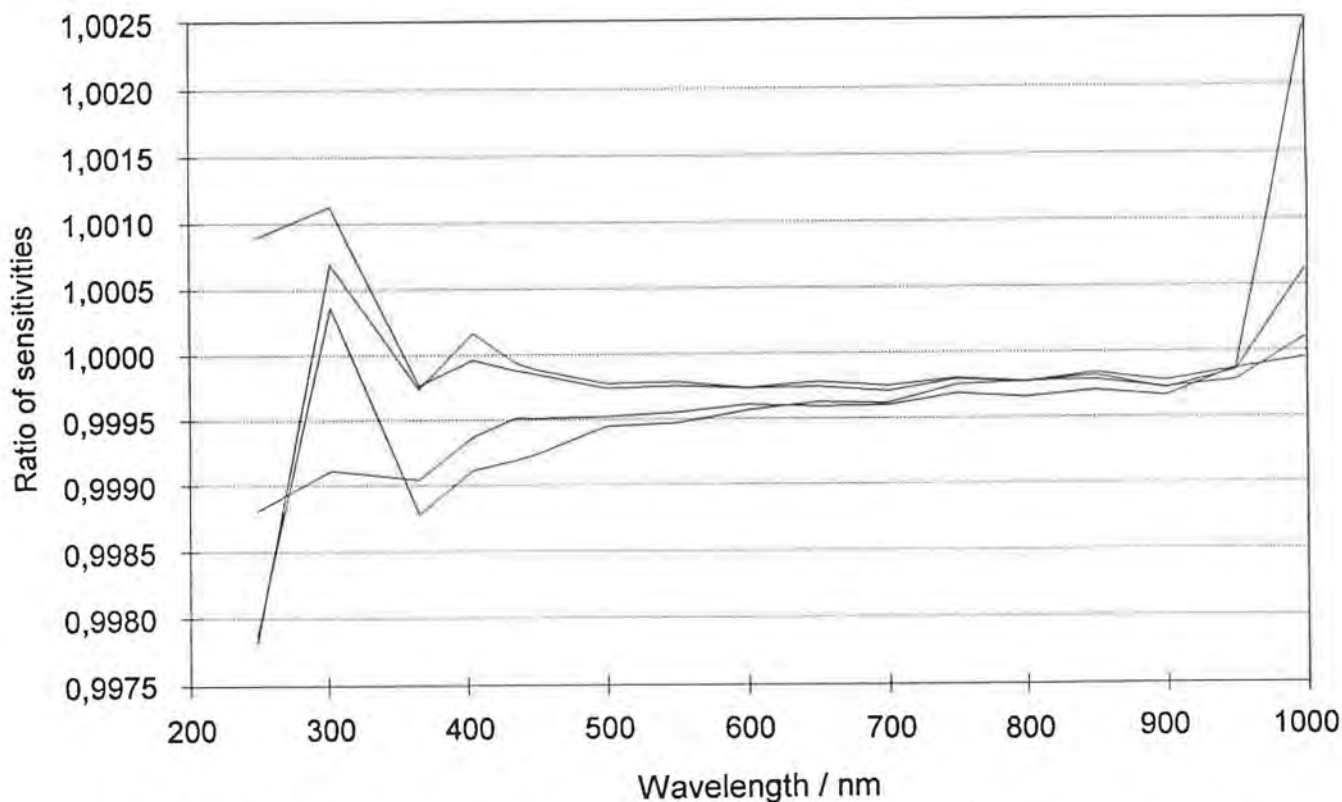


**Fig.2A:** : Ratio of trap sensitivity after return from the participant to that found before sending to participant..

## ***THE NATIONAL SCALES***

### ***IENGF (Turin, Italy)***

At the IENGF the photodiodes were measured at 365 nm and at all wavelengths between 400 nm and 900 nm (inclusive), the trap detector has not been calibrated. The sources were a metalhalide lamp and an incandescent lamp in combination with a Czerny-Turner double monochromator or interference filters. The absolute spectral responsivity scale is deduced using a QED-200 or an ESR.

Spot size:	5 mm diameter
Temperature:	25 °C
Beam divergence (full angle):	No information given.
Bandwidth:	4 nm
Radiant power:	150 $\mu$ W (max.)

### ***IOM (Madrid, Spain)***

IOM used a commercial ECPR (Laser Precision RS-5900) which has been checked against a CRI cryogenic radiometer as an absolute standard. The detectors were calibrated directly against the ECPR if the power was above 10  $\mu$ W, otherwise a silicon detector was used as a transfer standard. The detectors were calibrated at all wavelengths between 365 nm and 1000 nm (inclusive).

Spot size:	5 mm diameter (diodes), 3 mm (trap).
Temperature:	(22 $\pm$ 0,5) °C
Beam divergence (full angle):	3° - 4,2° depending on source and detector.
Bandwidth:	3,2 nm
Radiant power:	30 $\mu$ W - 110 $\mu$ W (Hg source) 1,5 $\mu$ W - 20 $\mu$ W (QTH source)

### ***SP (Borås, Sweden)***

SP used a ECPR which were calibrated against a group of QED-100 and QED-200 detectors. The QED's themselves were checked against a cryogenic radiometer at VTT, Finland. For the calibration an EG&G UV444B photodiode was used as a working standard for wavelengths above 450 nm. The detectors were calibrated at all wavelengths. A Hg arc lamp or QTH lamp were used together with a monochromator.

Spot size:	5 mm diameter
Temperature:	21,5 °C - 23,5 °C
Beam divergence (full angle):	8 ° (diodes), nearly parallel (trap)
Bandwidth:	2,5 nm - 8 nm.
Radiant power:	150 μW (max.)

### *VSL (Delft, The Netherlands)*

A single grating Czerny-Turner monochromator was used in conjunction with an Ar arc or QTH lamps. The VSL scale was deduced from Hamamatsu S1337 photodiodes which had previously been calibrated at the NRC for absolute spectral responsivity. For wavelengths needed for the comparison but at which the photodiodes had not been calibrated at the NRC an interpolation formula was applied. The detectors were calibrated at all wavelengths.

Spot size:	2,5 mm diameter
Temperature:	22,5 °C
Beam divergence (full angle):	4,6
Bandwidth:	2 nm
Radiant power:	4 μW (max.)

## *COMPARISON OF THE NATIONAL SCALES*

### *PHOTODIODES*

Fig.3A is the equivalent of Fig.27 of the original report, it shows the ratio of the individual national spectral responsivity scales to that of the BIPM. The scale of the graph is identical to the one of Fig.27 of the original report to allow a better comparison of the figures.

It is obvious that there is a substantial spread between the individual national scales of the four laboratories (about 1% in general). Only the VSL curve shows a good agreement with the BIPM scale and hence with the group of four laboratories which were grouped closely together in the main part of the comparison.

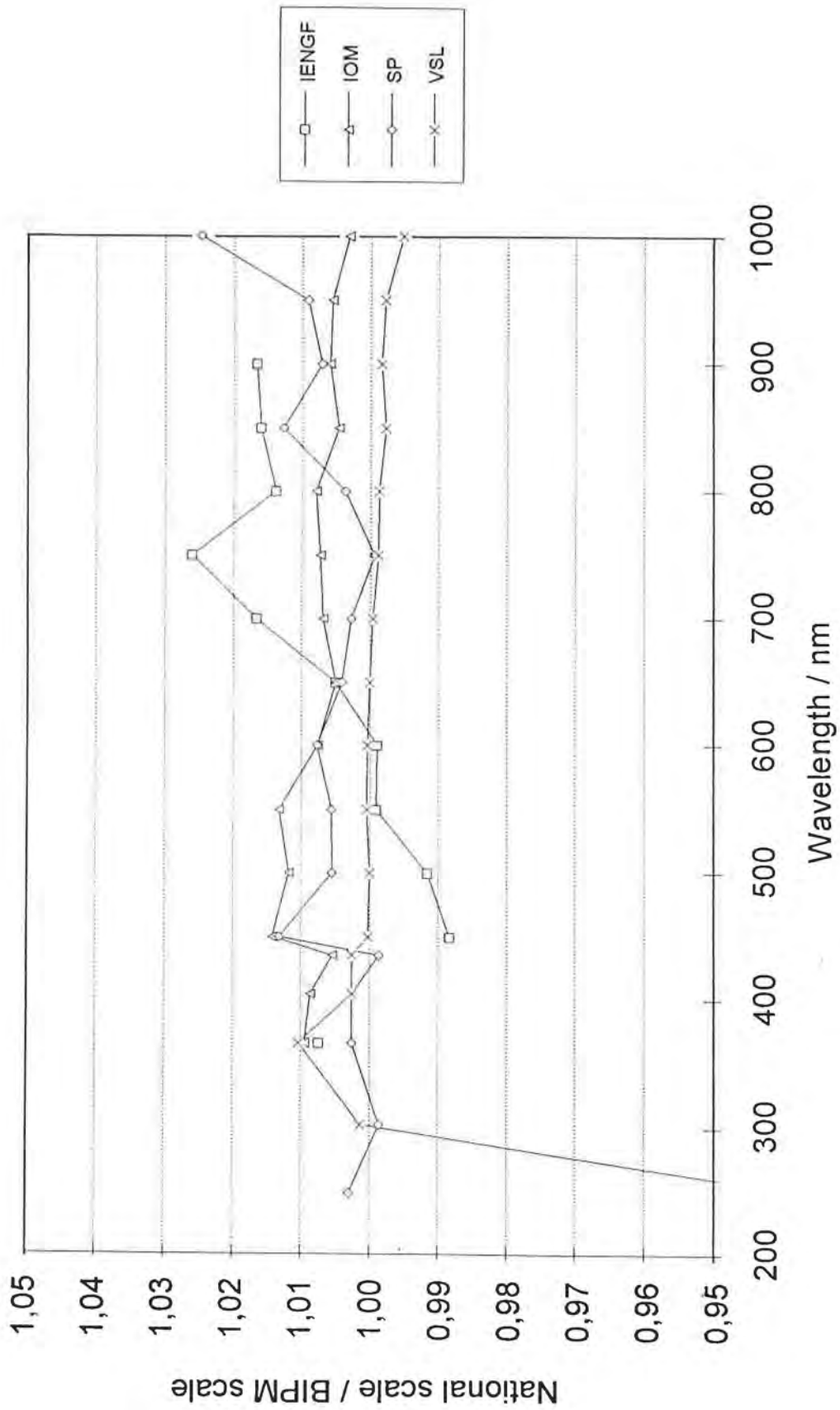
Fig.4A is the same as Fig.2A, zoomed to  $\pm 1\%$  as Fig.28 in the main report.

Table 3A gives the numerical data corresponding to the figures. From this table the ratio of the scales of any two participants can be deduced as in the ratio the BIPM value is eliminated.

lambda / nm	individual scale / BIPM scale			
<b>PHOTODIODES</b>				
	IENGF	IOM	SP	VSL
248,3			1,00307	0,93612
302,2			0,99865	1,00139
366,0	1,00742	1,00951	1,00259	1,01034
404,7		1,00864	1,00260	1,00260
435,8		1,00550	0,99870	1,00260
450,0	0,98832	1,01424	1,01317	1,00033
500,0	0,99156	1,01184	1,00556	1,00008
550,0	0,99915	1,01330	1,00565	1,00048
600,0	0,99898	1,00772	1,00776	1,00043
650,0	1,00510	1,00512	1,00423	1,00007
700,0	1,01664	1,00697	1,00281	0,99967
750,0	1,02610	1,00738	0,99936	0,99884
800,0	1,01378	1,00797	1,00369	0,99875
850,0	1,01604	1,00468	1,01271	0,99781
900,0	1,01663	1,00599	1,00715	0,99846
950,0		1,00562	1,00917	0,99790
1000,0		1,00314	1,02470	0,99525
<b>TRAPS</b>				
248,3			0,99982	0,91987
302,2	D		1,00165	0,99814
366,0	E	1,00515	1,00297	0,98837
404,7	R	1,00424	0,99934	0,99538
435,8	S	1,00302	1,00200	1,00074
450,0	S	1,00313	1,00770	0,99639
500,0	A	1,00605	0,99805	0,99595
550,0	M	1,00494	0,99808	0,99712
600,0	E	1,00190	0,99935	0,99735
650,0		1,00239	0,99408	0,99741
700,0	T	1,00406	0,99350	0,99778
750,0		1,00564	0,98982	0,99723
800,0	N	1,00340	0,99431	0,99936
850,0		1,00177	1,00110	0,99658
900,0		1,00307	0,99656	0,99658
950,0		1,00175	0,99692	0,99507
1000,0		1,00367	1,00371	0,99469

**Tab.3A:** Individual national scales compared to the BIPM scale.

As has been explained in the main report, it is possible to estimate the spread in the absolute calibrations of an individual laboratory from the results for the different photodiodes. Fig.5A (which corresponds to Fig.29) shows the spread as a function of wavelength.



**Fig.3A:** Comparison of the individual national scales, derived from the diodes, with the spectral responsivity scale of the BIPM

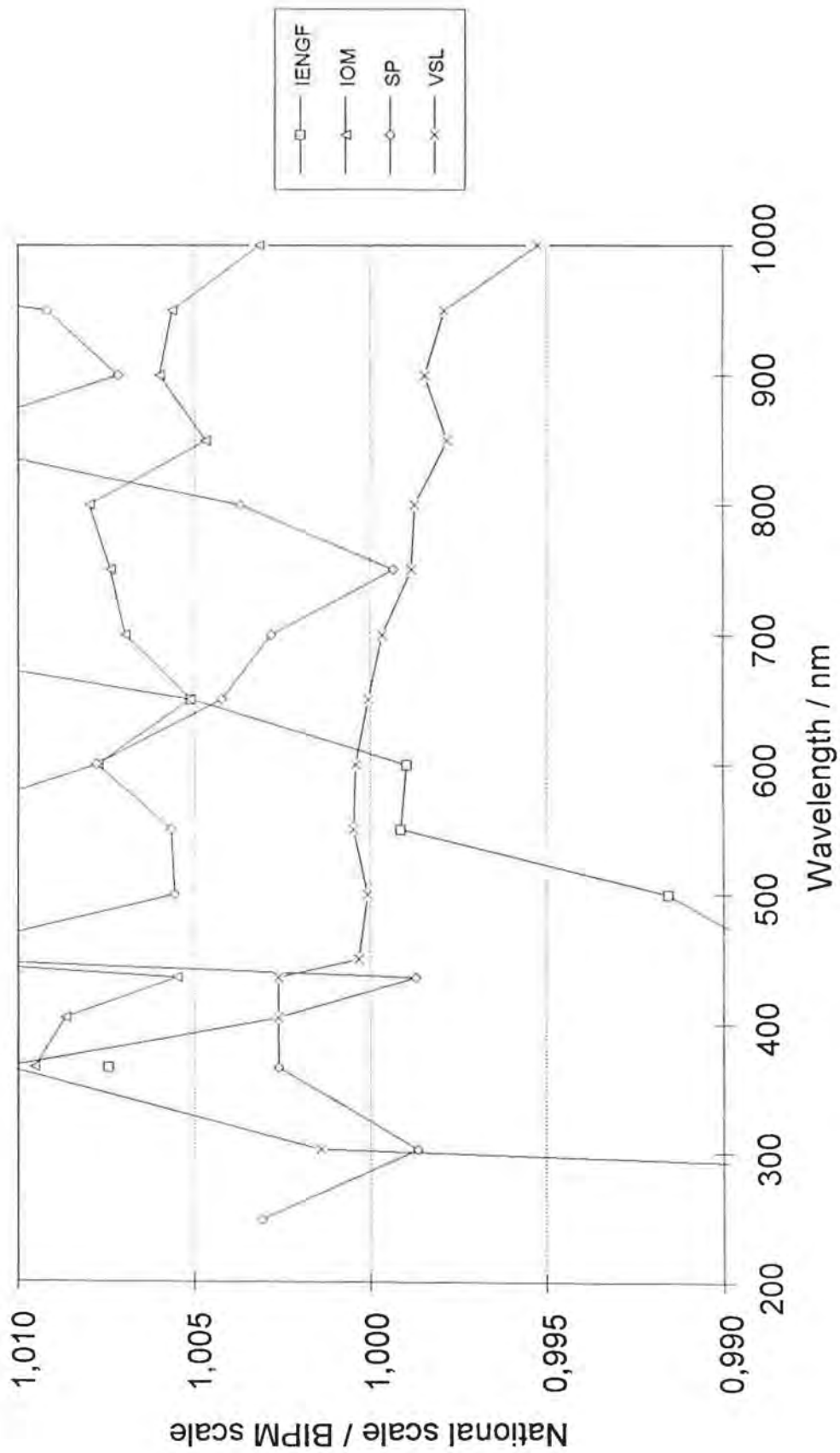


**Fig.4A:** Comparison of the individual national scales, derived from the diodes, with the spectral responsivity scale of the BIPM (zoom).

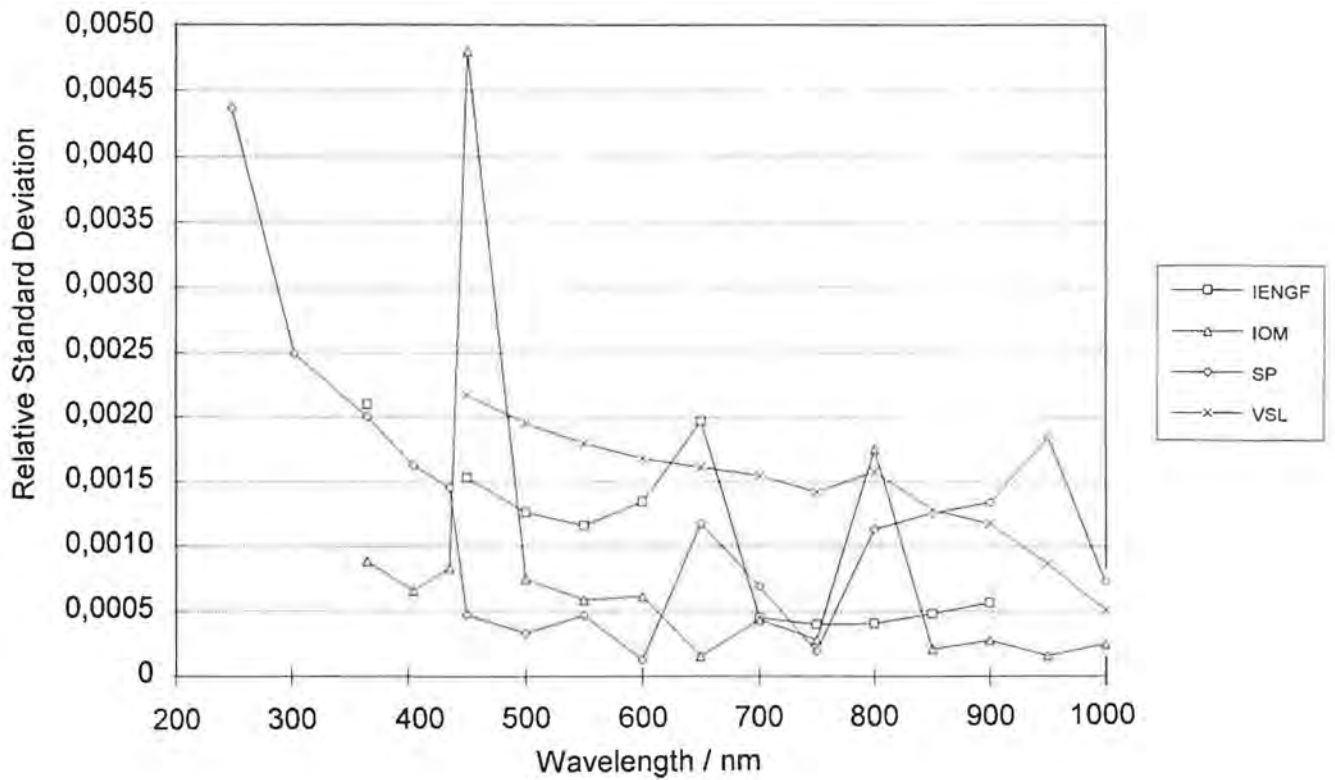


**Fig.5A:** Spread of calibration of the three photodiodes for each laboratory.

### **TRAPS**

The IENGF did not measure the trap detector. The results of the other three laboratories are shown in Fig.6A and Fig.7A, corresponding to Figs.30 and 31 in the main report.

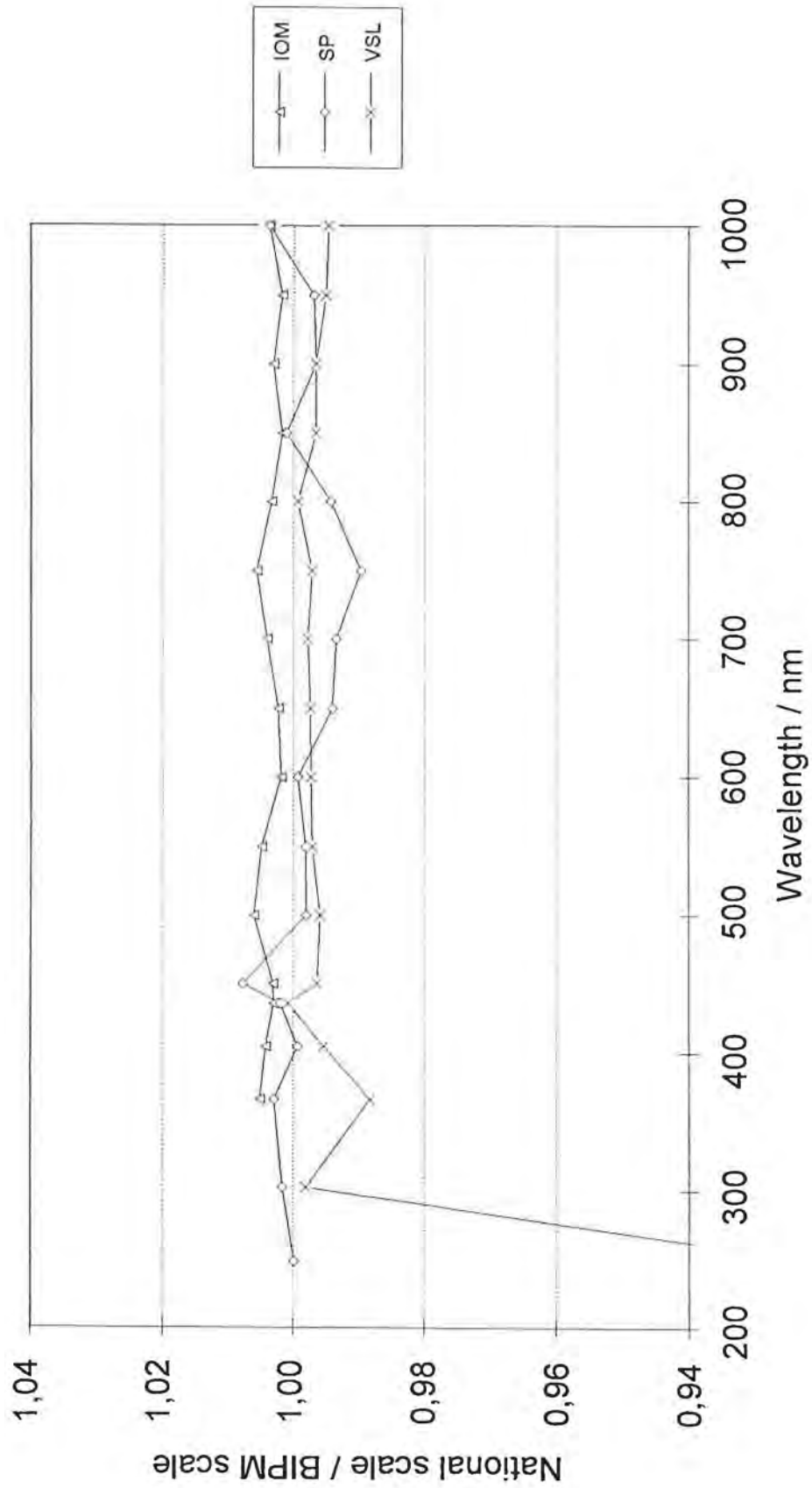


**Fig.6A:** Comparison of the individual national scales, derived from the traps, with the spectral responsivity scale of the BIPM .

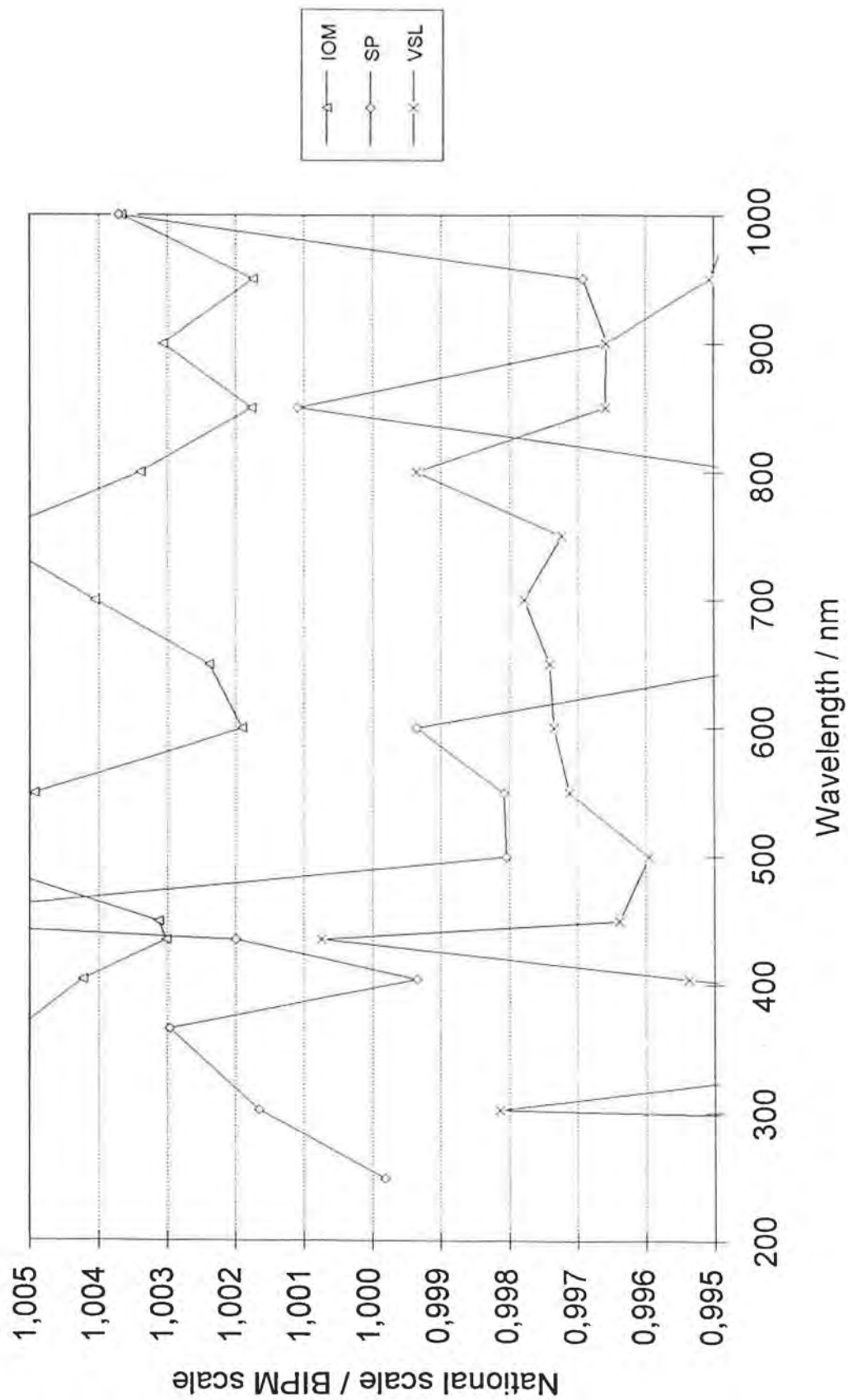
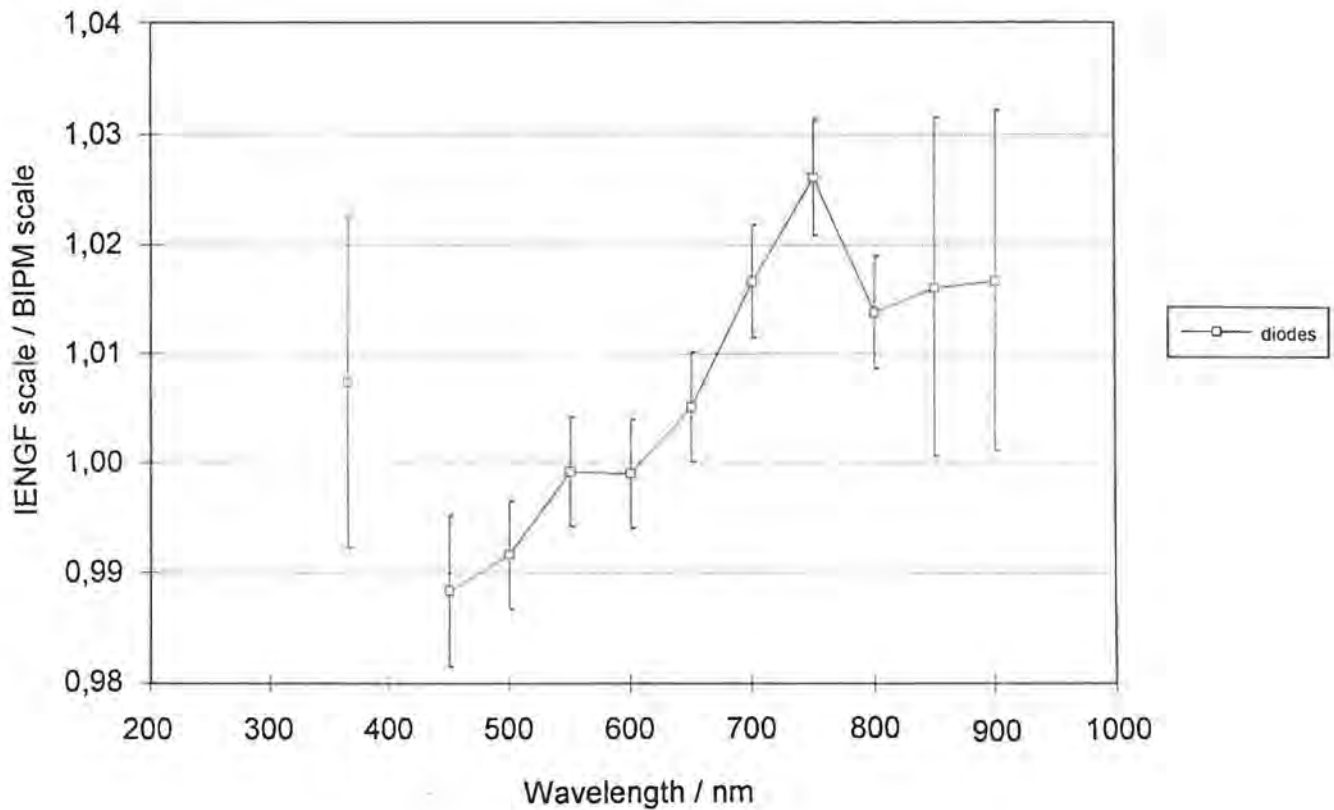


Fig.7A: Comparison of the individual national scales, derived from the traps, with the spectral responsivity scale of the BIPM (zoom).

**INDIVIDUAL NATIONAL SCALES)**

Figures 8A to 11A show the ratios of the individual scales to the BIPM scale for the photodiodes and the trap detector (if measured) as a function of wavelength. All laboratories which have calibrated the photodiodes as well as the trap detector show a significant and systematic difference in the calibrations of these two types of detectors.



**Fig.8A:** IENGf spectral responsivity scale compared to the scale of the BIPM.

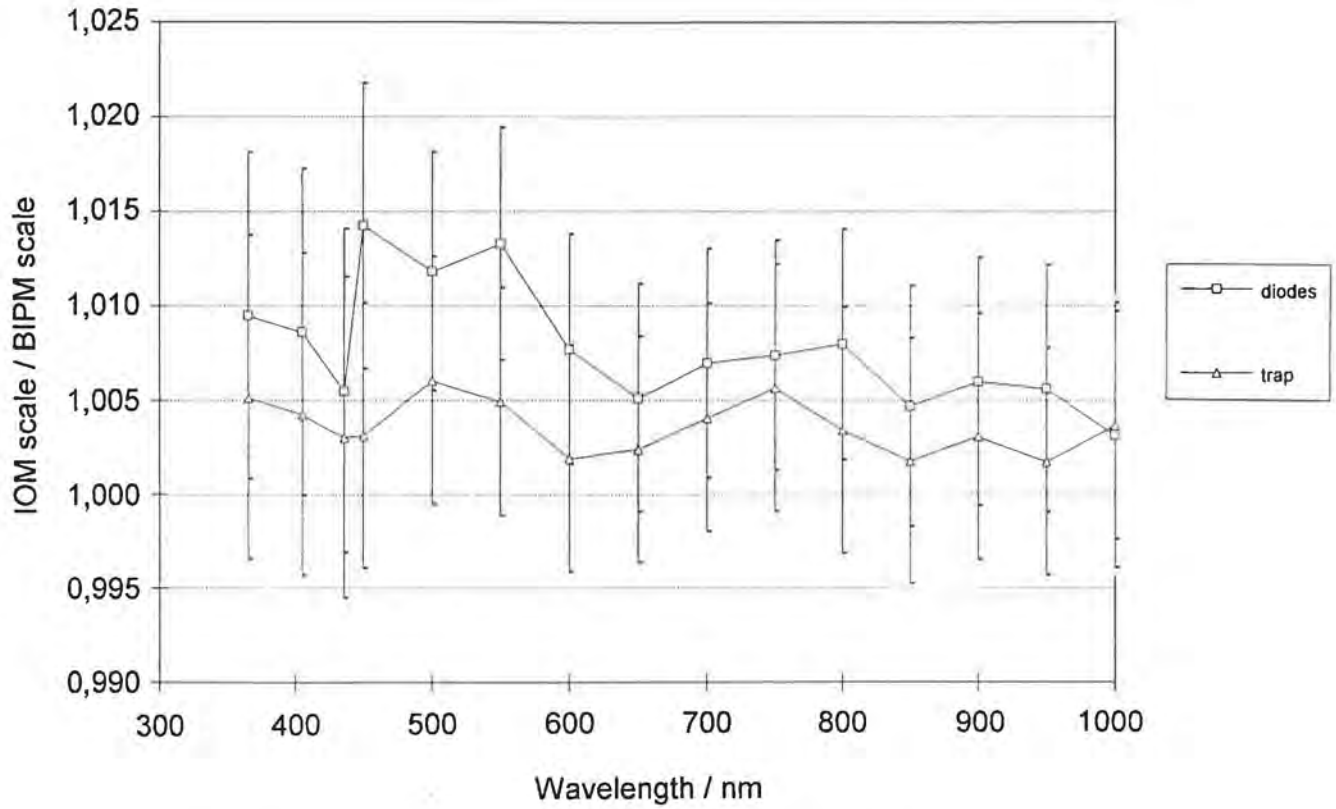


Fig.9A: IOM spectral responsivity scale compared to the scale of the BIPM.

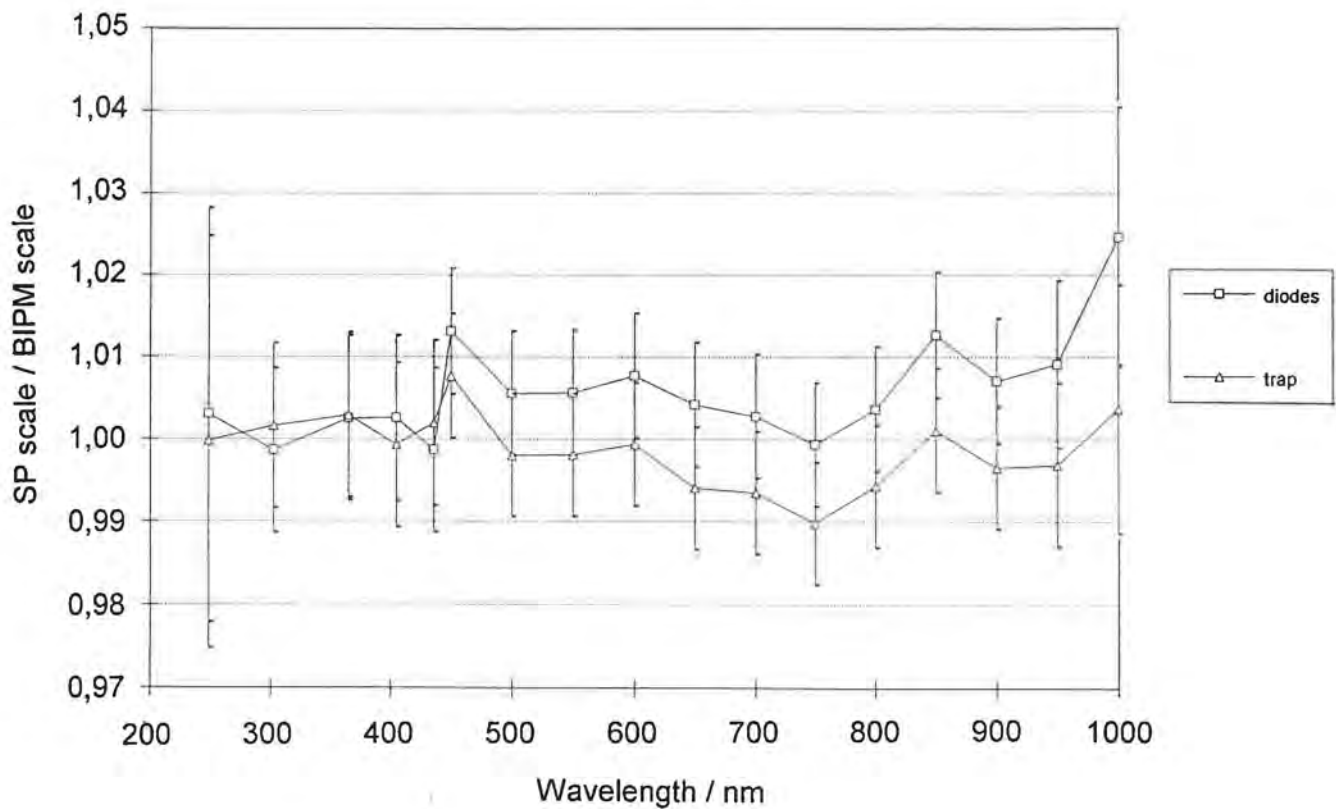
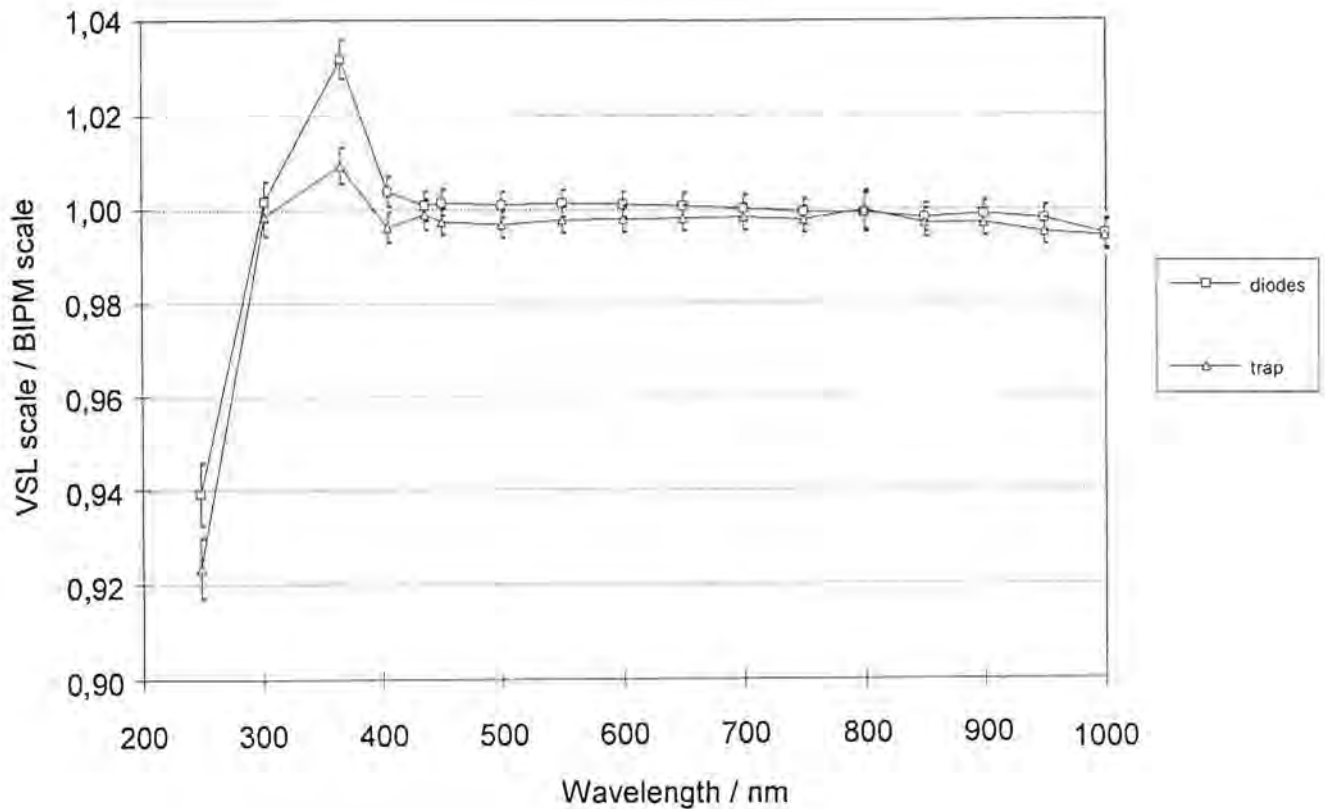


Fig.10A: SP spectral responsivity scale compared to the scale of the BIPM.



**Fig.11A:** VSL spectral responsivity scale compared to the scale of the BIPM.

### ***NEW DATA COMMUNICATED TO THE BIPM***

After distribution of the draft version of the report BIPM-94/9 to the participants, the NPL and the NIM communicated new values for their calibration data.

The NPL changed slightly their absolute calibration in the UV and found the reason why one of the photodiodes had a large discrepancy at 1000 nm.

The NIM had originally understood that the trap calibration should be done only at laser wavelengths. Although they had done the trap calibration at all wavelengths, the NIM did not communicate the results. After study of the main report they did send the calibration data to the BIPM. The NIM thinks that it is almost certain, that the offset of their photodiode calibration is due to the use of laser light in combination with a windowed photodiode, as it was suggested in the main report, page 57.

Table 4A gives the new data for the NPL and the NIM, figures 12A and 13A show the ratios of the individual scales to that of the BIPM scale.

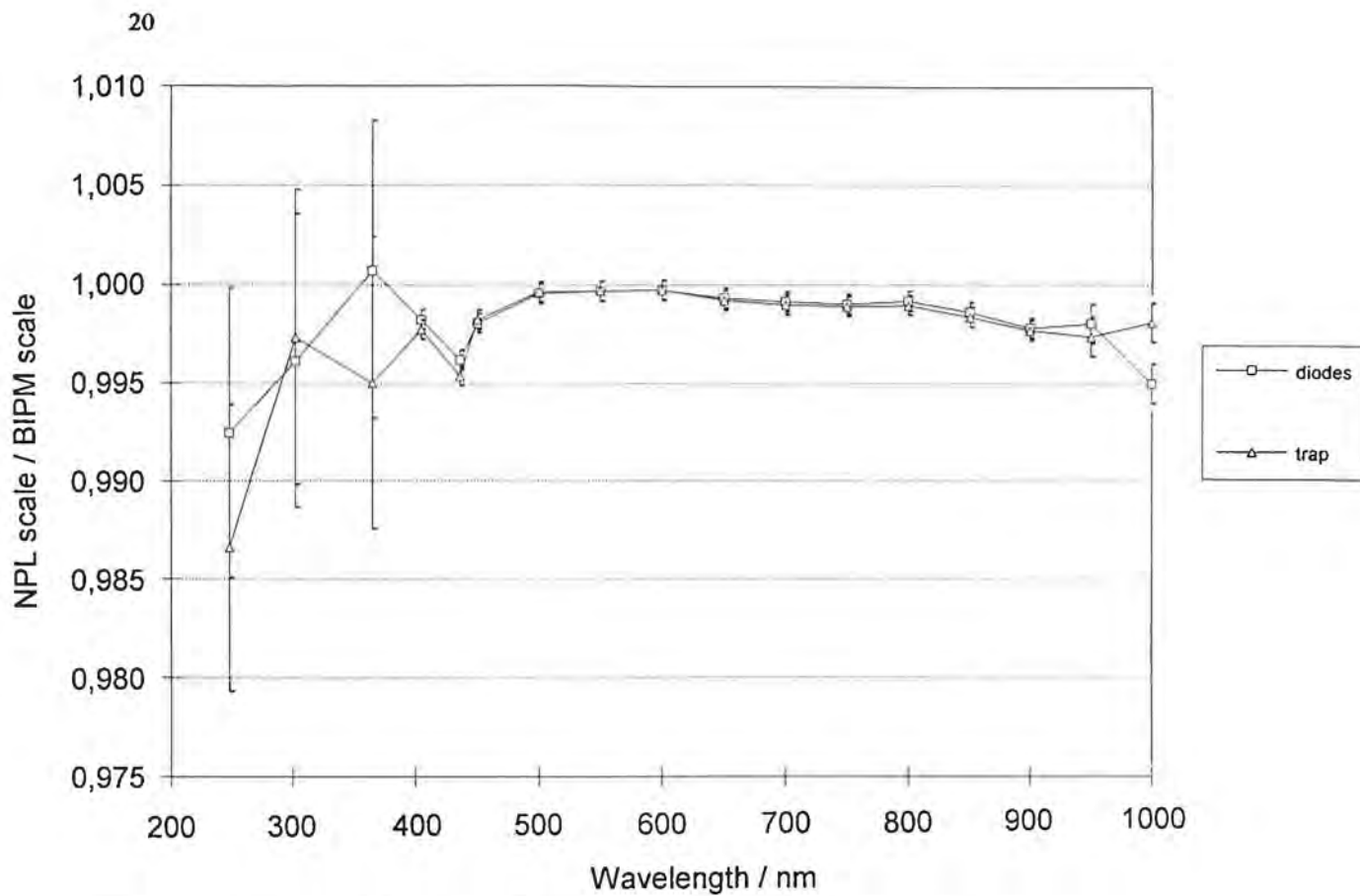


Fig.12A: NPL spectral responsivity scale compared to the scale of the BIPM.

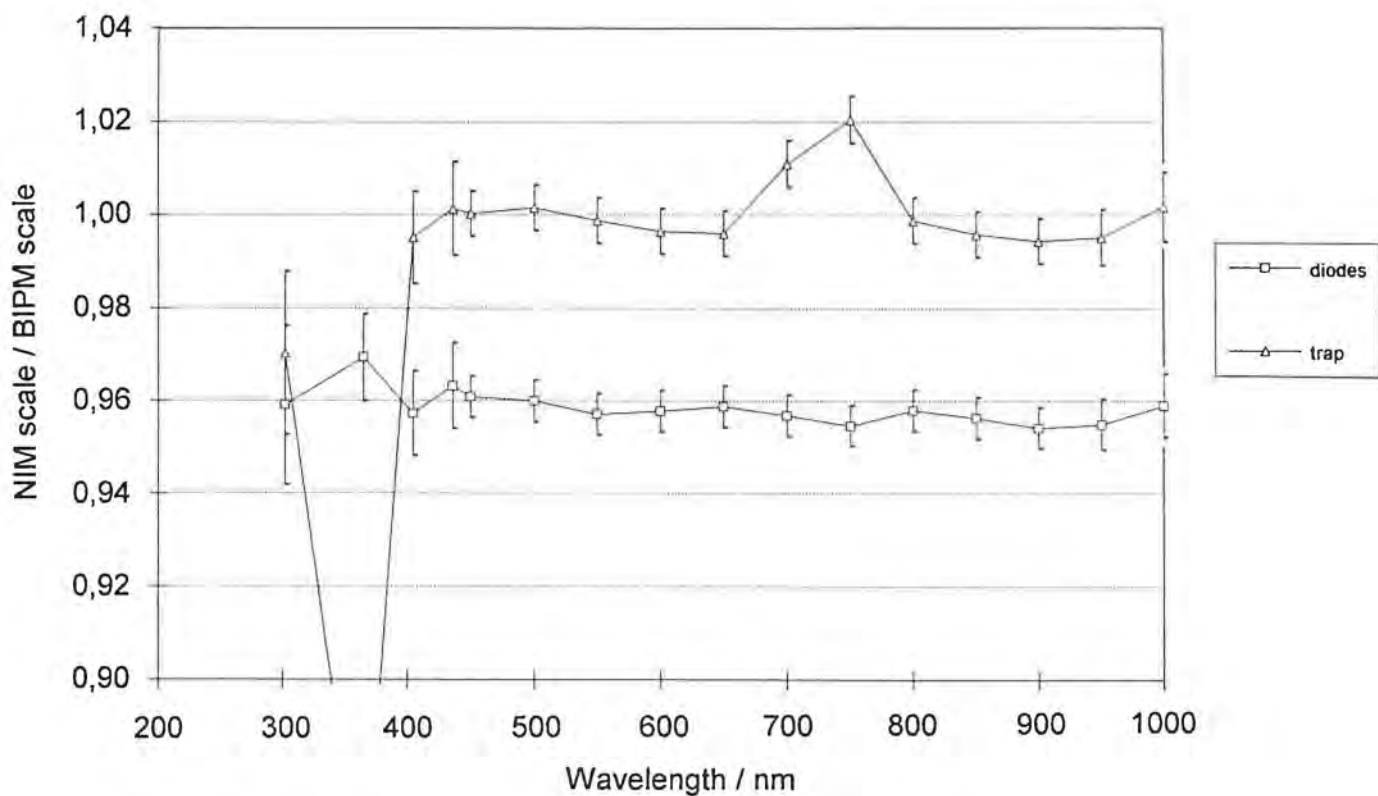


Fig.13A: NIM spectral responsivity scale compared to the scale of the BIPM.

lambda / nm	individual scale / BIPM scale	
<b>PHOTODIODES</b>		
	<b>NIM</b>	<b>NPL</b>
248,3		0,99245
302,2	0,95909	0,99610
365,0	0,96942	1,00072
404,7	0,95725	0,99823
435,8	0,96323	0,99617
450,0	0,96088	0,99805
500,0	0,95997	0,99956
550,0	0,95708	0,99967
600,0	0,95776	0,99975
650,0	0,95867	0,99934
700,0	0,95675	0,99915
750,0	0,95459	0,99902
800,0	0,95791	0,99917
850,0	0,95629	0,99862
900,0	0,95409	0,99780
950,0	0,95486	0,99801
1000,0	0,95895	0,99498
<b>TRAPS</b>		
248,3		0,98661
302,2	0,97034	0,99731
365,0	0,85041	0,99500
404,7	0,99521	0,99771
435,8	1,00143	0,99537
450,0	1,00032	0,99822
500,0	1,00156	0,99965
550,0	0,99886	0,99971
600,0	0,99652	0,99973
650,0	0,99607	0,99922
700,0	1,01096	0,99899
750,0	1,02045	0,99891
800,0	0,99878	0,99896
850,0	0,99583	0,99836
900,0	0,99433	0,99768
950,0	0,99512	0,99736
1000,0	1,00177	0,99808

**Table 4A:** Individual national scales compared to the BIPM scale (NIM and NPL)

## *CONCLUSIONS*

This annex to the main part of the report concludes the international comparison of spectral responsivity of silicon detectors. A total of 18 national laboratories and the BIPM have participated in this comparison. The results show an agreement of the scales within their uncertainties for most of the laboratories. However, some large deviations could be observed also, particularly in the ultra-violet.

The authors would like to thank all the participants for their effort.

## ***LIST OF FIGURES***

Fig.1A Change in spectral responsivity of diodes .....	8
Fig.2A Change in spectral responsivity of traps.....	8
Fig.3A Comparison of the individual national scales, derived from the diodes.....	12
Fig.4A Comparison of the individual national scales, derived from the diodes (zoom).....	13
Fig.5A Spread of calibration of the three photodiodes for each laboratory.....	14
Fig.6A Comparison of the individual national scales, derived from the traps.....	15
Fig.7A Comparison of the individual national scales, derived from the traps (zoom).....	16
Fig.8A IENGF spectral responsivity scale compared to the scale of the BIPM .....	17
Fig.9A IOM spectral responsivity scale compared to the scale of the BIPM .....	18
Fig.10A SP spectral responsivity scale compared to the scale of the BIPM .....	18
Fig.11A VSL spectral responsivity scale compared to the scale of the BIPM.....	19
Fig.12A NPL spectral responsivity scale compared to the scale of the BIPM.....	20
Fig.13A NIM spectral responsivity scale compared to the scale of the BIPM .....	20

## ***LIST OF TABLES***

Tab.1A Participants in the second round .....	6
Tab.2A Assignment of detectors to the laboratories for the first and second round.....	6
Tab.3A Individual national scales compared to the BIPM scale (second round participants).....	11
Tab.4A Individual national scales compared to the BIPM scale (NIM and NPL) .....	21